NASA CONTRACTOR REPORT

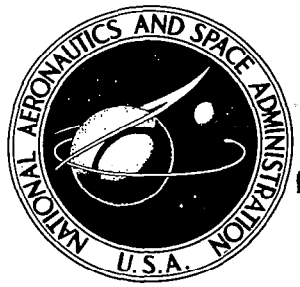

A NUMERICAL STUDY OF ELECTROMAGNETIC SCATTERING FROM OCEAN-LIKE SURFACES

by R. R. Lentz

Prepared by
THE OHIO STATE UNIVERSITY
Columbus, Ohio 43212

for Langley Research Center

NATIONAL AERONAUTICS AND SPACE ADMINISTRATION • WASHINGTON, D. C. • JULY 1972

1. Report No.	2. Government Accession No.	3. Recipient's Catalog No.
NASA CR-2091		

4. Title and Subtitle	5. Report Date
A NUMERICAL STUDY OF ELECTROMAGNETIC SCATTERING FROM OCEAN-LIKE SURFACES	July 1972
	6. Performing Organization Code

7. Author(s)	8. Performing Organization Report No.
R. R. Lentz	3030-1
	10. Work Unit No.

9. Performing Organization Name and Address	11. Contract or Grant No.
The Ohio State University Department of Electrical Engineering Columbus, Ohio 43212	NAS 1-9998
	13. Type of Report and Period Covered
12. Sponsoring Agency Name and Address	Contractor Report
National Aeronautics and Space Administration Washington, D.C. 20546	14. Sponsoring Agency Code

15. Supplementary Notes

16. Abstract

The integral equations describing electromagnetic scattering from one-dimensional conducting surfaces is formulated and numerical results are presented. The results are compared with those obtained using approximate methods such as physical optics, geometrical optics, and perturbation theory. The integral equation solutions show that the surface radius of curvature must be greater than 2.5 wavelengths for either the physical optics or geometric optics to give satisfactory results. It has also been shown that perturbation theory agrees with the exact fields as long as the root mean square surface roughness is less than one-tenth of a wavelength.

17. Key Words (Suggested by Author(s))	18. Distribution Statement
Rough surface scattering Scattering from ocean surface Electromagnetic scattering from stochastic surfaces	Unclassified - Unlimited

19. Security Classif. (of this report)	20. Security Classif. (of this page)	21. No. of Pages	22. Price*
Unclassified		138	$3.00

*For sale by the National Technical Information Service, Springfield, Virginia 22151

TABLE OF CONTENTS

A NUMERICAL STUDY OF ELECTROMAGNETIC SCATTERING FROM OCEAN-LIKE SURFACES

R. R. Lentz
The Ohio State University ElectroScience Laboratory

CHAPTER I

INTRODUCTION

The scattering of electromagnetic waves from the ocean surface has been of great interest for some time. In this work the scattering from one dimensional sea-like random surfaces is examined by a variety of computational methods, with a view to establishing what practical limitations must be satisfied on such surface parameters as radius of curvature, mean squared height, etc., in order that the statistical properties of the scattered radiation may be calculated with reasonable accuracy. The results of the computations are then used to discuss the applicability of the several theoretical models for sea-surface scattering (geometrical optics, physical optics, perturbation theory and the composite model) and the prospect for direct calculation of the scattered fields from the actual sea surface.

During the past few years, theoretical and experimental work here and abroad (Refs. [1]-[7]) has led to an understanding of the mechanisms responsible for scattering and emission of microwaves by the ocean. For off-normal backscatter, the "Bragg-scatter" from capillary and short wavelength components of the ocean surface, which can be calculated by perturbation theory, has explained the angular

and polarization dependence of the microwave radar return. When combined with the known height spectrum (Ref. [8]) of the ocean surface, it explains the weak dependence of backscatter on electromagnetic wavelength and wind velocity. Near the specular direction, i.e., near normal incidence for backscatter, the scattering is controlled by the slope distribution of the large scale structure of the surface. This part of the scattering is calculated by geometrical optics, and explains the dependence of the emissivity of the surface on wind velocity.

Nevertheless, the many assumptions required in finding the scattered fields by the perturbation or geometrical optics approximations, particularly assumptions about the Gaussian character of the surface height statistics, and the applicability of the theoretical approximations to the actual sea surface, have led to considerable discussion about the validity of the various theoretical solutions (Ref. [9]). Since straightforward verification by measurement is not practical, partly because of difficulty in the measurement process itself and partly because of the difficulty in specifying exactly what the surface was when the measurement was being made, it is desirable to have a direct method for calculating the scattering from a specific realization of the ocean surface. Direct calculations will allow a realistic assessment of the validity of the various theories, without any assumptions about the statistical properties of the surface. If a statistical average of the scattered fields over an ensemble of surface representations is required, it can be obtained (albeit at

some cost) by a direct summation of the scattered fields from the individual surface representations.

The specific surfaces considered here are cylindrical perfectly conducting surfaces as shown in Fig. 1. The surface generators are

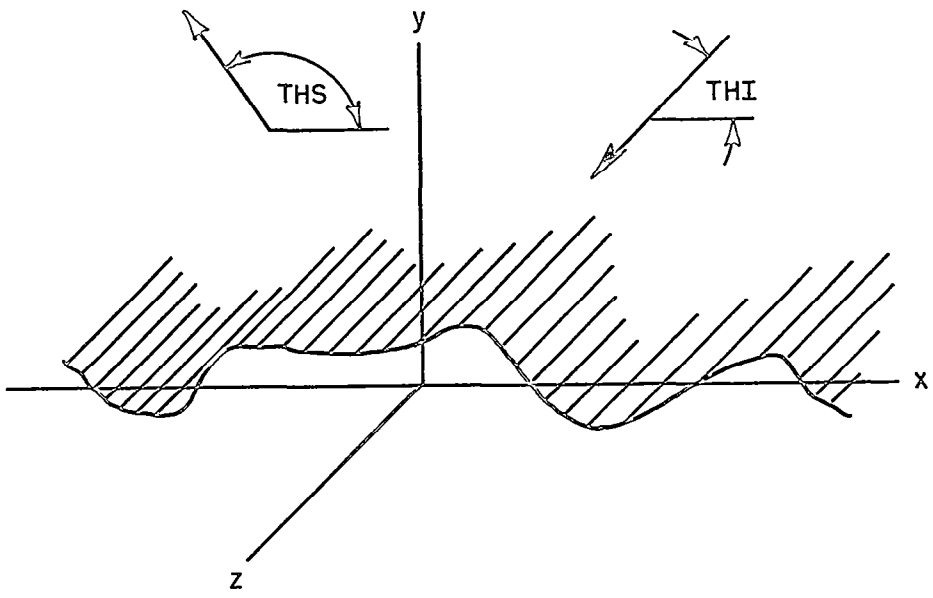

Fig. 1.--The scattering surface.

parallel to the z axis, and the surface elevation is specified by $y = H(X)$. The incident field is a plane wave whose direction of propagation lies in the x,y plane and makes an angle of THI with the positive x axis, while the observation direction makes an angle of THS with the positive x axis. Time dependence is assumed to be $e^{j\omega t}$ and has been suppressed throughout. All distances are measured in centimeters.

Three different methods for calculating the fields from such a surface are developed here. Although the details are discussed later it is desirable to outline each technique at this time.

The first approximate method is the geometrical optics technique (G.O.). For a given surface, and given scattering and incidence angles, the program locates the specular points on the surface (points where the local incidence angle equals the local scattering angle) and evaluates the radius of curvature at each specular point. The scattered far field is then found by summing the contribution from each of the specular points, including an extra 90° phase shift for the fields scattered from concave up portions of the surface. Shadowing of one section of the surface by another section may be taken into account.

The next approximation is the physical optics (P.O.) technique. For a given surface the scattered field is computed by integrating over the approximate surface current

$$\bar{J}_s = 2\hat{n} \times \bar{H}^i \tag{1}$$

where $\hat{n}$ is the outward normal to the surface and $\bar{H}^i$ is the incident magnetic field. Shadowing is always taken into account, as this is implicit in the physical optics formulation.

The last method developed here is based on a point matching solution to the integral equation satisfied by the true surface current $\bar{J}_s$. The scattered fields are then found by integrating over the surface currents. Test cases (e.g., the wedge problem) have shown this method to be by far the most accurate; hence it is used as a standard to which all others are compared. However, because of computer storage limitations, this program can not handle surfaces whose arclengths are greater than $\sim$60 electrical

wavelengths, whereas the G.O. and P.O. programs can, in principle, handle surfaces of any length provided sufficient computer time is available.

In order to avoid edge effects, tapering of the incident field is necessary in the integral equation solutions. The same tapering has been applied in both the G.O. and P.O. solutions so that they can be directly compared to the exact fields. The tapering applied here is illustrated in Fig. 14 of Chapter IV.

In the succeeding chapters each of these methods will be described in detail. By comparing the results for a series of test surfaces, the limitations of each method are established.

CHAPTER II

THE GEOMETRICAL OPTICS METHOD

The first approach to examining the scattering from a one dimensional rough surface is the geometrical optics method. By this is meant that the scattered field is computed by finding the specular points on the surface, and associating with each such point a scattered field amplitude and phase which depend on the geometrical properties of the surface at the specular point.

A. Geometrical Optics

Conservation of energy flux along a ray path will provide us with the geometrical optics field strengths (Ref. [10]).

Consider the two dimensional ray tube shown in Fig. 2. If u_o is the field strength at some reference point at a distance ρ from the caustic and u is the field strength at distance $\rho + \ell$ from the caustic, then the conservation of energy in the ray tube requires

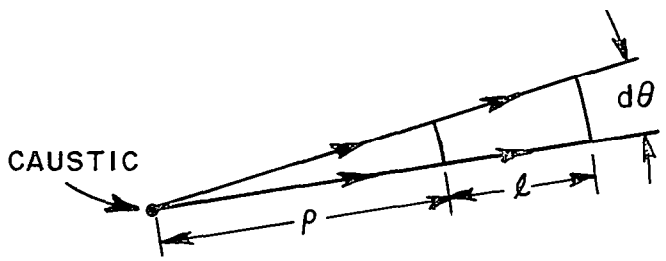

Fig. 2.--Ray tube geometry.

(2) $$u_o^2 \rho \, d\theta = u^2 (\rho + \ell) \, d\theta$$

so that one may write

(3) $$u(\ell) = u_o \sqrt{\frac{\rho}{\rho+\ell}} \; e^{-jk\ell}.$$

The factor $e^{-jk\ell}$, with λ_e the electrical wavelength and

(4) $$k = 2\pi/\lambda_e$$

accounts for the phase shift between ρ and $\rho+\ell$. Equation (3) fails at ℓ equal to $-\rho$. This location (at the confluence of the rays) is termed a caustic. Kay and Keller (Ref. [11]) have demonstrated that at points beyond the caustic (ℓ less than $-\rho$) Eq. (3) is still valid if a phase shift of +90° is introduced.

To use geometrical optics it is necessary to find all points on the scattering body at which the law of reflection is satisfied locally for the particular set of THI and THS under consideration. Once these points are located Eq. (3) is used to calculate the scattered field. Figure 3 shows the geometry for the calculation of the scattered field from one such specular point. By the law of reflection, the local incidence and scattering angles are equal and are marked ANG in the figure. The distances marked r_c and ρ are the radius of curvature and the distance from the specular point to the optical image of the source (i.e., the caustic distance) respectively. The distance ρ is given by a cylindrical mirror formula as

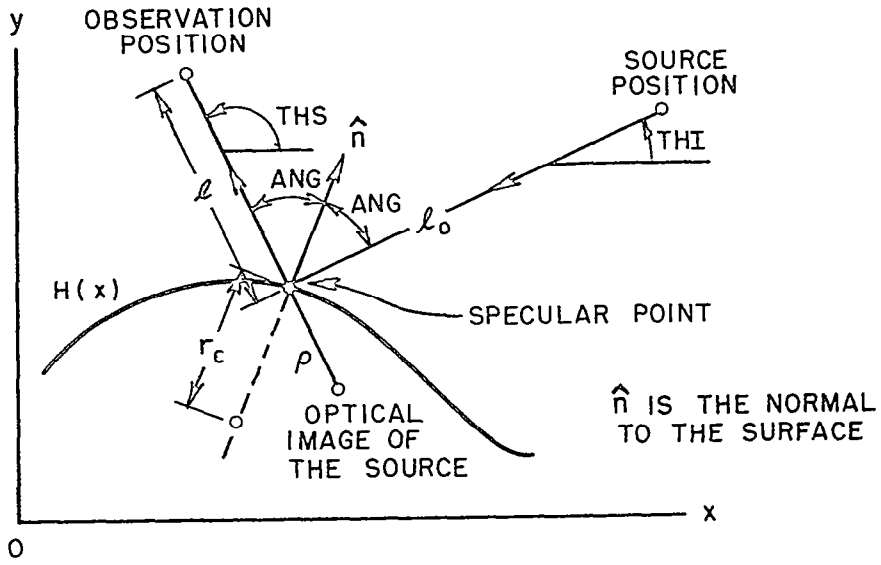

Fig. 3.--Specular point geometry.

$$(5) \qquad \frac{1}{\rho} = \frac{2}{|r_c| \cos (ANG)} + \frac{1}{\ell_o} .$$

In the cases considered here the distance to the line source, ℓ_o, will be assumed to be infinite, hence

$$(6) \qquad \rho = \frac{|r_c| \cos (ANG)}{2} .$$

If the specular point is taken as the reference position then Eq. (3) gives u_s, the scattered field at the observation position

$$(7) \qquad u_s = R\, u_i \sqrt{\frac{\rho}{\rho+\ell}}\; e^{-jk\ell}$$

$$= R\, u_i \sqrt{\rho}\; e^{-jk\ell}/\sqrt{\ell} \text{ for } \ell >> \rho \text{ (far field)}$$

where u_i is the incident field evaluated at the specular point and R is a reflection coefficient. If the electric field is parallel to the surface generators (T.M. case) and u_i is taken as the incident electric field, then u_s is taken as the scattered electric field with R = -1. If the magnetic field is parallel to the surface generators (T.E. case) and u_i is taken as the incident magnetic field, then u_s is the scattered magnetic field and R = +1. For dielectric scatterers the corresponding Fresnel reflection coefficients are to be used for R. This makes the geometrical optics program the easiest to convert from perfectly conducting bodies to penetrable bodies.

Up to this point the scattering surface has been assumed to be concave down at the specular point. If the body is concave up at the specular point then the caustic position is above the surface instead of below, the scattered rays pass through the caustic on the way to the observation point if the observer is in the far field, and thus a phase shift of +90 degrees must be introduced. The distant scattered fields may then finally be written

$$(8)\quad E_z^s(\ell) = -E_z^i\Big|_{\substack{\text{Specular}\\ \text{Point}}} \sqrt{\frac{|r_c|\ \cos\ (ANG)}{2}}\ \frac{e^{-jk\ell}}{\sqrt{\ell}}\ \varepsilon$$

for the T.M. case and

$$(9)\qquad H_z^s(\ell) = H_z^i\Big|_{\substack{\text{Specular}\\ \text{Point}}} \sqrt{\frac{|r_c|\ \cos\ (ANG)}{2}}\ \frac{e^{-jk\ell}}{\sqrt{\ell}}\ \varepsilon$$

for the T.E. case, where ε is +1 if the surface is concave down at the specular point and +j if the surface is concave up at the specular point.

On an actual surface there may be several specular points contributing to the total scattered field, so it is important to preserve the phase relationships among them. Phase reference is taken at the origin, and an incident wave of unit amplitude is assumed, i.e.,

$$E_z^i = e^{-j\overline{k} \cdot \overline{R}} \qquad \text{(T.M. case)} \tag{10}$$

$$H_z^i = e^{-j\overline{k} \cdot \overline{R}} \qquad \text{(T.E. case)} \tag{11}$$

where

$$\overline{k} \cdot \overline{R} = \frac{2\pi}{\lambda_e}(-x \cos (THI) - H(X) \sin (THI)). \tag{12}$$

With the aid of the geometry shown in Fig. 4, the scattered far field is found from Eqs. (8) and (9), with $\ell = \ell_1 + \ell_2$, where

$$\ell_2 = -\overline{R} \cdot \hat{D}_s = - x \cos (THS) - H(x) \sin (THS), \tag{13}$$

and

$$\hat{D}_s = \cos(THS)\hat{x} + \sin (THS)\, \hat{y} \tag{14}$$

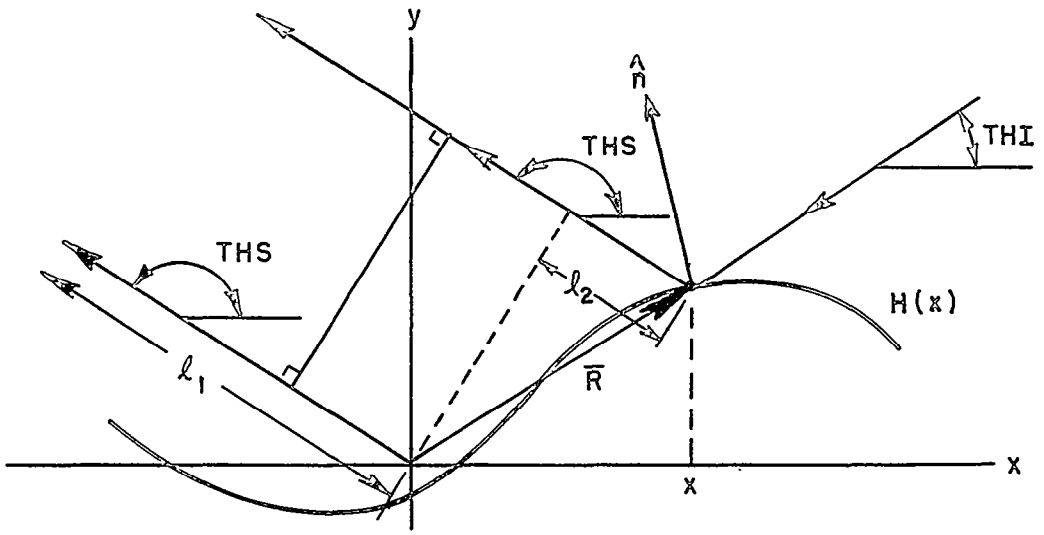

Fig. 4.--Far field scattering geometry.

is the unit vector in the scattering direction. Since $\ell_1 >> \ell_2$, Eq. (8) becomes, for the T.M. case

$$(15) \qquad E_z^s(\ell_1) = -\sqrt{\frac{|r_c| \cos (ANG)}{2}} \quad \frac{e^{-jk\ell_1}}{\sqrt{\ell_1}} \varepsilon \quad e^{jkQ(x)}$$

where

$$(16) \qquad Q(x) = x (\cos (THI) + \cos (THS)) + H(x) (\sin (THI) + \sin (THS)).$$

Similarly, for the T.E. case

$$(17) \qquad H_z^s(\ell_1) = \sqrt{\frac{|r_c| \cos (ANG)}{2}} \quad \frac{e^{-jk\ell_1}}{\sqrt{\ell_1}} \varepsilon \quad e^{jkQ(x)}$$

The total scattered field in the THS direction is the sum of the fields scattered by each of the specular points. The numerical values of the scattered fields as calculated by the programs of Appendix A, and plotted in the various figures of Chapter V are denoted by E_z^s and H_z^s, and have been normalized with respect to the actual fields $E_z^s(\ell_1), H_z^s(\ell_1)$ by

$$(18) \qquad \begin{Bmatrix} E_z^s \\ H_z^s \end{Bmatrix} = \sqrt{\ell_1}\, e^{jk\ell_1} \begin{Bmatrix} E_z^s(\ell_1) \\ H_z^s(\ell_1) \end{Bmatrix} .$$

It is clear that Eqs. (15) and (17) fail if the radius of curvature is infinite at the specular point. This is because the source was assumed at infinity, i.e., $\ell_0 \to \infty$. If ℓ_0 were to be held finite then from Eq. (5)

$$(19) \qquad \lim_{r_c \to \infty} \rho = \ell_0$$

and the singularity in Eqs. (15) and (17) would not occur. In addition to the singularities caused by an infinitely distant source, there are a number of other shortcomings of the G.O. approximation. Among them are: a failure to account for wedge diffraction effects (radius of curvature goes to zero), a failure to account for diffraction from shadow boundaries into shadowed regions (Ref. [12]), a failure to properly predict the scattered fields if the surface

features subtend only a few Fresnel zones (Ref. [13]), and finally a failure to predict any scattered field if no specular point exists on the body.

Implicit in the geometrical optics technique is the concept of shadowing, that is, a specular point cannot contribute to the scattered field unless it can be seen by both the source and the observer. The program developed here can account for shadowing of this type.

B. Discussion of the Geometrical Optics Program

For geometrical optics calculations the first order of business is the location of the specular points. Figure 5 shows the geometry.

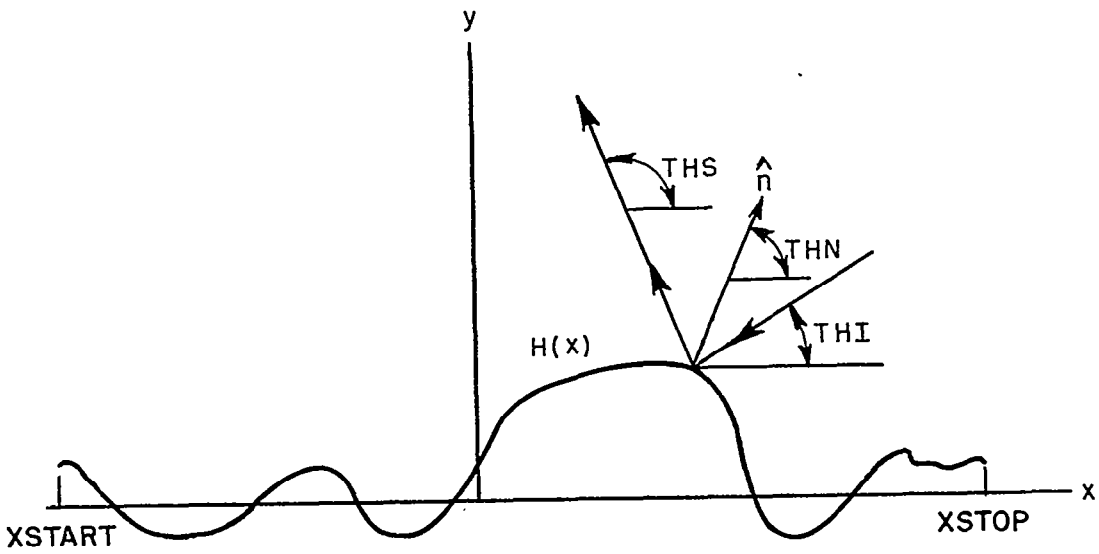

Fig. 5.--Geometry for specular point location.

The surface height profile is described by H(X) and the regions under investigation lies between XSTRT (X START) and XSTOP. THI and THS have already been defined; THN (THETA of the NORMAL) is the angle between the normal ($\hat{n}$) to the surface and the positive x axis. Clearly

(20) $THN(x) = \pi/2 + Tan^{-1}\ (dH(x)/dx)$.

The law of reflection gives (x,H(X)) as a specular point when

(21) $THS - THN(X) = THN(X) - THI$

i.e.,

(22) $(THS + THI)/2 = THN(X)$.

The program calculates the function

(23) $E(X) = (THS + THI)/2 - (\pi/2 + Tan^{-1}\ (dH(X)/dx)$

for many points in the interval (XSTRT, XSTOP) and when this function changes sign a specular point has been located. The collection of points so located is stored in an array XN(J). To save running time two searches are made, first a coarse grain search and then, in the neighborhood of each specular point, a finer grain pass is made.

The search must satisfy two requirements. First, it must be fine enough to locate all specular points; this requires that the surface must be sampled often enough to get an adequate description of its structure. For example if the surface were described by a Fourier series then one would expect that sampling every twentieth of the minimum mechanical wavelength would be sufficient. Secondly, the specular positions must be located to within a small fraction of an electrical wavelength so that the phase relationships among the various specular points are correctly maintained. In the light of

these considerations a first search might be made at a step size of (the minimum mechanical wavelength)/20. The fine grain search would then be made with a step size of say (λ_e/20.0) or (1st step size/2.0) whichever is the smallest. In the program, the coarse step size is called DLTAX (DELTA X) and the fine step size is called DLTAXOO. The local angle of incidence for each specular point is stored in an array ANG(J). This angle is used in the computation of the scattered field and is shown in Fig. 5. Once a complete pass is made over the surface, the scattered fields are computed. It should be noted that whenever any one of THI, THS, H(X) is changed, the complete pass must be made again.

The actual program, given in Appendix A, makes the scattered field computation for two cases:

1) all specular points contributing,
2) scattering from concave up specular points neglected when calculating the scattered field.

The second case, clearly incorrect, was an attempt to see how the computed fields would correspond to the results of certain statistical theories which neglect the concave up specular points. In the program the electric field calculated from the first case is called ESCNS (ELECTRIC FIELDS SCATTERED WITH NO SHADOWING) and from the second case ESCDNS (ELECTRIC FIELD SCATTERED FROM CONCAVE DOWN POINTS WITH NO SHADOWING).

Geometrical optics allows shadowing to be taken into account without much extra effort. The three types which may occur (specular point not illuminated by source, specular point not visible

to observer, both) are shown in Fig. 6. Each point in the array of specular points, XN , is examined for inbound shadowing in the following way. A line is passed through the specular point XN_j, $H(XN_j)$ with slope tan(THI). The equation of the line is

$$YI(X) = Tan(THI)x + (H(XN_j) - Tan(THI)\ XN_j) \tag{24}$$

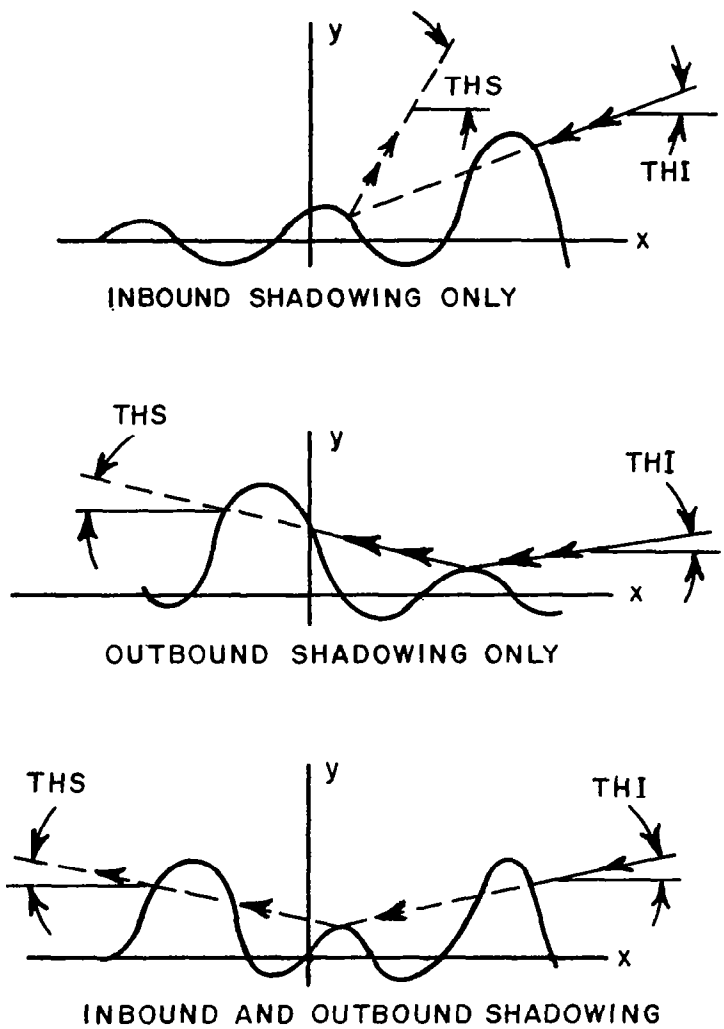

Fig. 6.--Specular point shadowing.

Then x is incremented in the proper direction until one of the following occurs. The first possibility is that at some point x, YI(x) becomes greater than the maximum value that H(x) can attain for any value of x in the interval XSTRT, XSTOP. This value of H(x) is called HMAX and must be supplied for each surface being considered. If the surface is a sum of sinusoids then HMAX is equal to the sum of the individual magnitudes. The second possibility is that at some point the value of x is incremented out of the interval (XSTRT, XSTOP) being considered. The third and final possibility is that at some point x the line YI(x) intersects the surface profile H(x). When the first or second case occurs the specular point is not shadowed. In the third case the specular point is inbound shadowed and for that particular j, XN(j) is set equal to a number much larger than XSTOP. This allows XN_j to be skipped when the contribution from each of the specular points is being computed. A very similar test is applied for outbound shadowing.

When both the inbound and the outbound shadowing tests are completed the array of specular point positions contains values which are either in the range XSTRT < X < XSTOP or XN_j >> XSTOP. The scattered field is calculated as in the case where shadowing is neglected except that when XN_j > XSTOP the field from this specular point is not put into the sum. The scattered field with shadowing accounted for is called ESCWS (ELECTRIC FIELD SCATTERED WITH SHADOWING) and the scattered field calculated with only concave down non-shadowed specular points contributing is called ESCD.

C. Using the Geometrical Optics Program

While the storage requirement is minimal, the running time of this program depends largely on the step sizes which have to be used during the search for the specular points, and the number of scattering angles. This means that as the length of the surface increases, the time per pass required to find the specular points goes up and the number of passes over the surface also increases, since to see detail in the scattered field pattern the scattering angle must be examined at a larger number of points (finer grain). The half-power beamwidth of a uniformly illuminated aperture of width XSTOP-XSTRT,

$$\text{beamwidth} \cong \frac{0.88\ \lambda_e}{\text{XSTOP} - \text{XSTRT}} \quad \text{radians} \tag{25}$$

affords a crude estimate of the fineness of the grain which must be taken. The increment in THS should be less than a fifth of this.

The program has been checked for several cases, two of which will now be mentioned. The simplest check was the comparison with hand calculations for a surface described by

$$H(x) = 50 \cos(2\pi x/800) \tag{26}$$

with x in the range (-200,200). This surface has only one specular point or none at all depending upon THI and THS. Another check was performed for a sinusoidal surface like the one shown in Fig. 7.

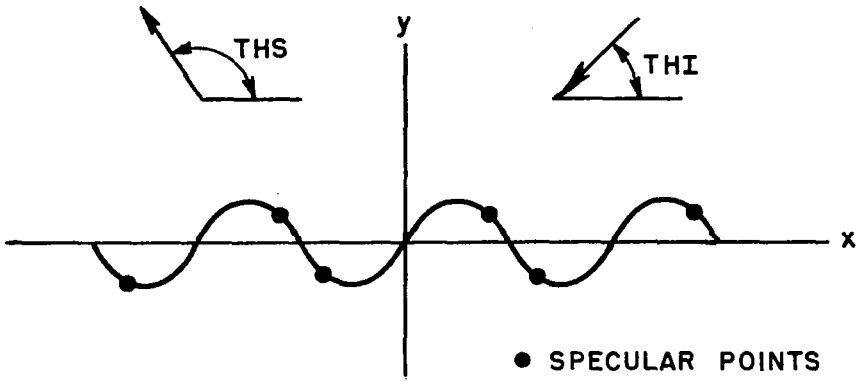

Fig. 7.--Specular points on a sinusoidal surface.

In this case the specular return comes from a collection of regularly spaced points which look like a pair of linear arrays of point sources. The program found the specular points and calculated the total scattered field correctly.

CHAPTER III

THE PHYSICAL OPTICS METHOD

The next complexity of approximation to the scattered fields to be considered here is given by the physical optics method.

A. The Physical Optics Approximation

Physical optics (P.O.), (Ref. [14]), approximates the true surface currents on a perfectly conducting body by the currents

$$\text{(27)} \qquad \bar{J}_s = \begin{cases} 2\hat{n} \times \bar{H}^i & \text{on the portions of the surface which are illuminated} \\ \bar{0} & \text{on the portions of the surface which are shadowed} \end{cases}$$

where $\hat{n}$ is the outward normal to the surface and $\bar{H}^i$ is the incident magnetic field evaluated at the surface. These approximate currents are then used in the radiation integral to calculate the scattered fields. The P.O. surface current is exact if the scattering body is perfectly conducting half space and the incident field is a plane wave. As the surface curvature decreases the P.O. currents depart more and more from the true currents; as the curvature at some point on the surface goes to zero (a wedge), the method fails entirely. Nor do the scattered fields predicted by P.O. satisfy the reciprocity theorem except for backscattering. Nevertheless, the P.O. method has a significant advantage over G.O. in that the fields remain

bounded even if the radius of curvature of the surface becomes infinite. Hence the flat facets of a surface can be approximately analyzed.

Whether or not P.O. provides any more useful information than G.O. is a question of long standing, and the answer seems to depend upon the geometry of the scattering body (Ref. [15]). For the kind of surfaces considered here it will appear that P.O. gives a good approximation to the scattered fields over a significantly wider range of surface characteristics than G.O. It is important to note that in this work the far field radiation integral over the physical optics currents is evaluated numerically to give the scattered fields. Unlike a number of rough surface scattering theories (Ref. [16]), no stationary phase approximation to the far field radiation integral is used. It is well known (Ref. [17]) that when the stationary phase approximation must be made, one obtains the G.O. result and there is then no difference between the two approaches.

The far-zone scattered fields will now be calculated using the physical optics currents. In the T.M. case, (see Fig. 8) the incident electric field is a z polarized plane wave of unit magnitude and the incident magnetic field is

$$\bar{H}^i = e^{+jk(x\cos(THI)+H(x)\sin(THI))}[-\sin(THI)\hat{x} + \cos(THI)\hat{y}]/\eta \tag{28}$$

where η is the impedance of free space. Using Ref. [18] and the fact that the tangential electric field vanishes on the surface, the scattered electric field is given by

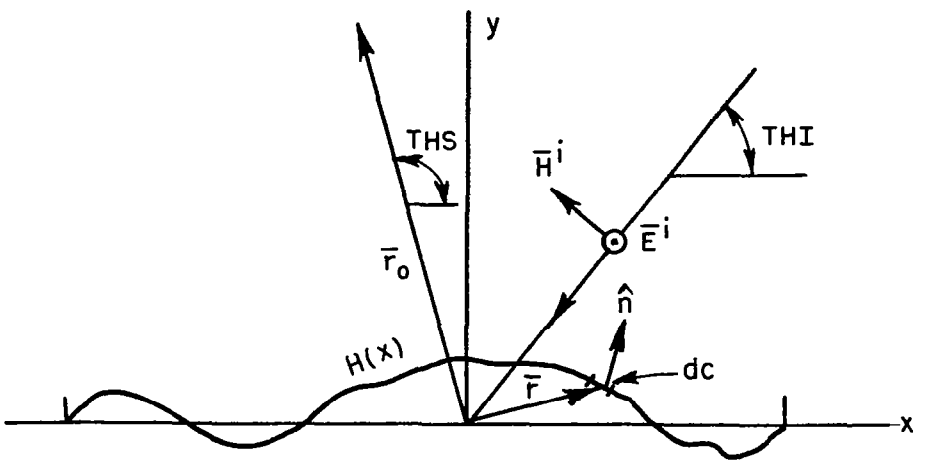

Fig. 8.--Geometry for T.M. physical optics.

$$(29) \qquad E^s(\bar{r}_o) = -\frac{j\omega\mu_o}{2\pi} \int_{c_{ill}} \int_{-\infty}^{\infty} (\hat{n} \times \bar{H}^i) \frac{e^{-jk|\bar{r}-\bar{r}_o|}}{|\bar{r}-\bar{r}_o|} \, dz \, dc$$

where $\bar{r}_o$ is the position vector to the observation point, $\bar{r}$ is the position vector of a point on the surface and $\hat{n}$ is the unit outward normal to the surface. The notation c_{ill} indicates that the integration is to be carried out only over those portions of the contour which are optically illuminated.

Since $\bar{H}^i$ and $\hat{n}$ are independent of z one can show, by using an appropriate integral representation for the Hankel function (Ref. [18]), that the scattered field is

$$(30) \qquad \bar{E}^s(\bar{\rho}_o) = -\frac{k\eta}{4} \int_{C_{ill}} (2\hat{n}\times\bar{H}^i)\, H_o^{(2)}(k|\bar{\rho}-\bar{\rho}_o|)\, dc$$

where all variables are confined to the x,y plane

$$(31) \qquad \bar{\rho}_o = x_o\,\hat{x} + y_o\,\hat{y}$$

$$(32) \qquad \bar{\rho} = x\,\hat{x} + y\,\hat{y}$$

and $H_o^{(2)}(x)$ is the Hankel function of the second kind and zero order. Using the large argument approximation for $H_o^{(2)}(x)$, the far field scattered electric field becomes

$$(33) \qquad E_z^s(\bar{\rho}_o) = -\left(\frac{2}{\pi k}\right)^{1/2} \frac{k}{2}\, e^{j\frac{\pi}{4}}\, \frac{e^{-jk|\bar{\rho}_o|}}{\sqrt{|\bar{\rho}_o|}} \int_{C_{ill}} \sin(THI-\tan^{-1}(\dot{H}))$$

$$e^{jkQ(x)}\sqrt{1+(\dot{H})^2}\, dx$$

where H(x) describes the surface height profile,

$$(34) \qquad \dot{H} = \frac{dH}{dx}\,,$$

and Q(x) is given by Eq. (16). As before, the factor

$$e^{-jk|\bar{\rho}_o|}\Big/\sqrt{|\bar{\rho}_o|}$$

has been suppressed in both the computed and reported values of the scattered electric field, so that the actual field $E_z^s(\bar{\rho}_o)$ is related to the print out value E_z^s by

$$(35) \qquad E_z^s = E_z^s(\bar{\rho}_o)\sqrt{|\bar{\rho}_o|}\; e^{+jk|\bar{\rho}_o|} \; .$$

When the incident magnetic field is $\hat{z}$ directed (transverse electric case) it is convenient to work with the scattered magnetic field. The latter is found from Ref. [18]

$$(36) \qquad 4\pi\, \bar{H}^s(\bar{r}_o) = 2 \int_{C_{ill}} \int_{-\infty}^{\infty} (\hat{n} \times \bar{H}^i) \times \bar{\nabla} \frac{e^{-jk|\bar{r}-\bar{r}_o|}}{|\bar{r}-\bar{r}_o|}\, dz\, dc$$

where $\bar{H}^i$ is the incident magnetic field (see Fig. 9). The two dimensional far field scattering becomes from Eq. (36)

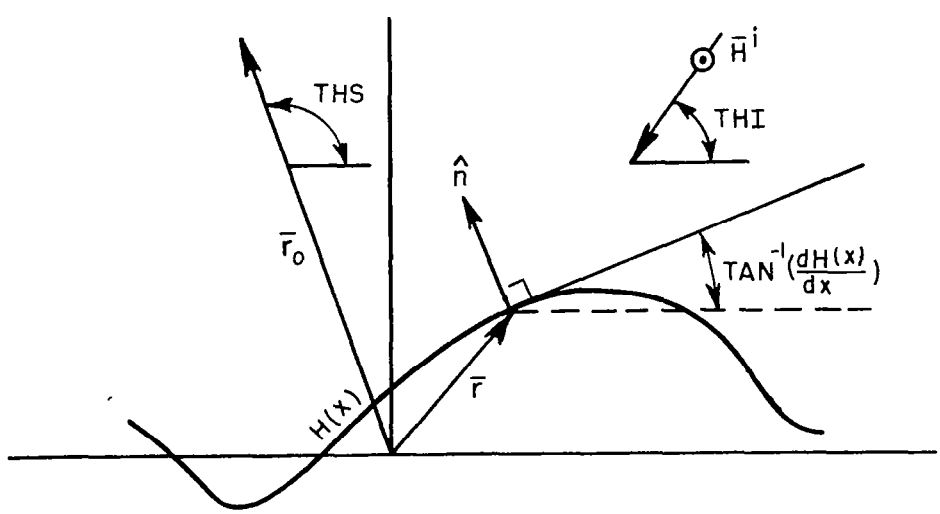

Fig. 9.--Geometry for T.E. physical optics.

$$(37) \qquad H_z^s(\bar{\rho}_o) = \frac{e^{-jk|\bar{\rho}_o|}}{\sqrt{|\bar{\rho}_o|}} \frac{e^{j\frac{\pi}{4}}}{\sqrt{\lambda_e}} \int_{c_{ill}} \sin(\tan^{-1}(\dot{H}) - THS) e^{jkQ(X)} \sqrt{1+\dot{H}^2}\, dx.$$

Again, the factor

$$\frac{e^{-jk|\bar{\rho}_o|}}{\sqrt{|\bar{\rho}_o|}}$$

is suppressed in the programs of Appendix A, so that the plotted or tabulated field strengths, H_z^s, are related to the true fields, $H_z^s(\bar{\rho}_o)$ by

$$(38) \qquad H_z^s = H_z^s(\bar{\rho}_o) \sqrt{|\bar{\rho}_o|}\, e^{jk|\bar{\rho}_o|} .$$

There are two further considerations that may be discussed at this time. For bistatic scattering it may happen that not all of the currents set up on the surface by the incident field are optically visible to the observer (see Fig. 10). In the physical optics programs developed here no account was taken of this possibility. Obviously such considerations do not arise for backscattering.

So far, in this chapter a perfectly conducting surface has been assumed. Physical optics can be generalized to treat dielectric surfaces by using a pair of equivalent electric and magnetic surface

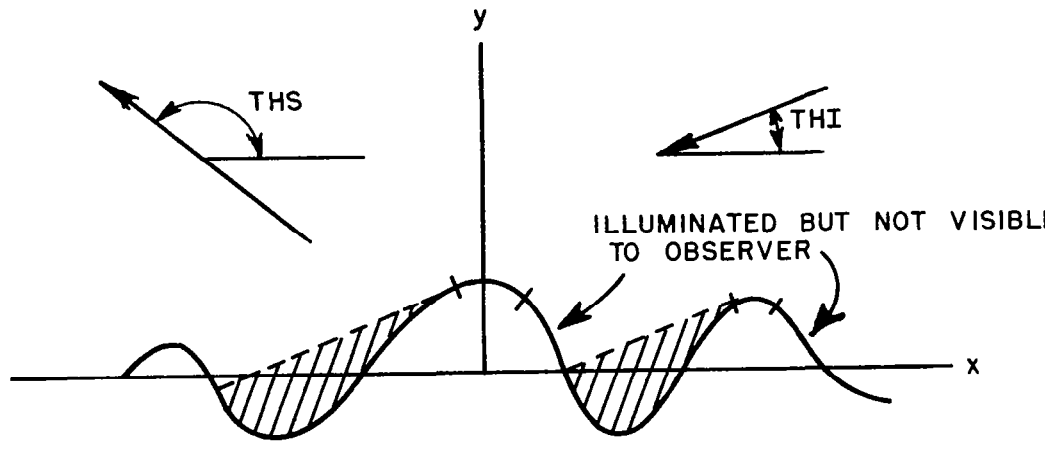

Fig. 10.--Optically invisible surface currents.

currents obtained from the fields of a plane wave incident on a dielectric half space (Ref. [19]). Since two integrations would be required to compute the scattered fields, it would seem that the running time should nearly double, but very little extra storage space would be required.

B. Discussion of the Physical Optics Computer Programs

For either polarization the physical optics program is divided into two parts. The first, and by far the most difficult, finds the shadow boundaries on the surface, since the integrations are to be performed only over the illuminated section of the contour. The second part performs the necessary integration to calculate the scattered far fields.

The program opens by considering the function H(X) which describes the surface between the defined endpoints ALEP (Left End Point) and REP (Right End Point). The search for shadow boundaries begins at REP by determining whether or not the right endpoint casts a shadow on the surface and proceeds from right to left (see Fig. 11).

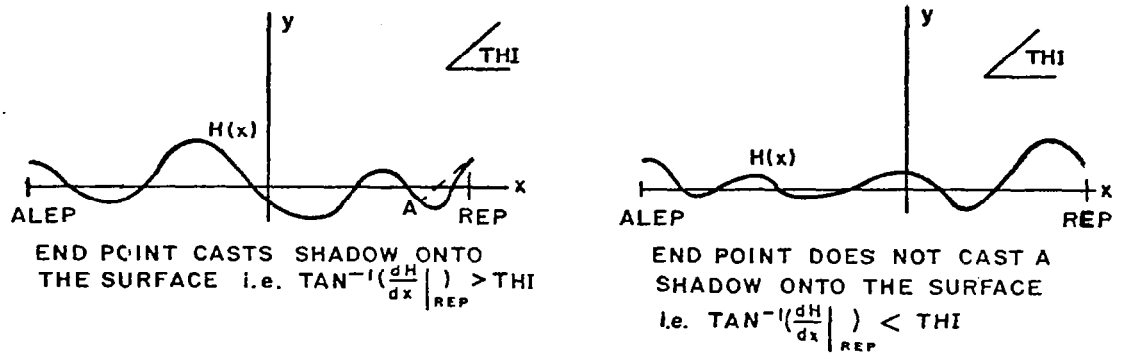

Fig. 11.--Shadowing at the right end point.

If THI (the incidence angle-required to be less than 90°) is greater than 80° it is assumed that no shadowing occurs. The starting point of the illuminated zone (either REP or A of Fig. 11) is stored in the first position of an array called SX (Shadow boundaries X coordinate). The value of x is decremented until either a point on the surface is reached where the tangent-slope condition

$$\frac{dH}{dx} = \tan(THI) \tag{39}$$

is satisfied, at which point a shadow zone begins, or x becomes less than ALEP, in which case the second entry in SX is ALEP. On the other hand if Eq. (39) is satisfied for some x between SX_1 and ALEP then this value of x is stored in SX_2, a line with slope tan(THI)

is passed thru the point, and its intersection (if any) with H(x) is found. If there are no such intersections, then all of the surface to the left of the point is shadowed. If an intersection does exist then the search for a point where the tangent-slope condition is satisfied begins again. This process continues until x is decremented past ALEP. The array SX thus stores the positions of points with an illuminated zone on their left in oddly subscripted locations and the points with an illuminated zone on their right in evenly subscripted locations (see Fig. 12). The size of the decrement used to locate the boundaries should be small enough to catch the surface features, and to locate the ends of the shadow zones within a fraction of a wavelength.

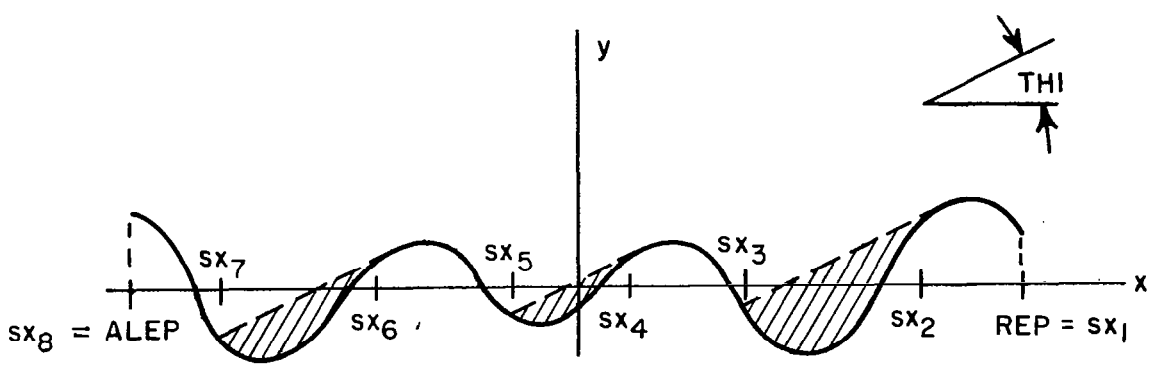

Fig. 12.--Illustration of shadowed and illuminated zones.

The integration over the illuminated sections of the surface to find the scattered fields is performed in a subroutine called BINT(XX,YY) (Bistatic radiation Integral) the arguments of which are the initial and final coordinates of one of the illuminated zones in

sx(J). The integration is repeated for each zone until all illuminated zones have been considered. The total scattered field (called S) for a particular THI and TNS is the sum of the zone fields. Except for normalization, the programs for the two polarizations differ only in the subroutine called FTBI(X) (Function To Be Integrated); the factor $\sin(THI-\tan^{-1}(\dot{H}))$ for the T.M. polarization is replaced in the T.E. case by $\sin(THS-\tan^{-1}(\dot{H}))$. The actual integration over the physical optics surface currents is performed by a five point Gaussian integration. In choosing the interval on the x axis over which the five point Gaussian integration is to be applied, two conditions must be met. The first is that the number of sample points along the contour must exceed five per wavelength. Presuming surface slopes of less than 60°, this means that ten sample points should be taken per electrical wavelength on the x axis. The second condition is that, if the surface were to be represented by a Fourier series, there should be 8-10 sample points per minimum mechanical wavelength along the x axis. Presuming, for example, that the first of the above conditions is the most stringent, each section of illuminated surface (i.e., between $x = SX_{j+1}$ and $x = SX_j$, j odd) would be divided into half electrical wavelength intervals plus a fractional interval, and five point Gaussian integration would be applied to each of the half electrical wavelength intervals, and to the last, fractional, interval.

C. Comments on the Use of the Physical Optics Programs

As in the case of G.O., the storage requirements are minimal, while running time depends upon the length of the surface and number of incidence and scattering angles which are investigated. For each THI the search for illumination boundaries is performed only once, but the integration must be repeated for each scattering angle considered. For many of the scattered field computations considered here the angle of incidence was held fixed and the scattering angle was varied between 0 and 180°. For such cases the time required to find the illuminated zones on the surface is small compared to the time required to do the integrations for the scattered field.

As the surface length is increased the time required goes up rapidly since the integration for each scattering angle takes longer and THS must be incremented with a finer grain to get an accurate reproduction of the structure in the scattered field pattern. The size of the increment for THS has already been discussed in connection with the geometrical optics program. For example, the time required to run a surface 16 electrical wavelengths long, with THS incremented by 0.5° from 0 to 180°, was 1.8 min. By comparison, 21 min. were required for a surface 100 electrical wavelengths long with increments in THS of 0.25° from 30° to 170°, i.e., 560 values of THS. The value of the increment in the last case appears to have been just adequate to see the detail in the pattern.

Among the checks of the P.O. program is a computation for a flat strip with no tapering of the illumination, for which a closed form

physical optics result is easily obtained. The agreement was excellent for both polarizations. In Chapter V, P.O. will be compared with the other two methods of computing the scattered fields. Special attention will be given to the range of surface parameters over which the P.O. approximation is valid.

CHAPTER IV

THE INTEGRAL EQUATION METHOD

In this chpater the third and most accurate method for calculating the scattering will be examined. Here the scattered field is obtained from the exact surface current, which is found from a moment method solution of an integral equation (see, e.g., Refs. [20], [21]). There are no restrictions on the curvature or form of the surface, but because of machine storage limitations only surfaces of rather short length (30 λ_e to 60 λ_e) can be handled.

A. Moment Methods

This section contains a brief introduction to the method of moments. For more information and other applications of this method refer to Ref. [22], on which the following is based.

The objective of the moment method is to determine, numerically, the function F which is a solution of the inhomogeneous operator equation

$$C(F) = G \tag{40}$$

where C( ) is a given linear operator and G is a given function. Suppose that F can be expanded in a set of basis functions b_n

$$F = \sum_{n=1}^{N} F_n \, b_n \, . \tag{41}$$

where F_n is the n-th unknown coefficient of the expansion of F in that basis. Note that if a computer is to be used, N will have to be finite. Using the linearity property of C

$$C(F) = C\left(\sum_{n=1}^{N} F_n\, b_n\right) = \sum_{n=1}^{N} F_n\, C(b_n) = G. \tag{42}$$

To convert the operator equation to a set of simultaneous equations an inner product, a scalar, $\langle h,g\rangle$ is defined for functions h,g and s and scalars α, β such that

$$\langle h,g\rangle = \langle g,h\rangle \tag{43}$$

$$\langle \alpha h + \beta g,s\rangle = \alpha\langle h,s\rangle + \beta\langle g,s\rangle \tag{44}$$

$$\langle h,h^*\rangle = 0, \text{ if } h \equiv 0. \tag{45}$$

Let $\{W_i\}$ be a set of weighting functions and take the inner product of both sides of Eq. (42) with W_m. Using the properties of the inner product, the original operator equation is converted to

$$\sum_{n=1}^{N} \langle W_m, C(b_n)\rangle\, F_n = \langle W_m, G\rangle \tag{46}$$

which is exactly the familiar matrix equation

$$\sum_{n=1}^{N} C_{mn}\, f_n = G_m \tag{47}$$

where

(48) $$C_{mn} = \langle W_m, C(b_n) \rangle$$

and

(49) $$G_m = \langle W_m, G \rangle .$$

The solution, F_i, to this system of equations can be found by any one of several methods, two of which are discussed in Appendix B. The solution may be exact or approximate depending upon N, b_n, and W_n.

For the integral equations to be solved here, the current is expanded in a basis of non-overlapping pulses of unit amplitude, while the weighting functions are chosen to be delta functions whose singularities occur at the centers of the pulses. The inner product is chosen to be

(50) $$\langle g,h \rangle = \int_c g\, h\, dc$$

where c is the contour of the scattering surface. This choice of basis and weight functions amounts to enforcing the integral equation at the centerpoints of the pulses, and is usually called "point-matching." For the operator equations considered in this work the system of simultaneous equations which result from point matching are well conditioned, i.e., suitable for computer solution (see Ref. [23]).

B. Integral Equation for Transverse Magnetic Polarization

In order to apply the point matching technique to the rough surface scattering problem, it is first necessary to find an appropriate linear operator. For this purpose the integral equation relating the unknown surface current to the known incident field has been chosen.

The incident electric field is $\hat{z}$ directed, the incident magnetic field is transverse (T.M. polarization) to the generators of the surface with contour c as shown in Fig. 13. If the total electric

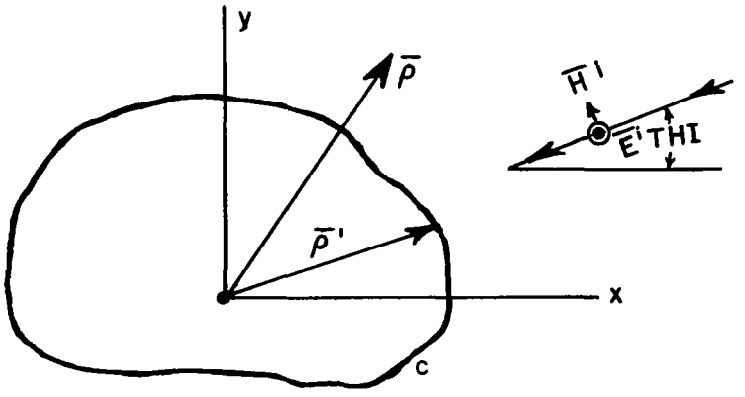

Fig. 13.--Geometry for T.M. scattering.

field is written as the sum of the incident field $\bar{E}^i$ and the scattered field $\bar{E}^s$, the boundary condition

$$\bar{E}^i + \bar{E}^s = 0 \tag{51}$$

must be satisfied on c. The scattered field is given in terms of the $\hat{z}$ directed surface currents, $J_z(\bar{\rho}')$, by (see Ref. [24])

$$(52) \qquad E_z^s(\bar{\rho}) = -\frac{k\eta}{4} \int_c J_z(\bar{\rho}') \, H_0^{(2)}(k|\bar{\rho}-\bar{\rho}'|) \, d\ell'$$

for the two dimensional case, where $H_0^{(2)}$ is the Hankel function of the second kind and order zero, η is the impedance of free space and k is the wave number, $2\pi/\lambda_e$. Combining this with the boundary condition (Eq. (51)) gives the integral equation for the unknown surface current

$$(53) \qquad E_z^i(\bar{\rho}) = \frac{k\eta}{4} \int_c J_z(\bar{\rho}') \, H_0^{(2)}(k|\bar{\rho}-\bar{\rho}'|) \, d\ell'$$

where $\bar{\rho}$, $\bar{\rho}'$ are now both confined to the contour c. Equation (53) can now be identified with Eq. (42) as follows:

$E_z^i(\bar{\rho})$ corresponds to G,

$J_z(\bar{\rho}')$ corresponds to F,

and the operator

$$\frac{k\eta}{4} \int_c (\quad) \, H_0^{(2)}(k|\bar{\rho}-\bar{\rho}'|) \, d\ell' \text{ corresponds to } C(\ ).$$

As it stands the integral equation requires the consideration of the current on the entire boundary c; if the entire contour of a two dimensional earth were to be included, the storage requirements for a moment method solution would be astronomical. It seems reasonable to assume that for standard radar wavelengths and with directive antennas, the surface current is appreciable over only a very small

portion of this contour. Thus it will be presumed that the surface current outside a certain illuminated region, which extends from -EP (End Point) to +EP, can be neglected (see Fig. 14). To simulate the

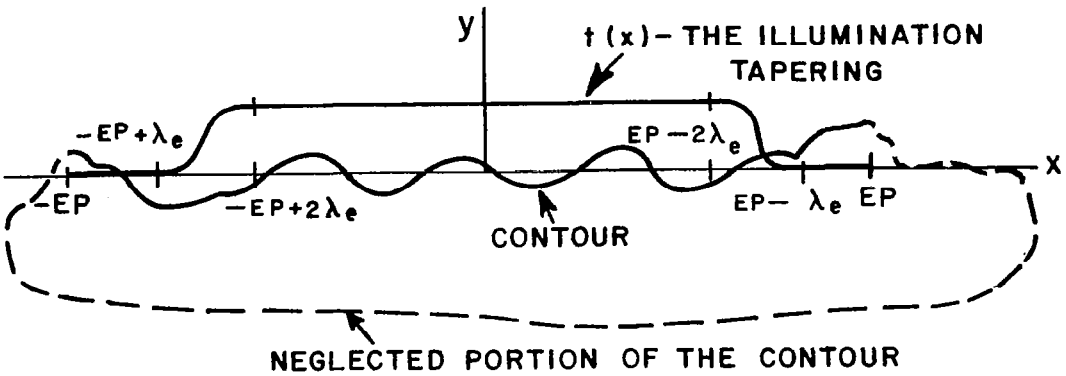

Fig. 14.--Modification of true contour to a shortened contour.

illumination of the surface by a directive antenna, an amplitude taper t(x) is introduced* in the following way. The amplitude of the incident field is taken as unity to within two electrical wavelengths from each end point. Between one and two electrical wavelengths from each end the field is sinusoidally tapered to zero. Over the last wavelength the incident field is taken to be zero. The incident field with tapering included, $E_z^i(\bar{\rho})$, is thus

*The use of amplitude tapering on a plane wave amounts to independently specifying the amplitude and phase, which makes such a field differ from a Maxwellian field. Changing the specification of the incident field would require no fundamental change in the methods and programs employed.

$$(54) \qquad E_z^i(\bar{\rho}) = t(x)\, e^{-j\bar{k}\cdot\bar{\rho}} = t(x)\, e^{+j\frac{2\pi}{\lambda_e}(\cos(THI)\, x + \sin(THI)\, H(x))}$$

The neglect of the surface currents beyond the endpoints (±EP) has been checked by lengthening the dead zone at each end of the region under consideration and noting the change in the surface currents and scattered fields. The results of this test are presented in Section D of the chapter and do indeed justify the assumption of negligible currents beyond the illuminated region.

Although tapering of the incident field is not needed in the P.O. or G.O. formulations, it has usually been included in the calculations so that the results of all the techniques can be fairly compared. The only cases in which tapering is not used are special tests of the individual methods.

The integral equation becomes

$$(55) \qquad E_z^i(\bar{\rho}) = \frac{k\eta}{4} \int_{-EP}^{EP} J_z(\bar{\rho}')\, H_0^{(2)}(k|\bar{\rho}-\bar{\rho}'|)\, d\ell'$$

with $\bar{\rho}$, $\bar{\rho}'$ both confined to the section of the contour for which $-EP \leq x \leq EP$.

The method of moments can now be applied. The surface is divided into segments of equal arclength DC, and the current, J_z, is expanded in a basis of non-overlapping pulse functions as

$$(56) \qquad J_z(\bar{\rho}') = \sum_{n=1}^{N} F_n \, P_{\frac{DC}{2}} \, (\bar{\rho}' - \bar{\rho}_n)$$

where $\bar{\rho}_n$ is the position vector of the midpoint of the n-th segment of the surface, F_n is a complex number representing the magnitude and phase of the current over the n-th segment of the contour, and the n-th basis function $P_{\frac{DC}{2}} \, (\bar{\rho}' - \bar{\rho}_n)$ is a pulse of unit amplitude and width DC along the contour c. Thus the actual surface current is to be approximated as shown in Fig. 15. For a reasonable representation of the surface current, the pulse width, DC, must be a fraction

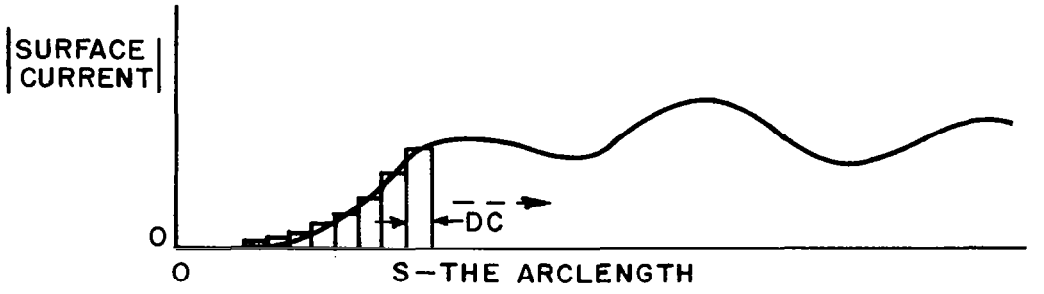

Fig. 15.--Approximation of the surface current.

of an electrical wavelength; $\lambda_e/10$ has been found to be satisfactory. The shape of the surface must also be considered in choosing DC, since the surface must be accurately modeled by strips of width DC. Hence, if λ_m is the shortest mechanical wavelength in the Fourier spectrum of the surface, then DC should also satisfy $DC \leq \lambda_m/10$. Of course the more restrictive of the two conditions should be met.

Applying the method of Section A of this chapter to Eq. (55)

$$(57)\qquad E_z^i(\bar{\rho}) = \frac{k\eta}{4}\int_{-EP}^{EP}\sum_{n=1}^{N} F_n\, P_{\frac{DC}{2}}(\bar{\rho}'-\bar{\rho}_n)\, H_o^{(2)}(k|\bar{\rho}-\bar{\rho}'|)\, d\ell'$$

$$= \frac{k\eta}{4}\sum_{n=1}^{N} F_n \int_{-EP}^{EP} P_{\frac{DC}{2}}(\bar{\rho}'-\bar{\rho}_n)\, H_o^{(2)}(k|\bar{\rho}-\bar{\rho}'|)\, d\ell'$$

$$= \frac{k\eta}{4}\sum_{n=1}^{N} F_n \int_{DC_n} H_o^{(2)}(k|\bar{\rho}-\bar{\rho}'|)\, d\ell'$$

where $\int_{DC_n}$ means "integrate over the n-th segment of the contour". Taking the inner product of Eq. (57) with the weighting functions,

$$(58)\qquad \langle \delta(\bar{\rho}-\bar{\rho}_m),\, E_z^i(\bar{\rho})\rangle = \frac{k\eta}{4}\sum_{n=1}^{N} F_n \left\langle \delta(\bar{\rho}-\bar{\rho}_m)\,,\, \int_{DC_n} H_o^{(2)}(k|\bar{\rho}-\bar{\rho}'|)\, d\ell' \right\rangle$$

so

$$(59)\qquad E^i(\bar{\rho}_m) = \frac{k\eta}{4}\sum_{n=1}^{N} F_n \int_{DC_n} H_o^{(2)}(k|\bar{\rho}_m-\bar{\rho}'|)\, d\ell'$$

which is the same as the NXN matrix form

$$(60)\qquad [C]\,[F] = [E]$$

where

$$(61)\qquad C_{mn} = \frac{k\eta}{4}\int_{DC_n} H_o^{(2)}(k|\bar{\rho}_m-\bar{\rho}'|)\, d\ell',$$

$$E_m = E_z^i(\bar{\rho}_m) \tag{62}$$

and F_n is the unknown amplitude and phase of the current in the n-th contour segment. Once Eq. (60) is solved, the surface current is known.

The far field scattering from the surface is found from the surface currents and Eq. (52) to be

$$E_z^s(\bar{\rho}) = \frac{k\eta}{4}\sqrt{\frac{2}{\pi k}}\, e^{k\frac{5\pi}{4}}\, \frac{e^{-jk|\bar{\rho}|}}{\sqrt{|\bar{\rho}|}} \int_{-EP}^{EP} J_z(\bar{\rho}')\, e^{jk(\bar{\rho}'\cdot\hat{\rho})}\, d\ell' \tag{63}$$

$$\cong \frac{k\eta}{4}\sqrt{\frac{2}{\pi k}}\, e^{j\frac{5\pi}{4}}\, \frac{e^{-jk|\bar{\rho}|}}{\sqrt{|\bar{\rho}|}} \int_{-EP}^{EP} \sum_{n=1}^{N} F_n\, P_{\frac{pc}{2}}(\bar{\rho}'-\bar{\rho}_n)\, e^{jk(\bar{\rho}'\cdot\hat{\rho})}\, d\ell'$$

$$\cong \frac{k\eta}{4}\sqrt{\frac{2}{\pi k}}\, e^{j\frac{5\pi}{4}}\, \frac{e^{-jk|\bar{\rho}|}}{\sqrt{|\bar{\rho}|}}\, DC \sum_{n=1}^{N} F_n\, e^{jk(\bar{\rho}'\cdot\hat{\rho})} .$$

The output of the computer programs is a normalized scattered field, E_z^s, which is related to the true scattered field, Eq. (63), by

$$E_z^s = E_z^s(\bar{\rho})\sqrt{|\bar{\rho}|}\, e^{jk|\bar{\rho}|} . \tag{64}$$

C. Discussion of the Computer Program for Transverse Magnetic Polarization

Several different programs were written using the above formulation of the problem. In the first part of this section the common

features of the programs will be discussed and later their differences and relative merits.

All of the T.M.I.E. (transverse magnetic integral equation) programs require that the surface have its arclength subdivided into segments of width DC, and have the endpoints and midpoints of these segments stored. The surface breakdown is shown in Fig. 16. The

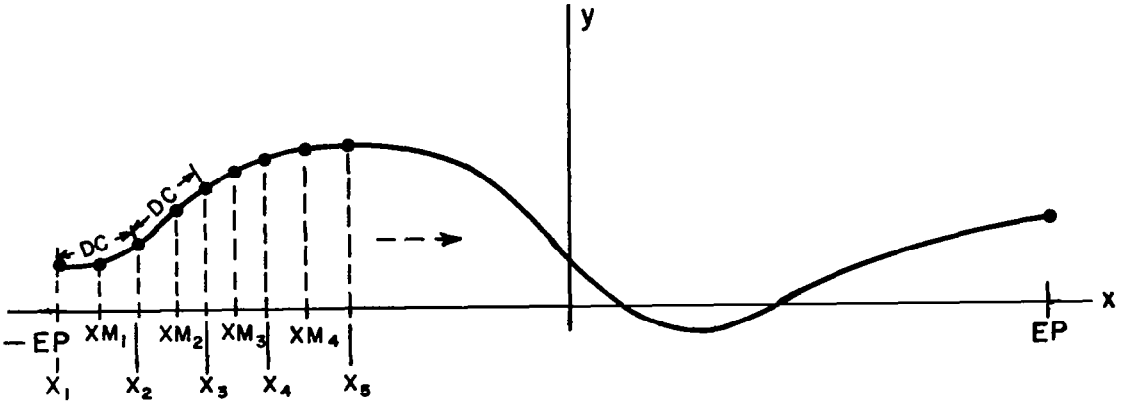

Fig. 16.--Breakdown of surface into segments of length DC.

j-th segment lies between x_j and x_{j+1}, while the j-th midpoint (XM_j) is such that $X_j<XM_j<X_{j+1}$. The surface is segmented by using the arclength formula and rectangular rule integration. After the surface subdivision is completed the programs differ somewhat depending on how the matrix elements are calculated.

Once the matrix elements have been calculated the first part of a two part solution of the system of equations begins. In all of the solution methods used the matrix is factored into an upper

and a lower triangular matrix, see Appendix B. The matrix elements depend only upon the surface profile H(x), and are independent of the incident field, THI or THS so that the factorization need be done only once for a given profile. In the second part of the solution the array [F] is loaded with the tapered incident electric field at each of the XM_j; the back substitutions (described in Appendix B) are then carried out to find the current coefficients, F_n. The scattered fields are then calculated from Eqs. (63) and (64).

The differences in the several programs for the T.M.I.E. lie mainly in the calculation of the matrix elements (Eq. (61)). The simplest way to evaluate Eq. (61) for $m \neq n$ is to presume that $H_o^{(2)}(k|\bar{\rho}_m - \bar{\rho}'|)$ is constant over the n-th interval; then

$$(65) \qquad C_{mn} \cong \frac{k\eta}{4} H_o^{(2)}(k|\bar{\rho}_m - \bar{\rho}_n|)\ DC$$

If $m=n$, a small argument approximation to $H_o^{(2)}(X)$ is made and integrated analytically, giving

$$(66) \qquad C_{mm} \cong \frac{k\eta}{4} DC\ H_o^{(2)}\left(\frac{k\ DC}{2\ e}\right)$$

where e is the base of the natural logarithm. In practice the matrix elements are simply the Hankel function and the $\frac{k\eta}{4} \cdot DC$ is accounted for when the fields are printed out. This approximation results in a symmetric matrix which, if efficiently stored, requires

only N(N+1)/2 storage locations. The length of surface which can be treated is increased by a factor of $\sqrt{2}$ over that which can be treated by methods requiring the storage of the full matrix. Appendix B gives the details of the storage and solution methods.

In another program, 5 point Gaussian integration, Ref. [25], is used to evaluate the C_{mn} for $m \neq n$, and when $m=n$ Eq. (66) is used. The matrix is no longer symmetric so all N^2 terms must be stored.

A third program was written which takes advantage of the fact that the currents are continuous on the surface except at sharp edges (Ref. [26]). Since the column vector [F] of Eq. (60) represents the current, continuity requires that adjacent entries be similar. Hence it is possible to interpolate. The currents at the even numbered stations may be approximated in terms of the adjacent currents by

$$F_{2n} = (F_{2n-1} + F_{2n+1})/2. \tag{67}$$

For simplicity, the original matrix will be assumed to be of odd order

$$N = 2\,kk + 1. \tag{68}$$

If, for example, N=7 then, using Eq. (67) in Eq. (60), one obtains the reduced system

$$E_1 = C_{11}F_1 + \frac{C_{12}}{2}(F_1+F_3) + C_{13}F_3 + \frac{C_{14}}{2}(F_3+F_5) + C_{15}F_5 + \frac{C_{16}}{2}(F_5+F_7) + C_{17}F_7$$

$$E_3 = C_{31}F_1 + \frac{C_{32}}{2}(F_1+F_3) + C_{33}F_3 + \frac{C_{34}}{2}(F_3+F_5) + C_{35}F_5 + \frac{C_{36}}{2}(F_5+F_7) + C_{37}F_7$$

(69)

$$E_5 = C_{51}F_1 + \frac{C_{52}}{2}(F_1+F_3) + C_{53}F_3 + \frac{C_{54}}{2}(F_3+F_5) + C_{55}F_5 + \frac{C_{56}}{2}(F_5+F_7) + C_{57}F_7$$

$$E_7 = C_{71}F_1 + \frac{C_{72}}{2}(F_1+F_3) + C_{73}F_3 + \frac{C_{74}}{2}(F_3+F_5) + C_{75}F_5 + \frac{C_{76}}{2}(F_5+F_7) + C_{77}F_7$$

where only odd rows have been retained, i.e., F_2, F_4, F_6 are considered known. Collecting terms,

$$(70)\quad E_k = (C_{k1} + \frac{C_{K2}}{2})F_1 + (\frac{C_{k2}}{2} + C_{k3} + \frac{C_{k4}}{2})F_3 + (\frac{C_{k4}}{2} + C_{k5} + \frac{C_{k6}}{2})F_5 + (\frac{C_{k6}}{2} + C_{k7})F_7$$

for $k = 1,3,5,7,$

and the number of unknowns has been reduced to kk. Since matrix manipulations are made using regular subscripts in the machine, it is very desirable to relabel the coefficients in the reduced system as follows

$$(71)\qquad C'_{mi} = \frac{C_{(2m-1),(2i-2)}}{2} + C_{(2m-1),(2i-1)} + \frac{C_{(2m-1),(2i)}}{2}$$

for the "interior" columns where $m=1,2,3,\cdots,kk$ and $i=2,3,\cdots,kk-1$. The first and last columns of the reduced matrix are

$$(72)\qquad C'_{m2} = C_{(2m-1),1} + \frac{C_{(2m-1),2}}{2} \qquad m=1,2,3,\cdots,kk$$

$$(73) \qquad C'_{m,kk} = \frac{C_{(2m-1),(2kk-2)}}{2} + C_{(2m-1),(2kk-1)}.$$

The C_{ij} are the elements of the original NXN matrix while C'_{ij} are elements of the kkXkk reduced matrix. In the computer program the C'_{ij} are called C_{ij} while the original matrix elements C_{ij} are labeled CO_{ij}.

When using the interpolation technique the surface is subdivided as usual except that, if an even number of segments is produced, then the last segment is dropped to make N odd. The system of equations is now

$$(74) \qquad [C][FP] = [E]$$

where [E] is filled with the incident electric field at the midpoints of the segments with odd subscripts and the matrix [C] is loaded according to Eqs. (71), (72) and (73). After the solution has been found the column vector FP(J) contains the currents on the segments with odd subscripts. The complete set of surface currents [F] is obtained by interpolation with

$$(75) \qquad \begin{aligned} F_{2j-1} &= FP_j && \text{for } j = 1,2,\cdots,kk \\ F_{2j} &= (FP_j + FP_{j+1})/2 && \text{for } j = 1,2,\cdots,kk-1. \end{aligned}$$

Once the column vector [F] has been filled in, the calculation of the scattered field proceeds as in Eqs. (63) and (64). The interpolation technique has been applied to the program which uses Gaussian integration to calculate the matrix elements.

The big advantage of interpolation is the dramatic increase in the size of the surface which can be handled for a given storage capacity. If the machine can handle an arclength of L using the non-symmetric, non-interpolation program then the symmetric matrix program can handle an arclength of $\sqrt{2}$ L while the interpolation technique will do an arclength of 2 L with the same amount of storage. The interpolation program still requires that all of the original matrix elements be evaluated to fill in the reduced matrix (Eqs. (71), (72) and (73)).

The integral equation programs require large amounts of storage and fairly long running times compared to either the G.O. or P.O. programs. The IBM 360-75 used here can hold a 275 x 275 complex matrix in high speed storage so that surfaces of length 27 λ_e, or 54 λ_e if interpolation is used, can be handled with DC = $\lambda_e/10$. As for the running time, consider the 16 λ_e long surface mentioned in Chapter III Section C, which took 1.8 minutes using the P.O. program. The scattering from the same surface was computed by the three T.M. integral equation methods. The symmetric formulation required 2.8 minutes and storage for 14,000 complex numbers. The program which uses Gaussian integration to evaluate the matrix coefficients required 5.0 minutes and twice as much storage,while the interpolation program required 3.3 minutes and storage for 7,000 complex numbers. Where speed is important the use of the symmetric I.E. program is indicated, while long surfaces are best handled by the two point interpolation program.

D. Tests of the Transverse Magnetic Integral Equation Programs

The shortened contour assumption is one of the most crucial in the construction of the integral equation programs (Fig. 14). The obvious way to test it is to extend the non-illuminated portion of the surface, which amounts to lengthening the contour without changing the non-zero portion of the illumination (see Fig. 17). If the approximation is indeed valid, then the current in the non-illuminated sections should fall off rapidly and the scattered fields should be the same in both cases. The assumption was tested on a sinusoidal surface, using the program with Gaussian integration. When regular tapering was used, the current at the outer ends of the dead zones was down by a factor of 30 from that in the central part of the contour. When the extended taper was used, the current at the new outer ends was down by a factor of 100. The scattered fields for the two cases are displayed in Fig. 18 and show clearly that the differences are insignificant. Thus it may be concluded that tapering of the incident field does permit the replacement of the true contour by the shortened contour.

The wedge, Fig. 19, for which asymptotic solutions are available, provides a test case for the integral equation programs. The angle of incidence, THI, was chosen to be 90°. In order to emphasize the corner contribution, a Gaussian tapering of the incident field was used, i.e.,

$$t(X) = e^{-(x/2\lambda_e)^2} . \tag{76}$$

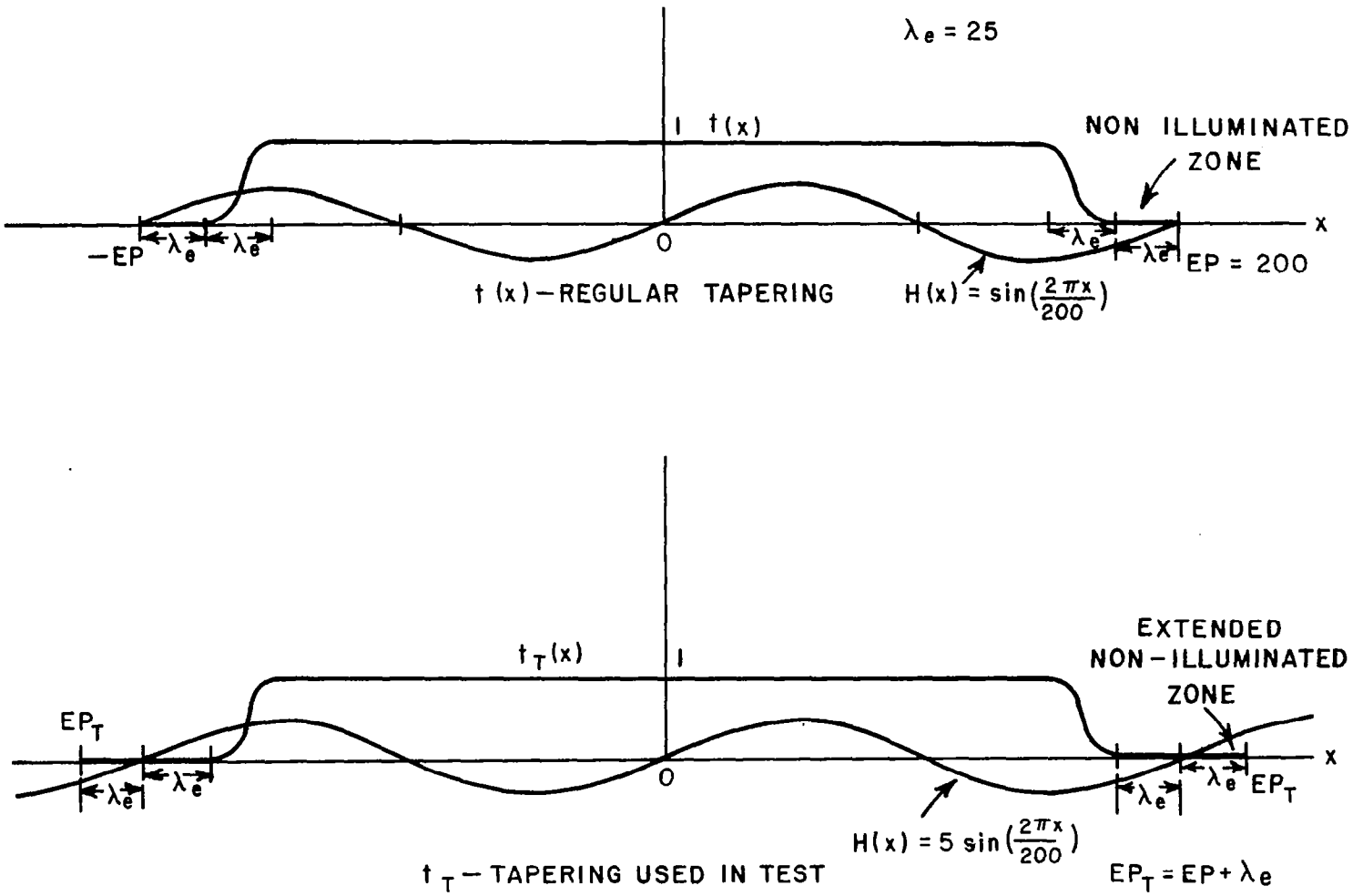

Fig.17.--Contour and tapering function used to test the shortened contour assumption.

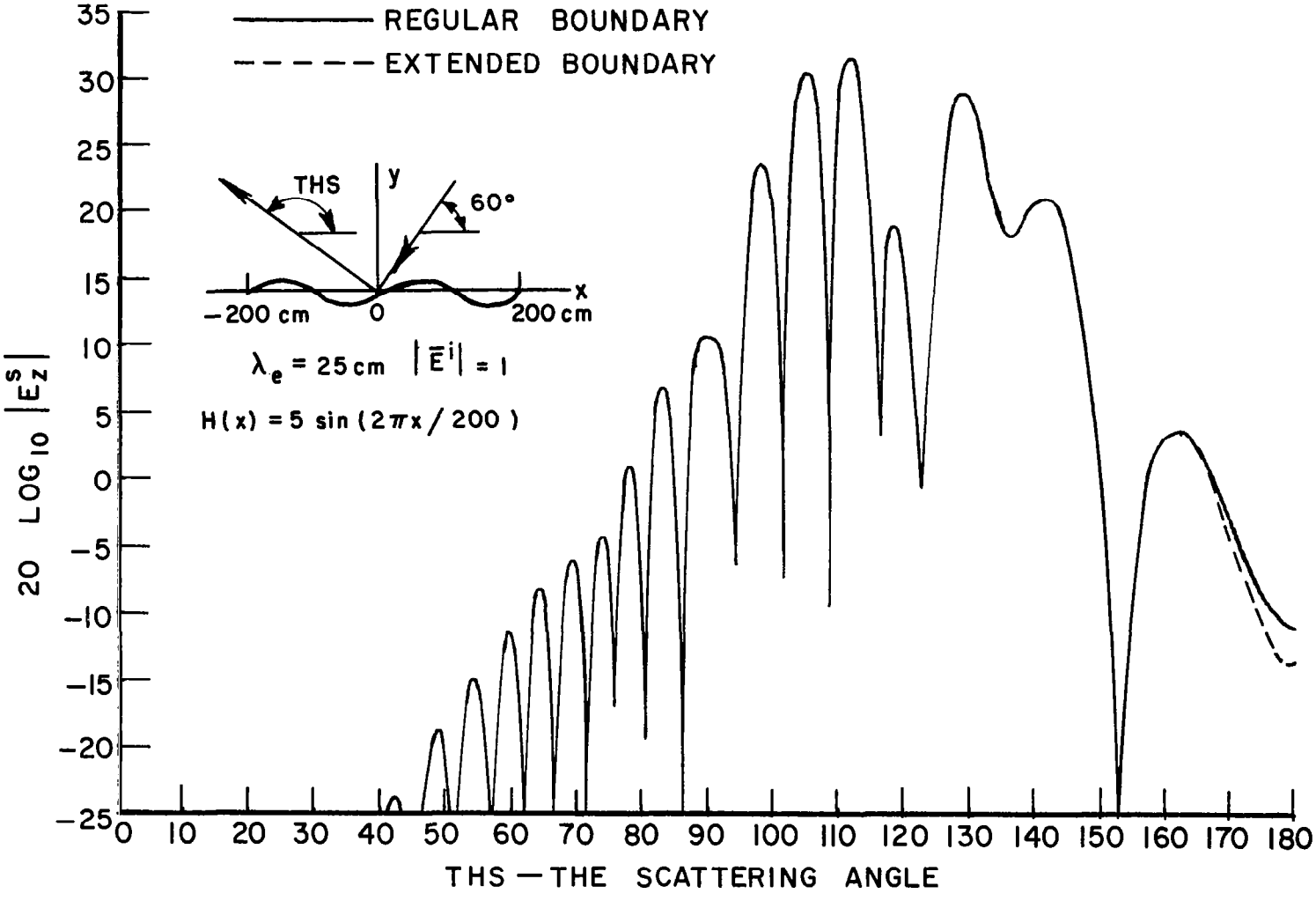

Fig. 18.--Scattered fields with and without extended boundaries, T.M. case.

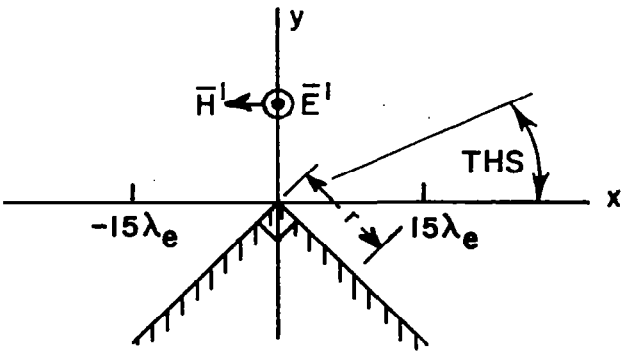

Fig. 19.--Geometry for wedge test.

The surface current, Fig. 20, shows the expected singularity at the corner. The computed scattered field is plotted in Fig. 21 along with the scattered field calculated independently using the geometrical theory of diffraction, Ref. [27]. Again, the agreement is seen to be excellent. All three T.M. integral equation programs produced essentially identical scattered fields. In a test of the self consistency of the three programs the scattering from the surface $H(X) = 5 \sin \frac{2\pi}{200} x$ was computed. The differences in the scattered fields are very minor and would not be perceptible on the scale of, e.g., Fig. 18.

In the light of the above tests, there seems to be no reason to prefer one T.M. integral equation program over the other two if numerical accuracy is the only criterion. If the running time or storage requirements must be considered then the preferred formulation can be determined by the comments at the end of Section C of this Chapter.

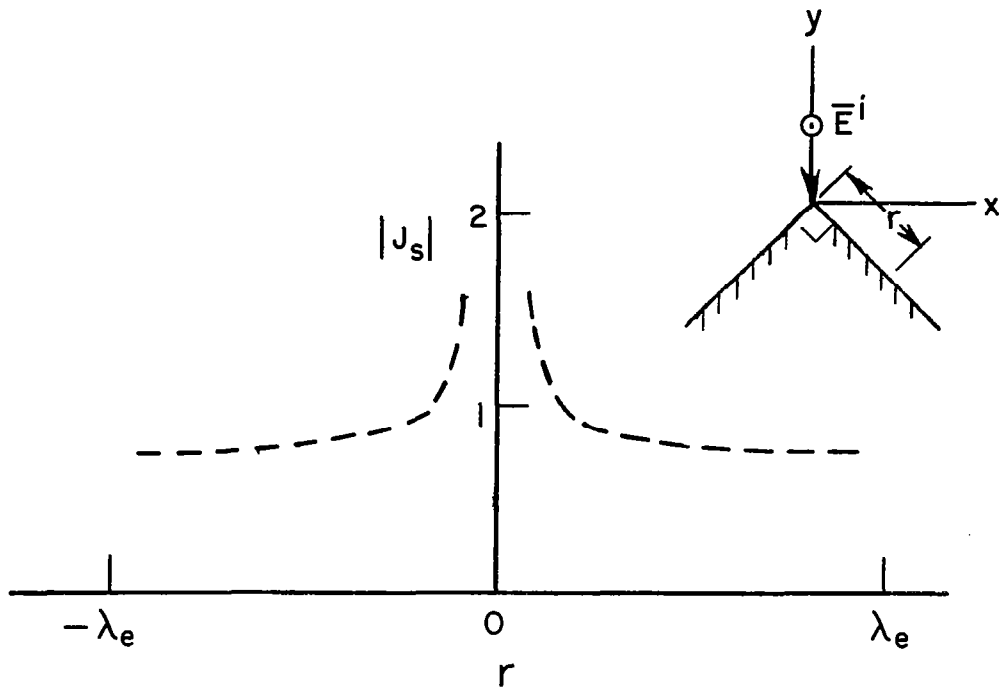

Fig. 20.--Computed $|J_s|$ on a wedge, T.M. case.

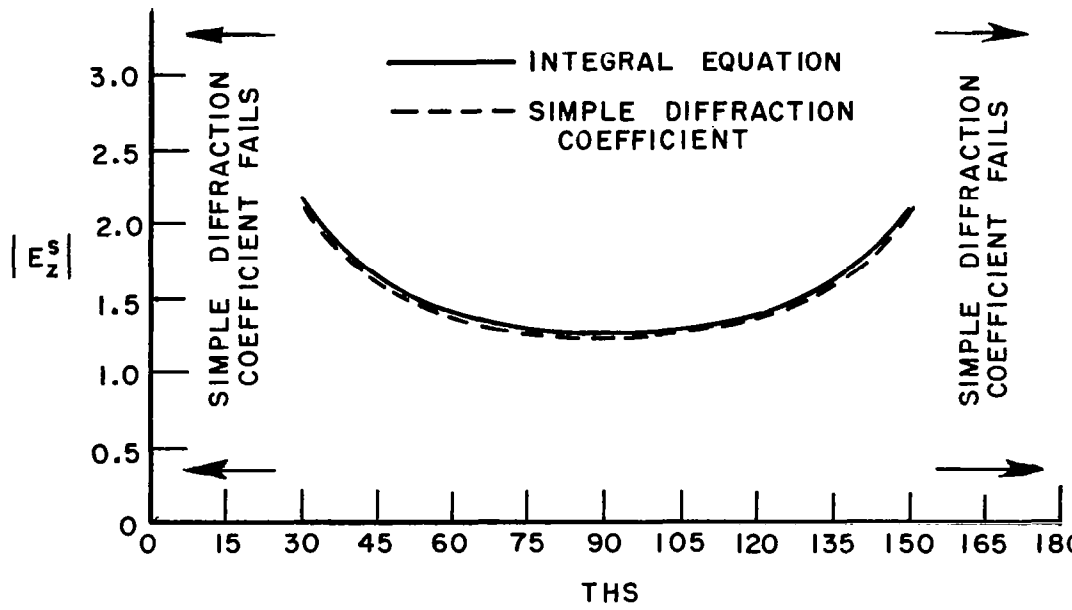

Fig. 21.-- Wedge scattered fields, T.M. case

E. Integral Equation for Transverse Electric Polarization

For the T.E. polarization, the incident magnetic field $\overline{H}^i$ is $\hat{z}$ directed and it will be convenient to work with the integral equation for the magnetic field given (Ref. [28]) by

$$(77) \qquad \overline{J}_s(\overline{r}) = 2\,\hat{n} \times \overline{H}^i(\overline{r}) + \frac{1}{2\pi}\,\hat{n}(\overline{r}) \times \int_s \overline{J}_s(\overline{r}') \times \overline{\nabla}' \frac{e^{-jk|\overline{r}-\overline{r}'|}}{|\overline{r}-\overline{r}'|}\,ds$$

where $\overline{r}$, $\overline{r}'$ are both position vectors of points on the surface, $\overline{H}^i(\overline{r})$ is the incident magnetic field, $\overline{J}_s(\overline{r})$ is the surface current, $\hat{n}$ is the outward normal to the surface and $\int$ indicates that the region about $\overline{r}' = \overline{r}$ is to be deleted from the integration. See Fig. 22.

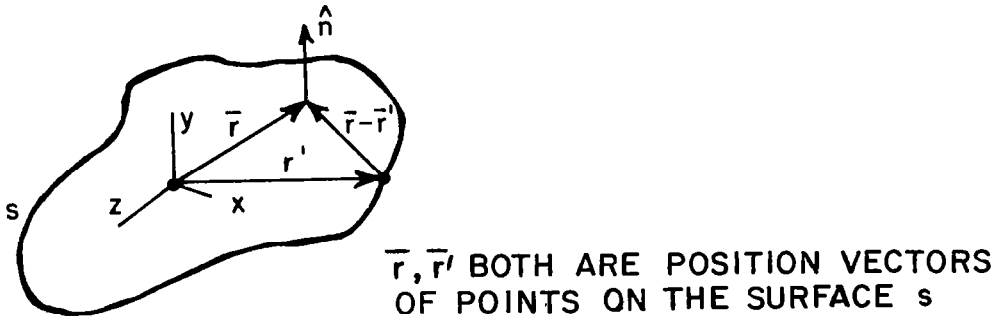

Fig. 22.--Three dimensional geometry for T.E. integral equation.

The two dimensional integral equation can be obtained by considering an infinitely long cylinder as shown in Fig. 23. When the incidence direction lies in the x,y plane the fields and surface current have no z dependence so that Eq. (77) can be reduced to

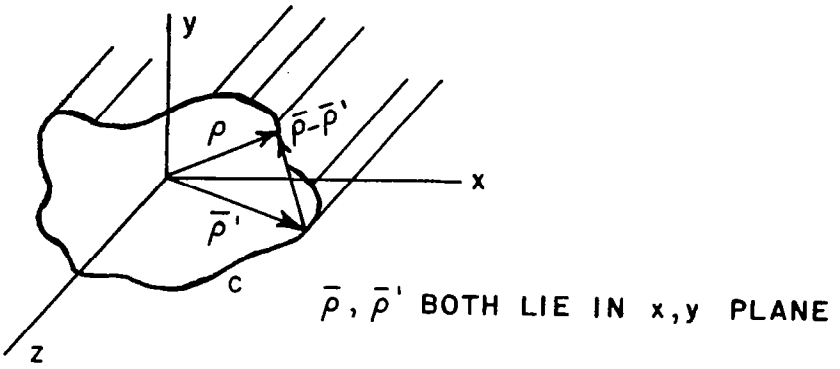

Fig. 23.--Two dimensional geometry for T.E. integral equation.

$$(78) \qquad \bar{J}_s(\bar{\rho}) = 2\,\hat{n}(\bar{\rho}) \times \bar{H}^i(\bar{\rho}) + \frac{k}{2j}\,\hat{n}(\bar{\rho}) \times \int_C \bar{J}_s(\bar{\rho}') \times (\hat{\bar{\rho}-\bar{\rho}'})\, H_1^{(2)}(k|\bar{\rho}-\bar{\rho}'|)\, dc'$$

where $(\hat{\bar{\rho}-\bar{\rho}'})$ is the unit vector in the $\bar{\rho}-\bar{\rho}'$ direction and $H_1^{(2)}(x)$ is the Hankel function of the second kind and order 1.

Just as in the T.M. case, tapering is introduced to account for the directional properties of radar antennas, and to limit the size of the system of linear equations which will result from Eq. (78). One may now assume that the surface currents are zero except near the illuminated region and the closed contour can then

be replaced by the open contour of Fig. 24. For this polarization the current flows transverse to $\hat{z}$ along the surface so

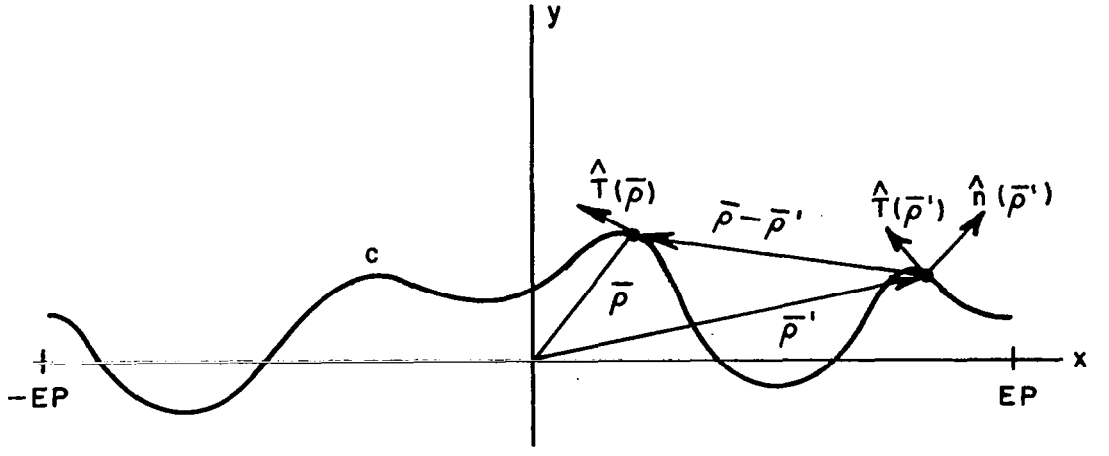

Fig. 24.--Open contour.

$$(79) \qquad \bar{J}_s(\bar{\rho}') = (\hat{z} \times \hat{n}(\bar{\rho}'))\, J_s(\bar{\rho}') = \hat{T}(\bar{\rho}')\, J_s(\bar{\rho}')$$

where $\hat{T}(\bar{\rho}')$ and $\hat{n}(\bar{\rho}')$ are the unit tangent vector and the unit normal vector to the surface, as shown in Fig. 24. $\hat{T}(\bar{\rho}')$ is given in terms of the profile, H(x), by

$$(80) \qquad \hat{T}(\bar{\rho}') = -\frac{[\hat{x} + \dot{H}(x')\hat{y}]}{\sqrt{1 + (\dot{H}(x'))^2}}$$

where $\dot{H}$ has the meaning assigned by Eq. (34). Using

$$(81) \qquad dc' = (1 + (\dot{H}(x'))^2)^{1/2}\, dx'$$

and Eqs. (78) and (79) with the tapered incident field

$$(82) \qquad H_z^i(\bar{\rho}) = t(x)\, e^{-j\bar{k}_i \cdot \bar{\rho}}$$

the integral equation becomes

$$(83) \qquad -t(x)\, e^{j\bar{k}_i \cdot \bar{\rho}} = \frac{J_s(\bar{\rho})}{2} + \frac{jk}{4} \int_{-EP}^{EP} \frac{J_s(\bar{\rho}') H_1^{(2)}(k|\bar{\rho}-\bar{\rho}'|)}{\sqrt{(x-x')^2+(H(x)-H(x'))^2}} \cdot [(H(x)-H(x'))-\dot{H}(x)(x-x')]\, dx'$$

where the integration over x' excludes a small region in the contour about the point described by $\bar{\rho}$.

The method of moments is applied to Eqs. (83) just as in the T.M. case. the current is expanded in a basis of non-overlapping pulse functions of width DC, delta functions are used as weighting functions and the scalar product is the same as in the T.M. case. The current is thus represented by

$$(84) \qquad J_s(\bar{\rho}') = \sum_{n=1}^{N} F_n\, P_{\frac{DC}{2}}\, (\bar{\rho}'-\bar{\rho}_n)$$

where, $\bar{\rho}'$, $\bar{\rho}_n$ lie on the contour c and $\bar{\rho}_n$ is the position vector of the midpoint of the n-th segment, the F_n's are the unknown expansion coefficients and the pulse functions $P_{\frac{DC}{2}}(\bar{\rho}'-\bar{\rho}_n)$ have been described in connection with the T.M. case. Placing this current in Eq. (83), taking the scalar product of both sides with the weighting functions and using the non-overlapping property of the basis functions results in

$$(85)\qquad -t(x_m)\, e^{-j\bar{k}_i\cdot\bar{\rho}_m} = \frac{F_m}{2} + \frac{jk}{4}\sum_{n=1}^{N} F_n \int_{-EP}^{EP} P_{\frac{ge}{2}}(\bar{\rho}'-\bar{\rho}_n)H_1^{(2)}(k|\bar{\rho}_m-\bar{\rho}'|)\,\frac{[(H(x_m)-H(x'))-\dot{H}(x_m)(x_m-x')]}{\sqrt{(x_m-x')^2+(H(x_m)-H(x'))^2}}\,dx' .$$

Since it is necessary to avoid $\bar{\rho}' = \bar{\rho}_m$ in the integration of Eq. (85), the summation will be forced to skip n=m giving as a system of equations

$$(86)\qquad -t(x_m)\, e^{-j\bar{k}_i\cdot\bar{\rho}_m} = \sum_{n=1}^{N} C_{mn} F_n$$

where

$$(87)\quad C_{mn} = \begin{cases} \frac{1}{2} & \text{if } m=n \\ \frac{jk}{4}\int_{x_n}^{x_{n+1}} H_1^{(2)}(k|\bar{\rho}_m-\bar{\rho}'|)\,\frac{[(H(x_m)-H(x'))-\dot{H}(x_m)(x_m-x')]}{\sqrt{(x_m-x')^2+(H(x_m)-H(x'))^2}}\,dx' & \text{if } m\neq n \end{cases}$$

and x_{n+1}, x_n are the upper and lower x coordinates of the endpoints of the n-th surface segment respectively.

Once Eq. (86) is solved for the coefficients of the surface current, F_m, the scattered field may be found from Ref. [18]

$$\bar{H}^s(\bar{r}) = \frac{1}{4\pi} \int_s \bar{J}_s(\bar{r}') \times \bar{\nabla}' \frac{e^{-jk|\bar{r}-\bar{r}'|}}{|\bar{r}-\bar{r}'|} \, ds'. \tag{88}$$

Specializing this to the far field scattering from an infinite cylinder and using the fact that $\bar{J}_s(\bar{r}')$ is independent of z and non zero only over a portion of the cylinder (see Fig. 25).

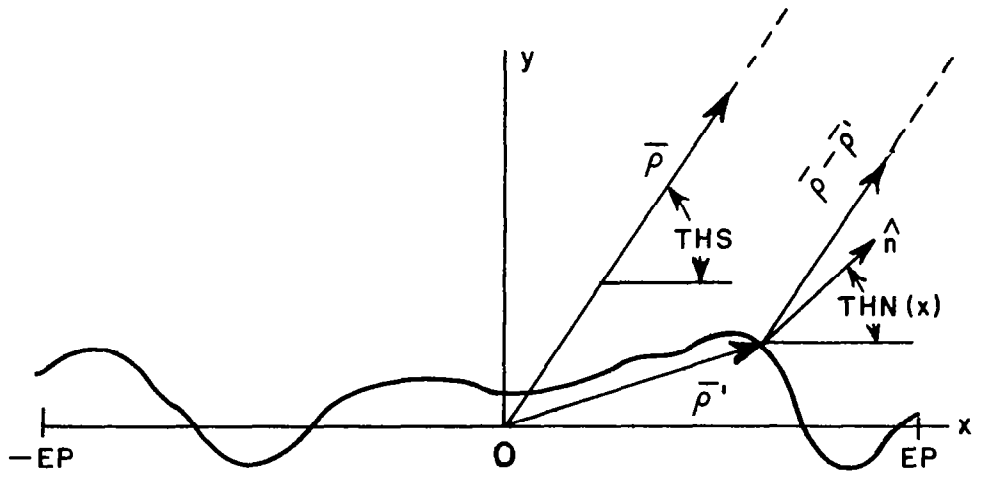

Fig. 25.--Geometry for calculation of far field scattering, T.E. case.

$$H_z^s(\bar{\rho}) = \frac{e^{-jk|\bar{\rho}|}}{\sqrt{|\bar{\rho}|}} \frac{j}{2} e^{j\frac{3\pi}{4}} \int_{-EP}^{EP} J_s(\bar{\rho}') \frac{[\sin(THS)-\dot{H}(x')\cos(THS]}{\sqrt{1+(\dot{H}(x'))^2}} \tag{89}$$

$$e^{jk(x'\cos(THS)+H(x')\sin(THS))} \, dc'$$

Substituting Eq. (84) whose coefficients are now known into Eq. (89) and assuming that the integrand is nearly constant over a surface segment of length DC,

$$(90) \qquad H_z^s(\bar{\rho}) = \frac{e^{-j\frac{3\pi}{4}}}{2\sqrt{\lambda}} \, DC \, \frac{e^{-jk|\bar{\rho}|}}{\sqrt{|\bar{\rho}|}} \sum_{n=1}^{N} F_n \cos(THS-THN(XM_n)) \cdot e^{jk(XM_n\cos(THS)+H(XM_n)\sin(THS))}$$

where THN(x) (THETA NORMAL) is given by

$$(91) \qquad THN(x) = (\pi/2) + \tan^{-1}(\dot{H}(x))$$

as shown in Fig. 25. The computed and plotted value of the scattered field, H_z^s, is given by

$$(92) \qquad H_z^s = H_z^s(\bar{\rho}) \sqrt{|\bar{\rho}|} e^{+jk|\bar{\rho}|} \, .$$

F. Discussion of the Computer Program for the Transverse Electric Polarization

The programs for the T.E. polarization are very similar to those for the T.M. polarization. As in the T.M. case the contour is broken up into segments of equal length DC. The same notation is used for the endpoints (x) and midpoints (XM) of the segments (Fig. 16). The T.E. and T.M. programs differ mainly in the values of the elements of the matrix [C], and in the driving side of the system of equations.

Also, for the integral equation used, the matrix is non-symmetric no matter how the coefficients are evaluated. Once again the system of equations, (Eq. (86)), is solved in such a way that different scattering and incidence angles do not require a completely new solution. Only the back substitution portion need be repeated (see Appendix B).

Several different programs have been written for the T.E. case, the major difference between them being the method used to evaluate the coefficients (Eq. (87)). The simplest way is to assume that the integrand is constant over the strip width so that

$$(93) \qquad C_{mn} = \begin{cases} \frac{1}{2} & \text{if } m=n \\ \frac{jk}{4}(DC)\,\frac{H_1^{(2)}(k|\bar{\rho}_m-\bar{\rho}_n|)}{|\bar{\rho}_m-\bar{\rho}_n|}\,[(H(XM_m)-H(XM_n))-\dot{H}(XM_m)(XM_m-XM_n)] & \text{if } m\neq n. \end{cases}$$

In practice, only the five point Gaussian integration was used to evaluate the off diagonal elements of [C], since it did not require much more running time than the simpler method. However, the interpolation technique retains all of its advantages and goes exactly as in the T.M. case with the C'_{ij} given by Eqs. (71), (72), and (73). Thus surface lengths of $27\lambda_e$ (or $54\lambda_e$ with interpolation) can be handled. As an example of the running times required, consider again the surface of length $16\lambda_e$ mentioned in Chapter 3 Section C. The T.E. physical optics program required 1.8 minutes while an equivalent run using the T.E. integral equation program required 5.0 minutes.

The interpolation program for this polarization took 3.5 minutes. Thus the interpolation program is superior to the non-interpolation program both with respect to storage requirement and running time.

G. Tests of the Transverse Electric Integral Equation Programes

The shortened contour assumption plays the same role and is tested in the same way in the T.E. integral equation programs as in the T.M. case. The contour is extended as shown in Fig. 17. When the regular tapering was used, the current at the outer ends of the dead zones was down by a factor of 70 from that in the central portion of the contour. When the extended surface was considered the current at the new outer ends was down by slightly more. The nearly identical scattered fields for the two cases are shown in Fig. 26.

The wedge provides a test case for which an independent result is available. The test geometry is as shown in Fig. 19 except that here the incident magnetic field is parallel to the corner of the wedge. Gaussian tapering of the incident field, Eq. (76), is used. In contrast to the current singularity in the T.M. case, the surface current in the T.E. case, Fig. 27, shows the expected $r^{2/3}$ behavior at the corner. The excellent agreement between the scattered fields calculated by the integral equation method and the fields obtained from the geometrical theory of diffraction, Ref. [27], is illustrated in Fig. 28. Both the non-interpolation and the interpolation T.E. integral equation programs gave the same result in this test.

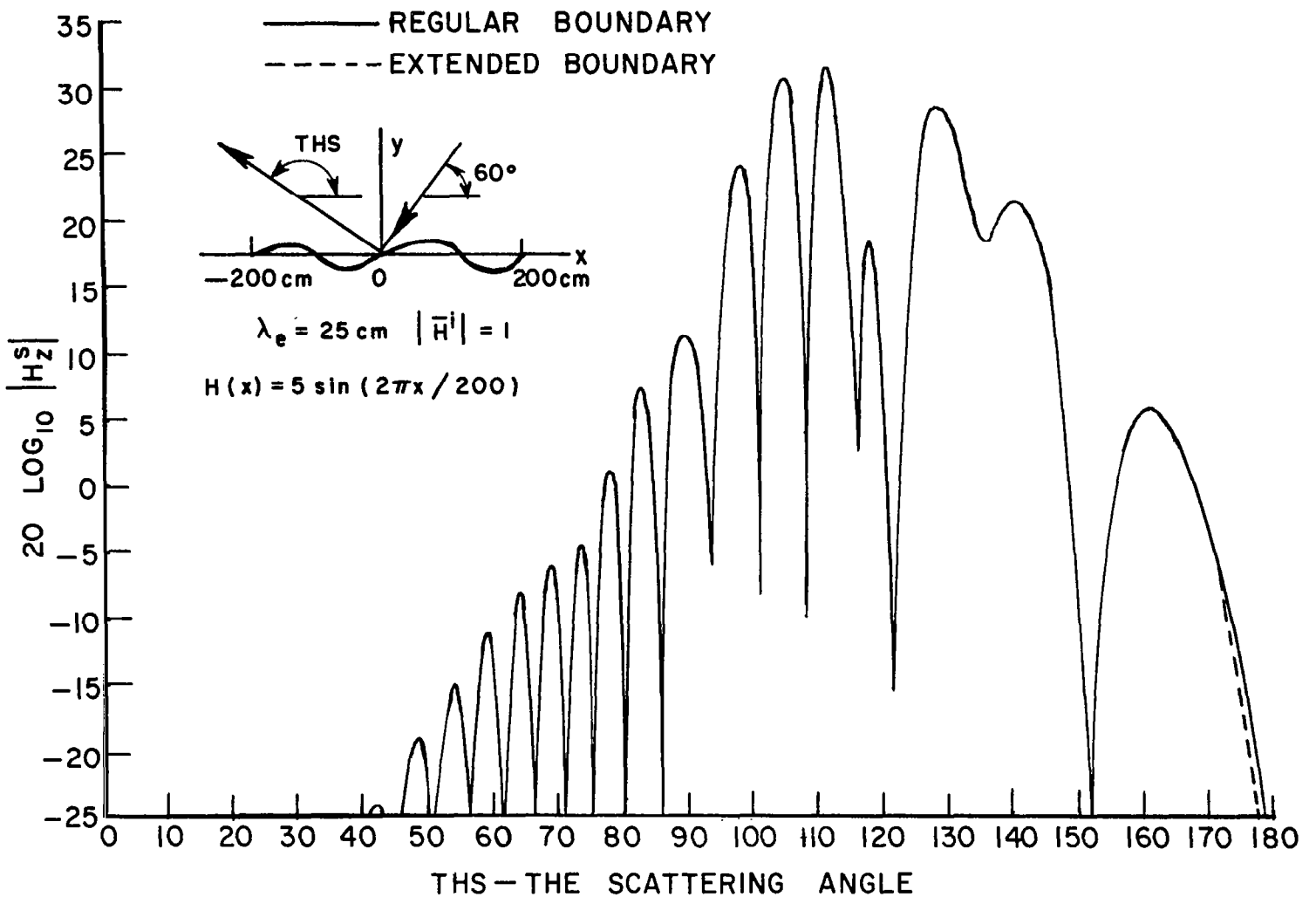

Fig. 26.--Scattered field with and without extended boundaries, T.E. case.

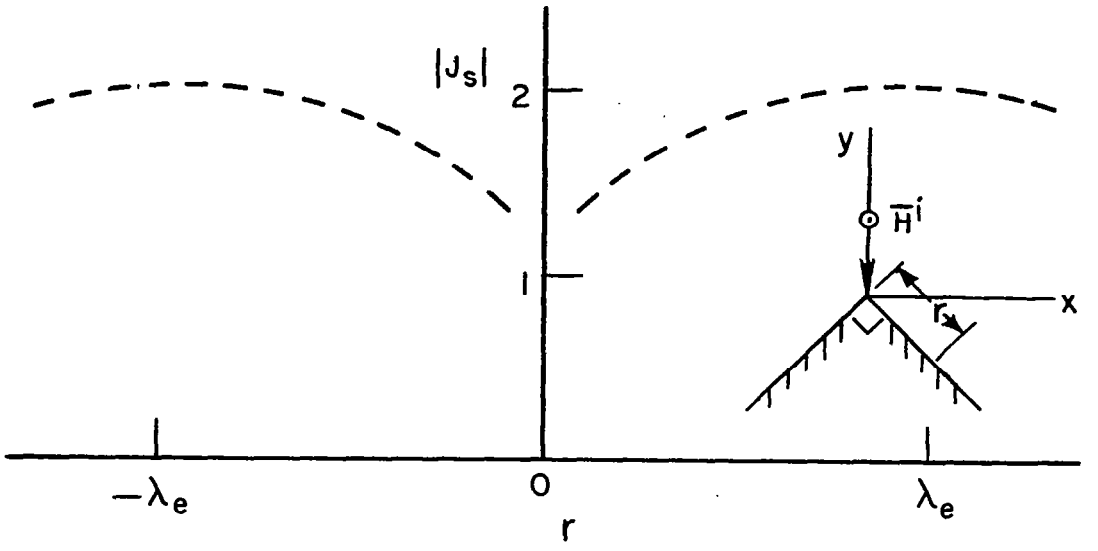

Fig. 27.--Computed $|J_s|$ near corner of wedge, T.E. case.

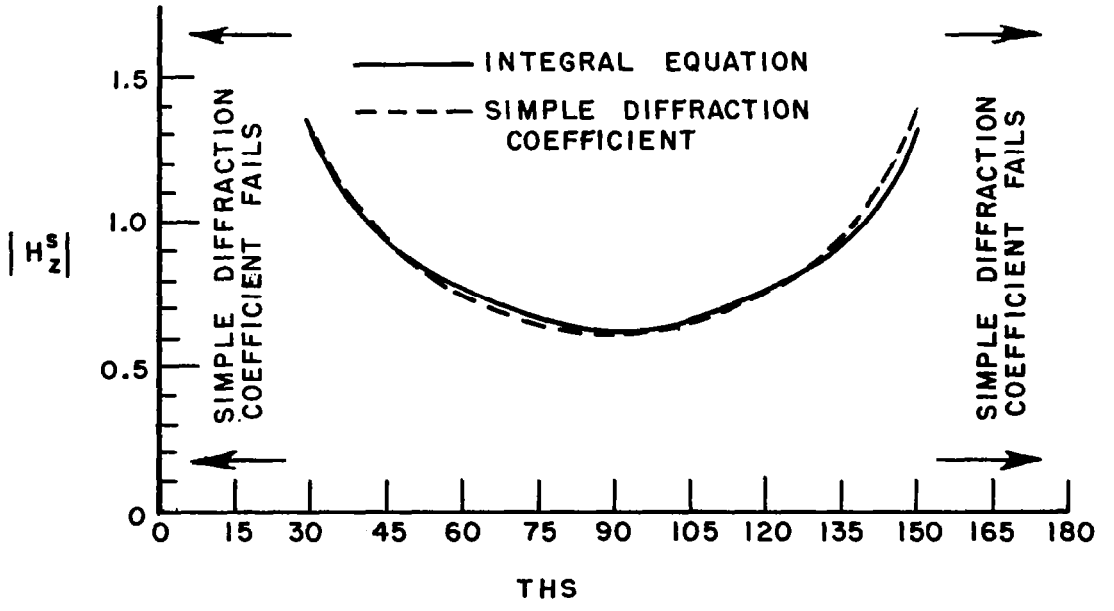

Fig. 28.--Wedge scattered fields, T.E. case.

The consistency of the two T.E. integral equation programs was checked on a surface with a height profile $H(x) = 5 \sin(2\pi x/200)$. The results were nearly identical.

The above tests indicate that so far as numerical accuracy is concerned the non-interpolation and interpolation T.E. integral equation programs do not differ. The interpolation program is preferred however because of the savings in storage.

CHAPTER V

APPLICATIONS

In this chapter the previously developed computer programs will be used to check the applicability of the geometrical optics, physical optics and perturbation approximations to the calculation of the scattering from non-uniform surfaces. The integral equation programs, which are believed to be exact, are used as standards.

The first surface to be considered has been especially chosen so that it fulfills the requirements necessary in order that physical and geometrical optics both give a valid approximation to the true scattered fields. The surface, a single half-cycle of a sine wave, has a profile $H(X) = 50 \cos(2\pi X/800)$ with x between 200.0 cm and -200.0 cm, and clearly has but one specular point. The incident field is tapered, and has an electrical wavelength of 25 cm. Unless otherwise noted, these conventions have been used throughout. The criteria for the successful application of G.O. and P.O. are met by this profile since the minimum radius of curvature is 12.8 λ_e and, having a maximum height of two λ_e, there are several Fresnel zones on the surface. The scattered fields predicted by the G.O., P.O. and I.E. programs are shown in Figs. 29 and 30 for the T.M. and T.E. polarizations respectively.

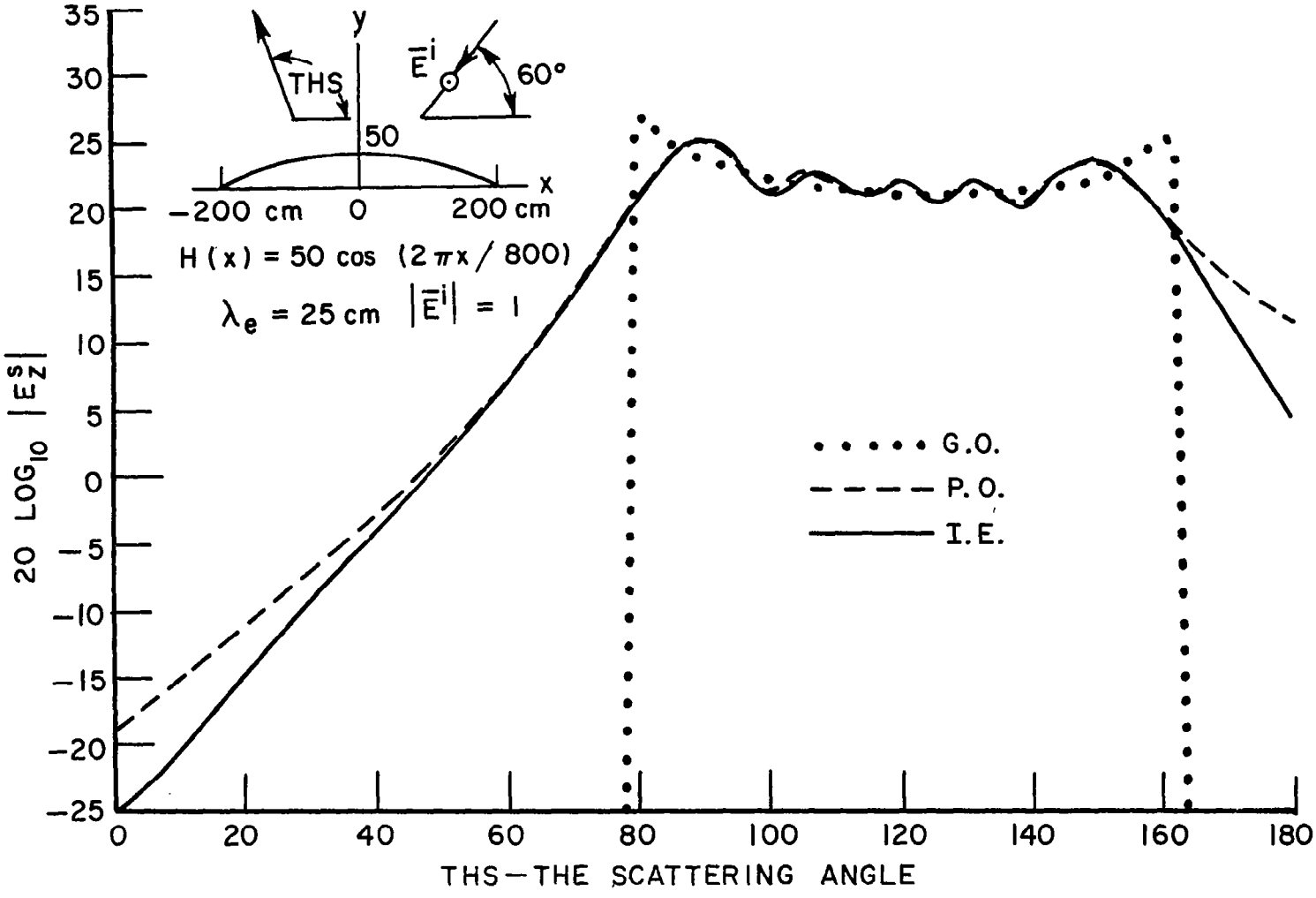

Fig. 29.--Scattering from 50 cos(2πx/800) as calculated by I.E., P.O., and G.O.; T.M. polarization.

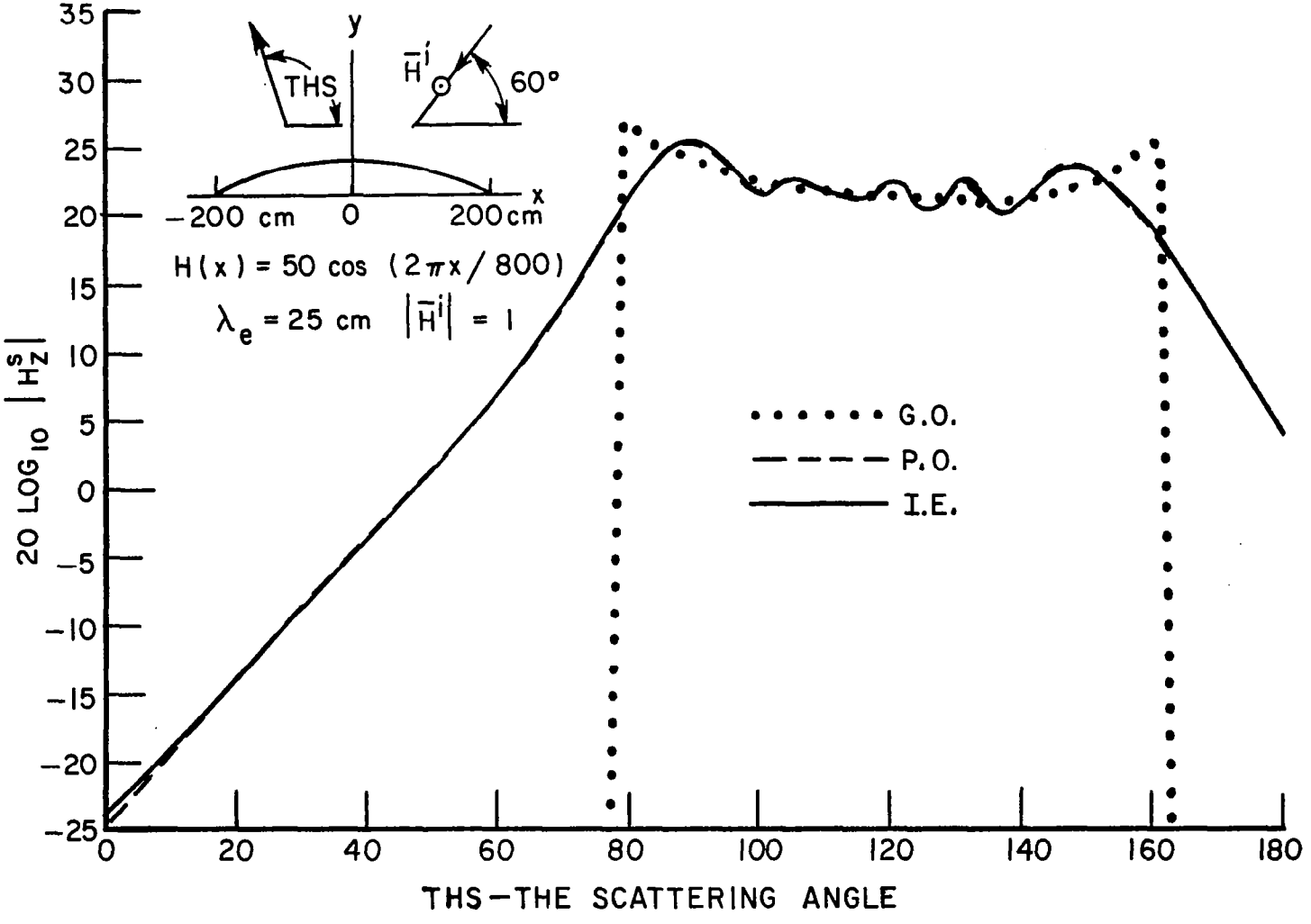

Fig. 30.--Scattering from 50 cos $2\pi x/800$ as calculated by I.E., P.O., and G.O.; T.E. polarization.

It is apparent that all methods give nearly the same result for THS between 87° and 155°. No scattered fields are predicted by G.O. for THS outside the range 78° and 163° since the normals to the surface have a limited range of directions as illustrated in Fig. 31. The

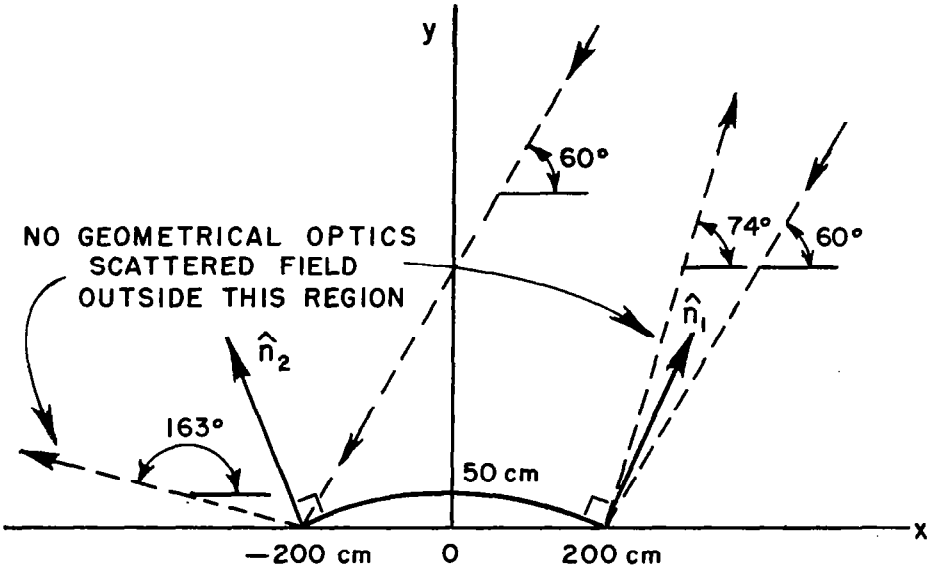

Fig. 31.--Limitation of scattering directions predicted by geometrical optics.

rise in the value of scattered field predicted by G.O. near 78° and 163° is due to the movement of the specular point into a region of the surface of increasing radius of curvature. However, as the specular point gets within two wavelengths of either endpoint the tapering of the incident field suppresses the expected singularity in the scattered field.

It should also be noted that for the P.O. results, the T.M. fields differ slightly from the correct fields for THS near grazing.

For either polarization the ripple observed in the scattered field and correctly predicted by P.O. is probably a consequence of the finite length of the surface. G.O., being a purely local theory, will not predict effects of this nature.

As a further check of the programs, the above profile was multiplied by minus one, i.e., instead of being concave down the surface was concave up. The amplitudes of the scattered fields remained unchanged but they all showed a phase shift of 90° due to what in G.O. theory is termed the caustic correction factor.

In order to establish more quantitatively the limitations on the G.O. and P.O. approximations, the scattered fields have been computed for a set of surfaces with height profile

$$H(X) = A \sin(2\pi X/200) \qquad -200 \text{ cm.} \leq x \leq 200 \text{ cm.}, \tag{94}$$

i.e., the surfaces are two complete mechanical wavelengths long. With THI fixed at 60°, the amplitude, A, was varied over a range of 5.0 cm. to 50.0 cm. so that the minimum radius of curvature, r_{cm}, varied from 8.0 λ_e to 0.8 λ_e. The important features of the scattered fields over this range of r_{cm} for each polarization are shown in Figs. 32-37 in order of decreasing r_{cm}. Some general trends are worthy of mention.

In the first place, as r_{cm}/λ_e decreases from 8 to 0.8, the agreement between the P.O. results and the exact fields goes from excellent to poor. It would appear that as long as the surface always has r_{cm}/λ_e greater than, say, 2.5, the P.O. approximation will

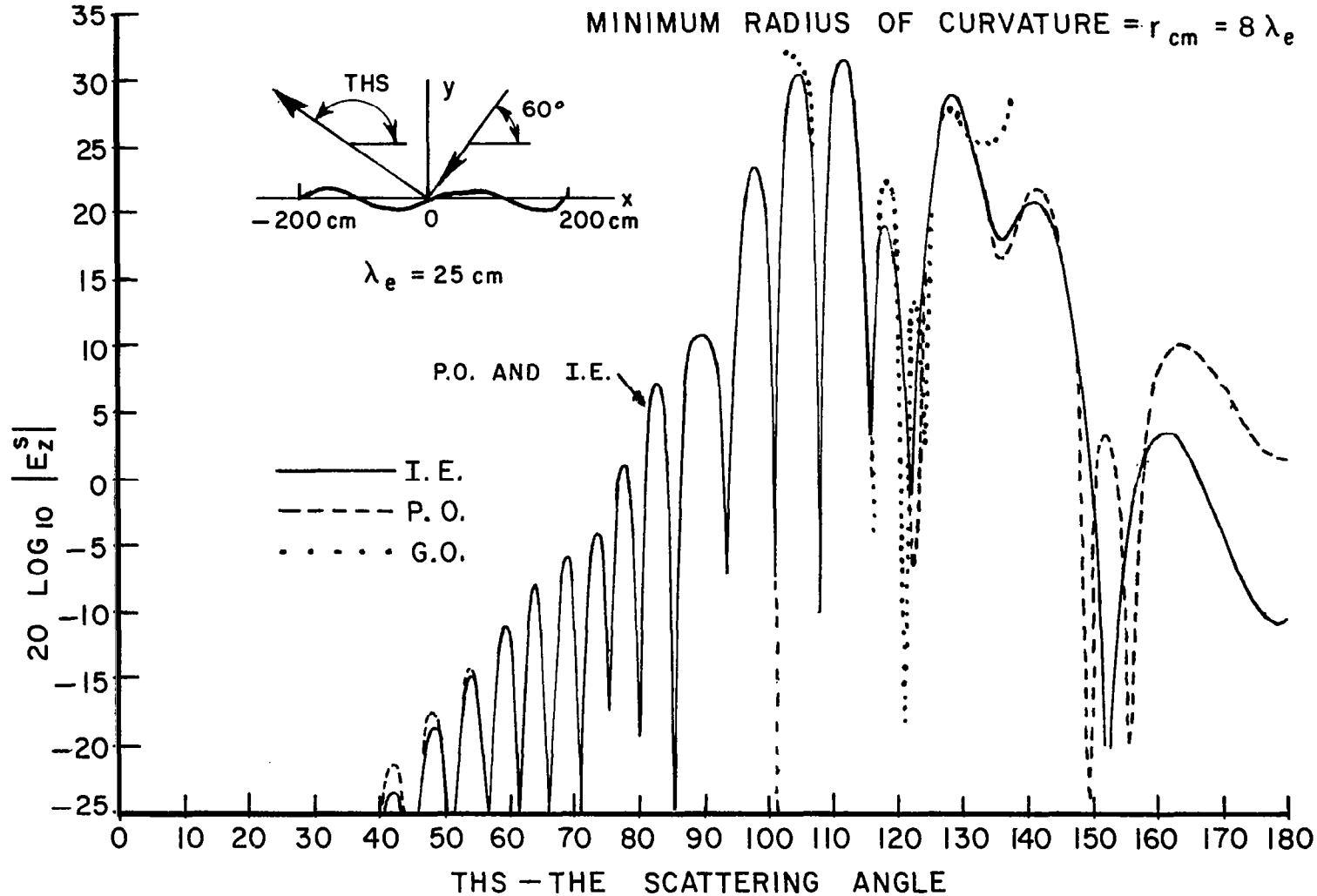

Fig. 32.--Scattered fields predicted by P.O., G.O., and I.E. methods for H(x)= 5 sin(2πx/200), T.M. polarization

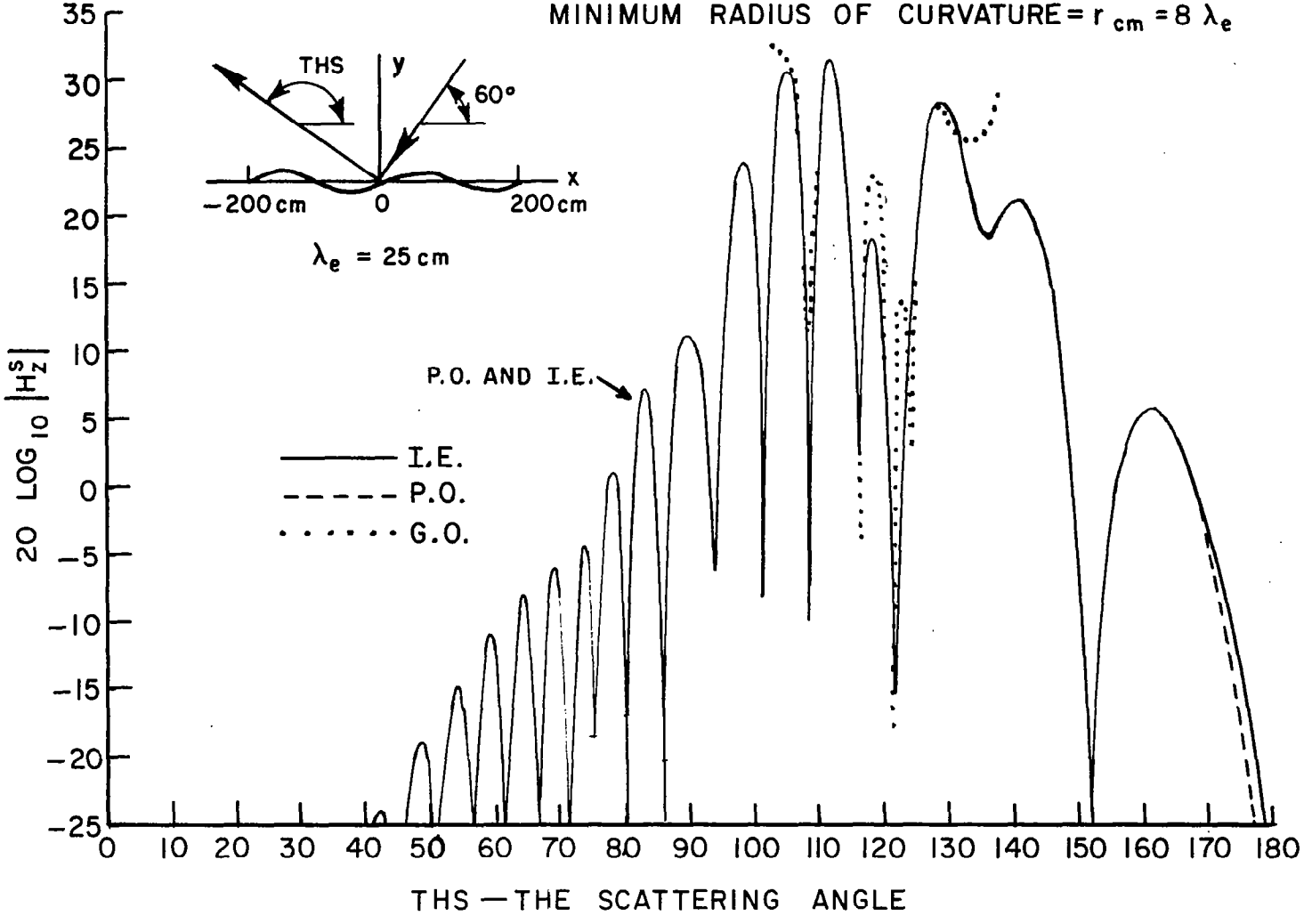

Fig. 33.--Scattered fields predicted by P.O., G.O., and I.E. methods for H(x)= 5 sin(2πx/200), T.E. polarization

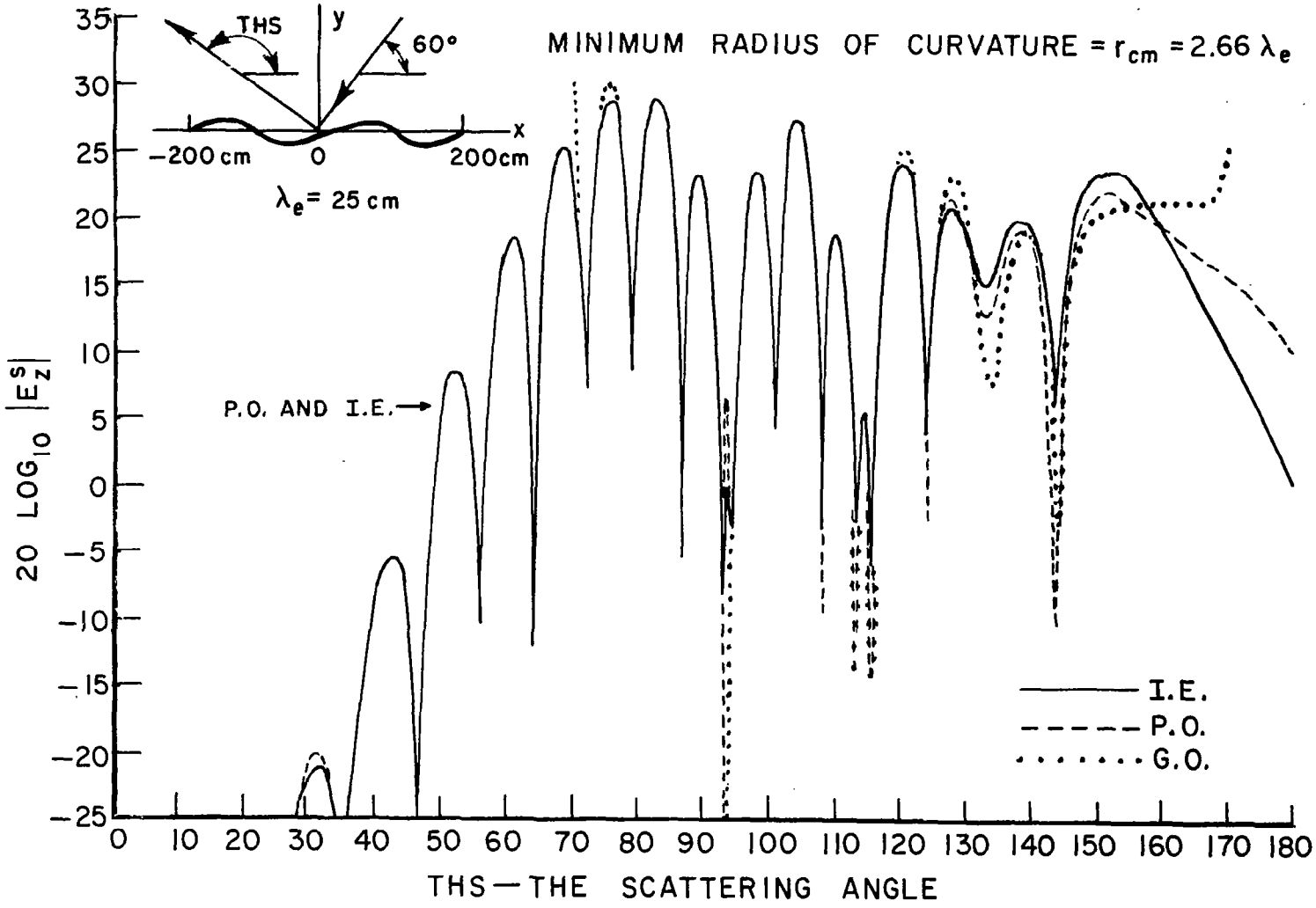

Fig. 34.--Scattered fields predicted by P.O., G.O., and I.E. methods for H(x)= 15 sin(2πx/200), T.M. polarization

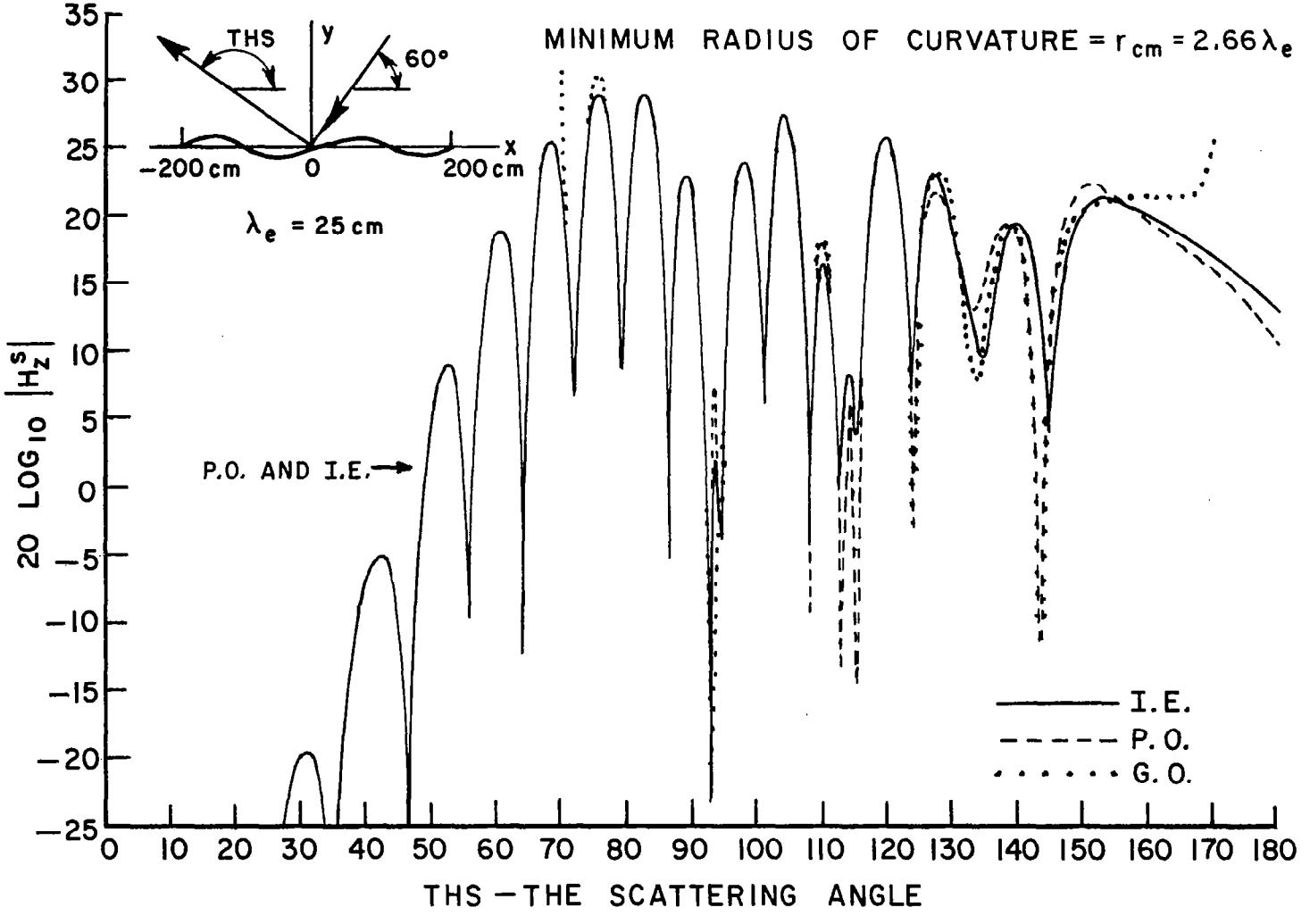

Fig. 35.--Scattered fields predicted by P.O., G.O., and I.E. methods for H(x)= 15 sin(2πx/200), T.E. polarization

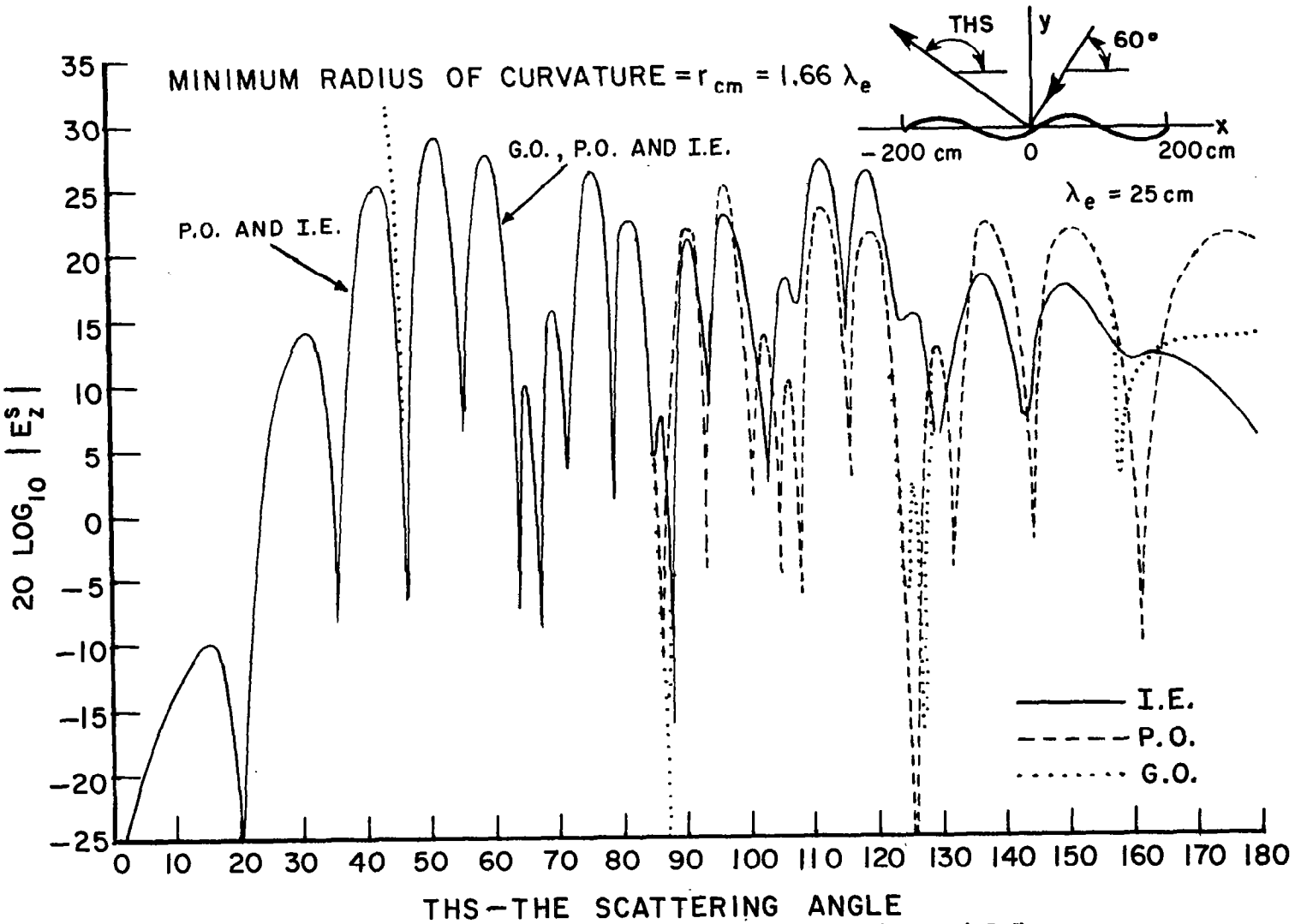

Fig. 36.—Scattered fields predicted by P.O., G.O., and I.E. methods for H(x)= 25 sin(2πx/200), T.M. polarization

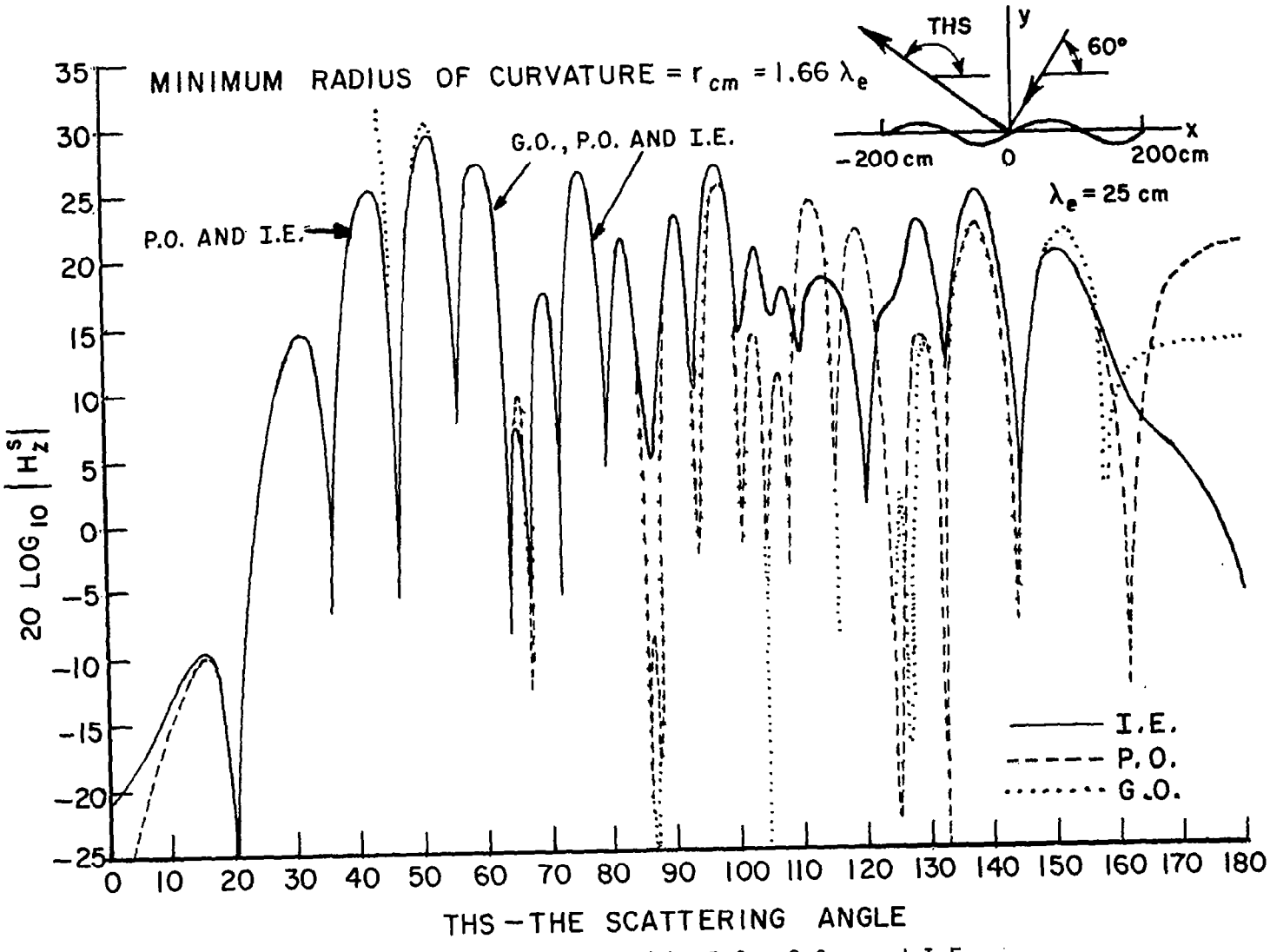

Fig. 37.--Scattered fields predicted by P.O., G.O., and I.E. methods for H(x)= 25 sin(2πx/200), T.E. polarization

give reliable values for the scattered field. Even for values of $r_{cm}/\lambda_e \simeq 1$, P.O. may still be considered usable, that is, it will reproduce the general structure of the scattered fields although with significantly lower accuracy. This limitation on the radius of curvature necessary for the successful application of the P.O. approximation is in agreement with the results of Ref. [29] in which the current on a sinusoidal surface of infinite extent is found. Except for scattering and incidence angles for which no specular points occur or for which a specular point coincides with a point of infinite radius of curvature, the G.O. and P.O. approximations give scattered fields very similar to each other even when they are not correct, e.g., Fig. 38. It is interesting to note that where the I.E. and P.O. (and hence the G.O.) fields agree the T.E. and T.M. fields are nearly identical but as the radius of curvature decreases the exact fields, T.E. and T.M., not only differ from the respective P.O. fields but from each other. This behavior is not entirely unexpected since for bodies with large radius of curvature in terms of wavelength the polarization independent G.O. is known to be a good approximation. As the radius of curvature goes to zero, e.g. a wedge, G.O. and P.O. both fail and the scattering is polarization dependent (see the wedge tests in Chapter IV).

The failure of G.O. when no specular point occurs on the surface or when a specular point coincides with a point of infinite radius of curvature makes it far less attractive than P.O., especially when numerical methods are involved. For example, when A=5, (see Fig. 32)

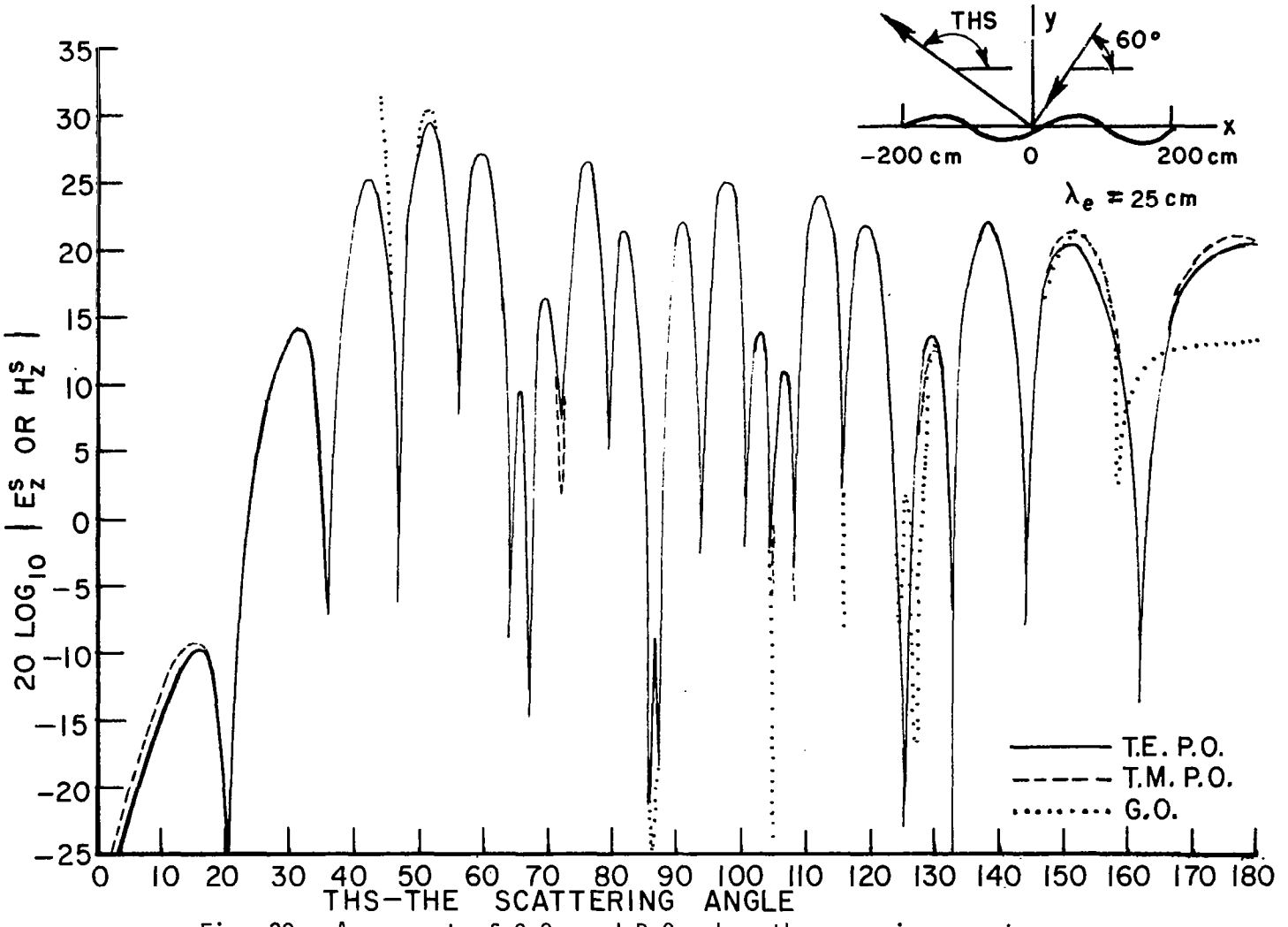

Fig. 38.--Agreement of G.O. and P.O. when they are incorrect.

G.O. predicts no scattered field outside the range 102° < THS < 138°, and gives fields which are singular at either end of the range. On the other hand, the P.O. approximation correctly predicts the scattered fields for a far wider range of THS, including backscatter, and the fields are always bounded.

It is also of interest to note that what might be called the "fine structure" of the scattering, particularly for THS < 80°, (see Fig. 32) is not due entirely to the finite length of the illuminated region as in Figs. 29 and 30 but is strongly controlled by the height profile.

Another approximate theory whose validity can be checked by the numerical methods developed here is the perturbation theory for the scattering from "slightly rough" surfaces as formulated in Refs. [30] and [31]. Perturbation theory predicts that if the amplitude of the surface profile is much less than the electrical wavelength of the incident fields, then the amplitude of the scattered field due to the perturbation of the surface is proportional to the surface height amplitude. This was checked by calculating, using the T.M. integral equation program, the scattering from a surface profile described by

$$(95) \qquad H(x) = c\,(\sin(2\pi x/50) + 1/2\,\sin(2\pi x/19.71))$$

for various values of c. The field scattered by slightly rough surfaces is dominated by the scattered field from the unperturbed surface (c=0) which is quite complex for the finite strips considered

here. Thus the behavior of the perturbed fields can best be illustrated by considering the difference between the actual field and the flat plate field. The perturbation in the scattered field, E_p, due to the perturbation in the height profile of the originally flat strip is then given by

$$E_p = E_z^s - E_{zo}^s \tag{96}$$

where E_z^s is the total scattered field as predicted by the computer program, and E_{zo}^s is the field scattered when c is zero (i.e., a flat strip). In order to test the prediction that $|E_p| \alpha c$, a low value of c (c=0.01 cm.), was chosen as a reference surface amplitude with reference scattered field $|E_{p1}|$, so that for a fixed scattering angle

$$\frac{|E_p|}{|E_{p1}|} = \frac{c}{c_1} \tag{97}$$

expresses the perturbation theory result. The exact fields are compared with perturbation theory in Fig. 39 for several values of c. The theory appears to fail at about $c/c_1 = 200$ which corresponds to a root mean square surface amplitude of approximately $\lambda_e/10$.

In addition to permitting the examination of the applicability of various electromagnetic approximations to the ocean surface scattering problem, the programs permit direct calculation of the scattered fields from any appropriate surface. One such application is to the calculation of the expected value of the backscattered power from an ensemble of ocean-like surfaces. Such an ensemble may be constructed from the known height spectrum, Ref. [32]. For the sea surface, the

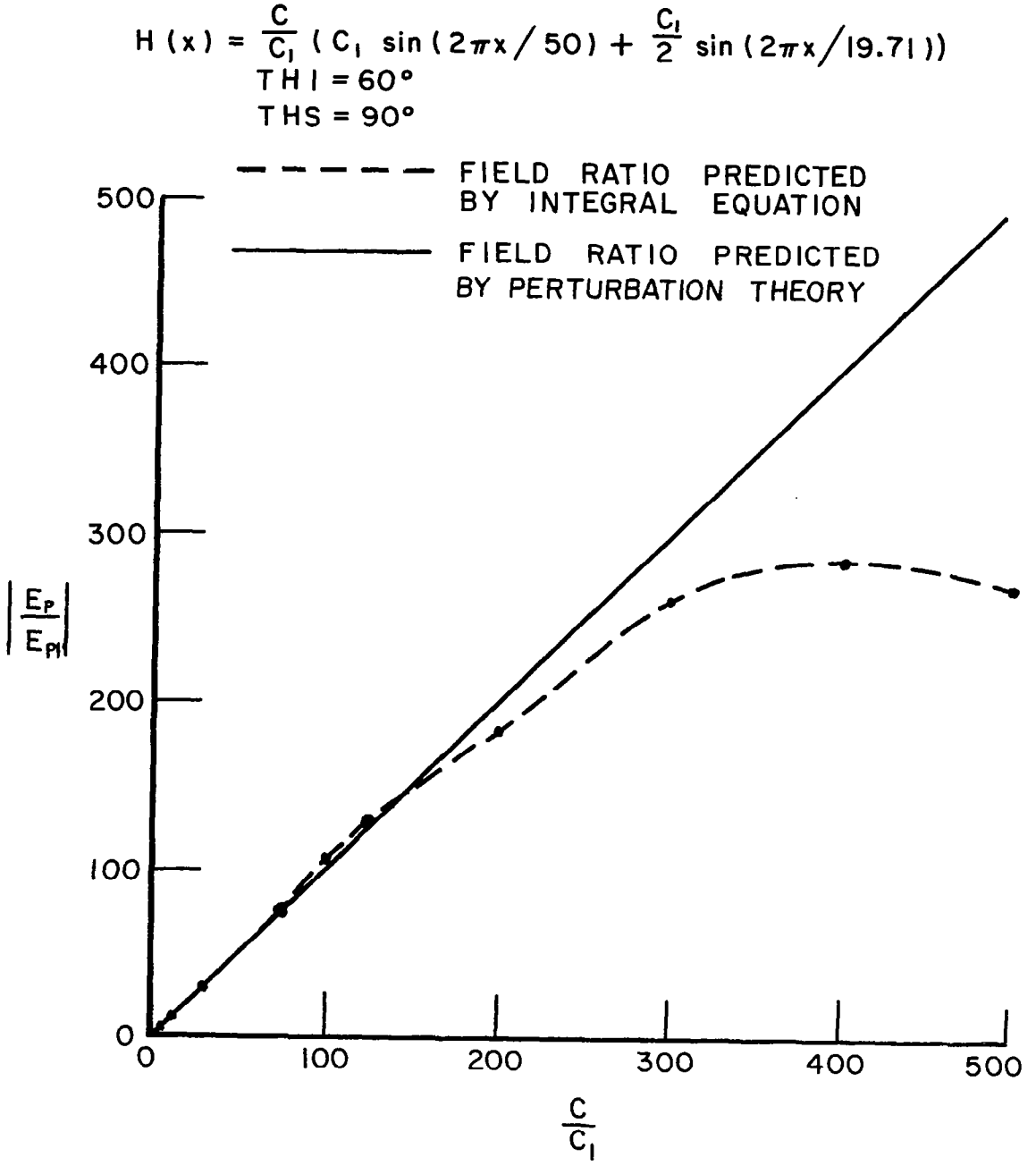

Fig. 39.--Perturbation theory test.

height spectrum, Fig. 40, decays approximately as k_m^{-4} over the significant range of wave numbers, where k_m is the mechanical wavenumber.

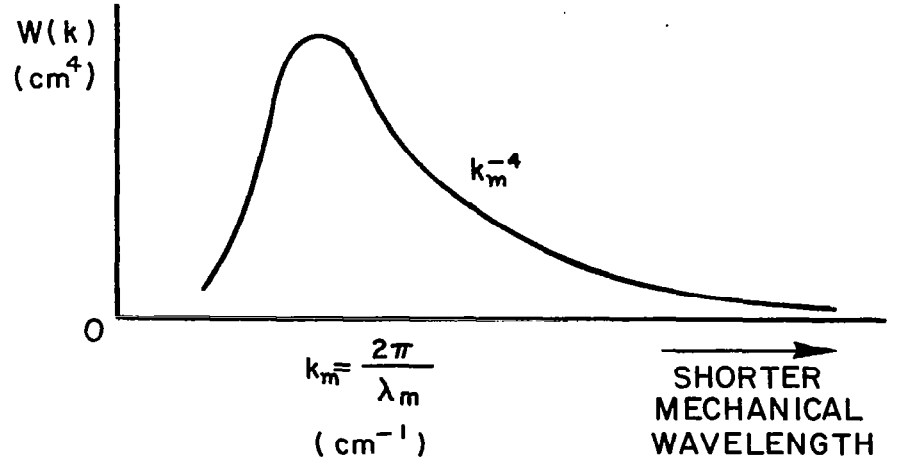

Fig. 40.--Sea surface height spectrum.

Thus a particular member of the ensemble can be chosen to be a finite sum of sinusoids with random phases whose amplitudes vary roughly as k_m^{-2}. If the k_m's are not harmonically related, the surface, like the ocean, will be aperiodic. One example of a surface of this type is given by the series

$$
\begin{aligned}
(98) \quad H(x) = {} & 2.5(0.4 \sin(2\pi x/200.0 + 0.78) \\
& + 0.8(10.0/20.0)^2 \sin(2\pi x/10.954 + 1.6) \\
& + 0.8(6.66/20.0)^2 \sin(2\pi x/6.28318 + 2.4) \\
& + 0.8(5.0/20.0)^2 \sin(2\pi x/4.795 + 0.4))
\end{aligned}
$$

illustrated in Fig. 41. An ensemble of surfaces of finite length can be generated by using successive non-overlapping sections of this surface.

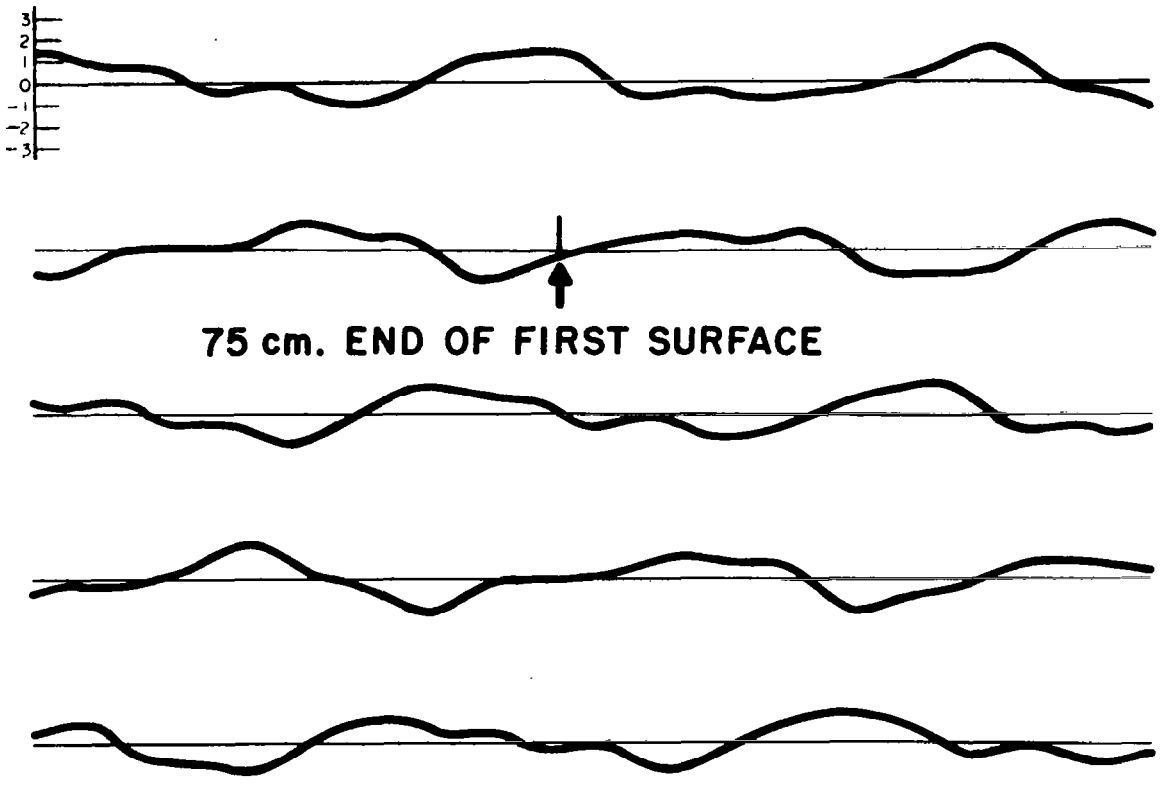

Fig. 41.--Four component representation of the surface

Physical optics was used to calculate the expected value of the backscattered power and field strength from a 75 member ensemble made from the surface described by Eq. (98). Each member of the ensemble was 75 electrical wavelengths long. On a CDC 6600 computer,

the time required for the run was about 40 minutes. The expected values $<|E_z^s|^2>$ are shown in Fig. 42; the expected value of E_z^s was found to be extremely small compared to the root mean square field.

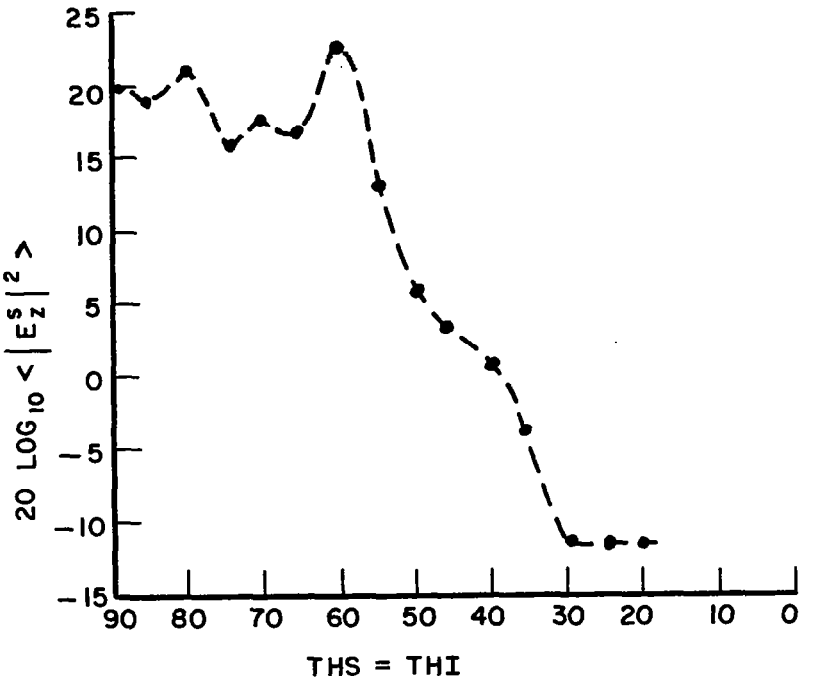

Fig. 42.--Expected value of backscattered $|E_z^s|^2$ from ensemble.

Notice that no special form of the slope distribution or other statistical properties of the surface have to be assumed. It is also possible to use a point by point, i.e. discrete, representation of the surface, such as might be generated by the prescribed statistical properties of the surface.

CHAPTER VI

SUMMARY AND CONCLUSIONS

In this work the scattering properties of cylindrical rough surfaces have been investigated by several numerical techniques in order to test the validity of previous theoretical work. The results, using as checks the integral equation solutions, show that geometrical optics is not usable for surfaces with radius of curvature smaller than 2.5 λ_e and may give poor results even when this condition is satisfied should the scattering geometry be such that no specular point exists or a specular point coincides with a point of infinite radius of curvature. With the exception of these two cases, geometrical optics and physical optics give nearly the same scattered fields.

It was found that the numerical evaluation of the scattered fields from the physical optics currents gives good results for almost any geometry (except perhaps deeply shadowed configurations) as long as the radius of curvature condition, $r_{cm} > 2.5\ \lambda_e$, is satisfied. Physical optics, although not always so accurate, has an advantage over the integral equation formulation in that the length of surface which can be treated is not limited by machine storage capacity.

The integral equation program has been used to check the perturbation theory prediction that the amplitude of the scattered field increases in proportion to the increase in the amplitude of the surface height profile. The numerical results confirm in a quantitative way the fact that the theory fails when the root mean square height is about one tenth of an electrical wavelength.

The physical optics program, because of its ability to handle long surfaces and its superiority to geometrical optics, has been applied to the direct calculation of the expected value of the scattered power from an ensemble of ocean-like surfaces which were constructed from a height spectrum similar to that of the sea. The computer time required, while lengthy, was not found to be prohibitive.

The extension of the programs to very long surfaces, to non-cylindrical surfaces or to dielectric surfaces appears feasible only for the G.O. and P.O. methods; the storage requirements for an I.E. solution in either case would be prohibitive. P.O. would probably be the easiest to modify to non-cylindrical surfaces, especially if shadowing were neglected. Since location of the specular points becomes much more complicated in the non-cylindrical case, the G.O. method would be more difficult to implement.

APPENDIX A

COMPUTER PROGRAMS

A listing of all the programs discussed in the text is presented here. To facilitate understanding of the programs, the symbols used in the programs have been used in the text whenever possible.

All programs require the plot subroutine listed at the end. The function subprograms AHAN20(x) and AHAN21(x) are required in the T.M. and T.E. integral equation programs respectively.

```
C       THIS PROGRAM IS FOR BISTATIC BACKSCATTERING
C       ESCNS IS THE RETURNED E FIELD WITH SHADOWING NOT ACCOUNTED FOR
C       ESCWS IS E SCATTERED WITH SHADOWING ACCOUNTED FOR
C
C       GEOMETRICAL OPTICS FOR THE OCEAN SURFACE
C
C        SPECULAR POINT SEARCH IS DONE IN TWO STEPS
C       #1 IS MECHANICAL WAVELENGTH DEPENDENT,#2 ISREFINNED MECHANICAL OR
C       ELECTRICAL WHICHEVER IS MORE STRINGENT.
C       DLTAX IS THE SEARCH SIZE#1,DLTAXOO IS SEARCH SIZE#2
C       DELSHA IS SHADOW TEST STEP SIZE
C       THIS PROGRAM CAN HANDLE 200 SPECULAR POINTS /PASS IE. ONE THI&ITHS
        DIMENSION XN(200),ANGLE(200)
        DIMENSION ACDNS(720),AWS(720),AWCS(720),ASNS(720),AOS(720)
        DIMENSION           ECDNS(720),EWS(720),EWCS(720),Y(10),ESNS(720)
        REAL  PI,PI2
        REAL  MTWO
        COMPLEX ESCNS,ESCWS,ENS
        COMMON CA,CB,CKA,CKB,PHA,PHB,CC,CKC,PHC
        COMPLEX  ESCDNS,ESCD
        NAMELIST/CAT/CA,CB,CKA,CKB,PHA,PHB,CC,CKC,PHC,WAVE,THID
        NAMELIST/CUT/ESNS,ASNS,ECDNS,ACDNS,EWS,AWS,EWCS,AWCS,AOS
C
C       THE FUNCTION WHICH DESCRIBES THE SURFACE IS
C       H(X)=CA*SIN((CKA*X)+PHA)+CB*SIN((CKB*X)+PHB)+CC*SIN((CKC*X)+PHC)
        CA=10.0
        CKA=6.28318/200.0
        PHA=0.0
        CB=0.0
        CKB=0.0
        PHB=0.0
        CC=0.0
        CKC=0.0
        PHC=0.0
        HMAX=ABS(CA)+ABS(CB)+ABS(CC)
        PI=3.14159
        PI2=1.5707963
        TPI=6.283185
C       WMMIN IS THE MINIMUM MECHANICAL WAVELENGTH
        WMMIN=TPI/AMAX1(CKA,CKB,CKC)
        DLX=0.01000
        TWDLX=20.0*DLX
C       NANI IS THE NUMBER OF ANGLES TO BE INVESTIGATED
        NANI=360
        XSTRT=-200.0
        XSTOP=-XSTRT
C       THS IS THE ANGLE BETWEEN THE POS. X AXIS AND THE SCATTERING DIREC.
C       THI IS THE ANGLE BETWEEN THE POS. X AXIS AND THEINC. DIRECTION

        THI=60.0*3.1415927/180.0
C       WAVE IS THE ELECTRICAL WAVELENGTH
        WAVE=25.0
        DLTAX=WMMIN/10.0
         DLTXOO=AMIN1((DLTAX/5.0),(WAVE/20.0))
        DELSHA=WMMIN/10.0
        XSKIP=XSTOP+(10**9)
        TANTHI=TAN(THI)
        THID=THI*180.0/3.14159
        CSTHI=COS(THI)
        SNTHI=SIN(THI)
        NAMELIST/TOM/DLTAX,DLTXOO,DELSHA
        WRITE(6,TOM)
        DO 93 IRE=1,NANI
        ASNS(IRE)=0.0
        ACDNS(IRE)=0.0
        AWS(IRE)=0.0
        AWCS(IRE)=0.0
        ESNS(IRE)=0.0
        ECDNS(IRE)=0.0
```

```
      EWS(IRE)=0.0
      EWCS(IRE)=0.0
   93 CONTINUE
      DO 17 IJ=1,NANI
      THS=FLOAT(IJ)*0.8726646 E-02
      THSD=THS*57.29578
      AOS(IJ)=THSD
      WRITE(6,356) THID,THSD
  356 FORMAT(11H INC ANGLE=,E15.8,13H SCATT ANGLE=,E15.8)
      SUCOS=CSTHI+COS(THS)
      SUSIN=SNTHI+SIN(THS)
      N=0
C     FIRST FIND POSITIONNS OF SPECULAR RETURN AND STORE THEM
C    THE FIRST POSITION CAN NOT BE A SPECULAR POINT
      XP=XSTRT
      SUMD2=(THI+THS)/2.0
      E=SUMD2-(TH(XP)+PI2)
  102 XP=XP+DLTAX
      EO=E
      E=SUMD2-(TH(XP)+PI2)
      IF(E.EQ.0.0) GO TO 100
      IF(((EO.GT.0.0).AND.(E.LT.0.0)).OR.((EO.LT.0.0).AND.(E.GT.0.0)))
     2  GO TO 100
      GO TO 101
  100 N=N+1
      XN(N)=XP
      ANGLE(N)=THS-(TH(XP)+PI2)
  101 IF (XP.LE. XSTOP) GO TO 102
      IF(N.EQ.0) GO TO 372
C     THIS IS TO REFINE THE POSITION OF THE SPECULAR POINT
      DO 25 K=1,N
      XSO=XN(K) -DLTAX
      E=SUMD2-(TH(XSO)+PI2)
  222 XSO=XSO+DLTX00
      EO=E
      E=SUMD2-(TH(XSO)+PI2)
      IF(E.EQ.0.0) GO TO 252
      IF(((EO.GT.0.0).AND.(E.LT.0.0)).OR.((EO.LT.0.0).AND.(E.GT.0.0)))
     2  GO TO 252
      GO TO 253
  252 XN(K)=XSO
      ANGLE(K)=THS-(TH(XSO)+PI2)
  253 CONTINUE
      IF (XSO.LT.XN(K)) GO TO 222
   25 CONTINUE
      ESCNS=CMPLX(0.0,0.0)
      ESCDNS=CMPLX(0.0,0.0)
      DO 10 K=1,N
      PHASE=(TPI/WAVE)*((SUCOS*XN(K))+(SUSIN*H(XN(K))))
      RC=RS(XN(K))*COS(ANGLE(K))
      IF(RC.LT.0.0) PHASE=PHASE+(PI/2.0)
      ENS=-((SQRT(ABS(RC/2.0)))*CEXP(CMPLX(0.0,PHASE)))
C     TAPPERING INCLUDED
      XG=XN(K)
      IF(XG.GT.(XSTOP-WAVE)) ENS=CMPLX(0.0,0.0)
      IF(XG.LT.(XSTRT+WAVE)) ENS=CMPLX(0.0,0.0)
      IF((XG.GT.(XSTOP-(2.0*WAVE))).AND.(XG.LE.(XSTOP-WAVE)))
     2ENS=ENS*(0.5-(0.5*SIN((3.14159/WAVE)*(XG-(XSTOP-(1.5*WAVE))))))
      IF((XG.GE.(XSTRT+WAVE)).AND.(XG.LE.(XSTRT+(2.0*WAVE))))
     2ENS=ENS*(0.5+(0.5*SIN((3.14159/WAVE)*(XG-(XSTRT+(1.5*WAVE))))))
      ESCNS=ESCNS+ENS
      IF(RS(XN(K)).LE.0.0) GO TO 10
      ESCDNS=ESCDNS+ENS
   10 CONTINUE
      ACD=CABS(ESCDNS)
      IF(ACD.LT.1.0 E-05) GO TO 59
      ANACD=57.29578*ATAN2(AIMAG(ESCDNS),REAL(ESCDNS))
   59 CONTINUE
      IF(ACD.LT. 1.0 E-05) ANACD=0.0
```

```
      ESMAG=CABS(ESCNS)
      ESANG=ATAN2(AIMAG(ESCNS),REAL(ESCNS))*180.0/3.1415927
      WRITE(6,726)  ESMAG,ESANG
  726 FORMAT(' ','MAG. OF SCATT. E FIELD=',E15.8,'PHASOR ANGLE=',E15.8,
     23X,'WITHOUT SHADOWING'  )
      WRITE (6,121) ACD,ANACD
  121  FORMAT(' ','SCATT. FIELD NO SHADOW CONCAVE DOWN TIPS ONLY=',E15.8,
     2'PHASOR ANGLE=',E15.8)
      ESNS(IJ)=ESMAG
      ECDNS(IJ)=ACD
      ASNS(IJ)=ESANG
      ACDNS(IJ)=ANACD
C     NOW FIND THE SHADOWING EFFECT
C     INBOUND SHADOWING
      IF (ABS(THI-PI2).LT.0.05) GO TO 500
      DO 327 K=1,N
      BI=H(XN(K))-(TANTHI*XN(K))
      STEPI=DELSHA
      IF (TANTHI.LT.0.0) STEPI=-DELSHA
      XI=XN(K)+STEPI
      GO TO 471
  470 XI=XI+STEPI
  471 YI=(TANTHI*XI)+BI
      IF (YI.LE.H(XI)) XN(K)=XSKIP
      IF(ABS(XN(K)).GT.XSTOP) GO TO 499
      IF(ABS(XI).GT.XSTOP) GO TO 499
      IF(YI.LE.HMAX) GO TO 470
  499 CONTINUE
  327 CONTINUE
  500 CONTINUE
C     OUT BOUND SHADOWING
      IF(ABS(THS-PI2).LT.0.05) GO TO 639
      TANTHS=TAN(THS)
      DO 633 KK=1,N
      IF (XN(KK).GT.XSTOP) GO TO 633
C     THE ABOVE CARD MAKES SURE THAT TIME IS NOT SPENT ON A PT, ALREADY
C     KNOWN TO BE SHADOWED
      BO=H(XN(KK))-(TANTHS*XN(KK))
      STEPO=DELSHA
      IF(TANTHS.LT.0.0) STEPO=-DELSHA
      XO=XN(KK)+STEPO
      GO TO 671
  670 XO=XO+STEPO
  671 YO=(TANTHS*XO)+BO
      IF(YO.LE.H(XO)) XN(KK)=XSKIP
      IF(ABS(XN(KK)).GT.XSTOP) GO TO 699
      IF (ABS(XO).GE.XSTOP) GO TO 699
      IF (YO.LE.HMAX) GO TO 670
  699 CONTINUE
  633 CONTINUE
  639 CONTINUE
C      END OF SHADOWING EFFECT
      ININ=0
      ESCWS=CMPLX(0.0,0.0)
```

```
      ESCD=CMPLX(0.0,0.0)
      DO 19 K=1,N
C      NEXT CARD SKIPS THE SHADOWED SPECULAR POINTS
      IF (XN(K).GT.XSTOP ) GO TO 19
      ININ=K
      PHASE=(TPI/WAVE)*((SUCOS*XN(K))+(SUSIN*H(XN(K))))
      RC=RS(XN(K))*COS(ANGLE(K))
      IF(RC.LT.0.0) PHASE=PHASE+(PI/2.0)
      ENS=-((SQRT(ABS(RC/2.0)))*CEXP(CMPLX(0.0,PHASE)))
C     TAPPERING INCLUDED
      XG=XN(K)
      IF(XG.GT.(XSTOP-WAVE)) ENS=CMPLX(0.0,0.0)
      IF(XG.LT.(XSTRT+WAVE)) ENS=CMPLX(0.0,0.0)
      IF((XG.GT.(XSTOP-(2.0*WAVE))).AND.(XG.LE.(XSTOP-WAVE)))
     2ENS=ENS*(0.5-(0.5*SIN((3.14159/WAVE)*(XG-(XSTOP-(1.5*WAVE))))))
      IF((XG.GE.(XSTRT+WAVE)).AND.(XG.LE.(XSTRT+(2.0*WAVE))))
     2ENS=ENS*(0.5+(0.5*SIN((3.14159/WAVE)*(XG-(XSTRT+(1.5*WAVE))))))
      ESCWS=ESCWS+ENS
      IF(RS(XN(K)).LE.0.0) GO TO 19
      ESCD=ESCD+ENS
 19   CONTINUE
      IF( ININ.EQ.0) WRITE(6,3149)
      IF(ININ.EQ.0) GO TO 23
      ABESCD=CABS(ESCD)
      IF(ABESCD.LT. 1.0 E-05) GO TO 58
      ANESCD=57.29578*ATAN2(AIMAG(ESCD),REAL(ESCD))
 58   CONTINUE
      IF(ABESCD .LT. 1.0E-05) ANESCD=0.0
      ESMAGS=CABS(ESCWS)
      ESANGS=ATAN2(AIMAG(ESCWS),REAL(ESCWS))*180.0/3.1415927
 3149 FORMAT(' ','NO SCATTERED E FIELD WITH SHADOWING')
      IF(ININ.NE.0) WRITE(6,776) ESMAGS,ESANGS
 776  FORMAT(' ','MAG OF SCATT. E FIELD WITH SHADOWING=',E15.8,'PHASOR
     2ANGLE=',E15.8)
      IF(ININ.NE.0) WRITE(6,2118) ABESCD,ANESCD
 2118 FORMAT(' ','SCAT FIELD WITH SHAD. CONCAVE DOWN ONLY=',E15.8,
     2' PHASOR ANGLE=',E15.8)
      EWS(IJ)=ESMAGS
      EWCS(IJ)=ABESCD
      AWS(IJ)=ESANGS
      AWCS(IJ)=ANESCD
      GO TO 23
 372  WRITE (6,3152) THID,THSD
 3152 FORMAT(' NO SPECULAR POINTS FOR THID=',E15.8,'   AND THSD=',E15.8)
 23   WRITE(6,779)
      WRITE(6,779)
 779  FORMAT(1H )
 17   CONTINUE

C       FOR THE PLOTS
      DO 536 IKO=1,NANI
      IND=IKO-1
      THSD=AOS(IKO)
      Y(1)=ESNS(IKO)
 536  CALL PLOT(THSD,Y,1,IND,50.0,0.0)
      DO 537 IKO=1,NANI
      IND=IKO-1
      THSD=AOS(IKO)
      Y(1)=EWS(IKO)
 537  CALL PLOT(THSD,Y,1,IND,50.0,0.0)
      DO 538 IKO=1,NANI
      IND=IKO-1
      THSD=AOS(IKO)
      Y(1)=ECONS(IKO)
 538  CALL PLOT(THSD,Y,1,IND,50.0,0.0)
      DO 539 IKO=1,NANI
      IND=IKO-1
      THSD=AOS(IKO)
      Y(1)=EWCS(IKO)
```

```
  539  CALL PLOT(THSD,Y,1,IND,50.0,0.0)
       DO 936 KKRL=1,NANI
       ANGOS=FLOAT(KKRL)/2.0
       IF(ESNS(KKRL).LE.0.0001) GO TO 936
       DBNS=20.0*ALOG10(ESNS(KKRL))
       WRITE(6,937) DBNS,ANGOS
  937  FORMAT('   DBNS=',E15.8,'   ANGOS=',E15.8)
   936 CONTINUE
       DO736 KKRL=1,NANI
       ANGOS=FLOAT(KKRL)/2.0
       IF( EWS(KKRL).LE.0.0001) GO TO 736
       DBS=20.0*ALOG10(EWS(KKRL))
       WRITE(6,737) DBS,ANGOS
  737  FORMAT('  DBS=',E15.8,'  ANGOS=',E15.8)
  736  CONTINUE
       STOP
       END


       FUNCTION RS(X)
       COMMON CA,CB,CKA,CKB,PHA,PHB,CC,CKC,PHC
C      THIS GIVES THE RADIUS OF CURVATURE AT X
       HP=(CA*CKA*COS((CKA*X)+PHA))+(CB*CKB*COS((CKB*X)+PHB))
      2+(CC*CKC*COS((CKC*X)+PHC))
       HPP=-((CA*CKA*CKA*SIN((CKA*X)+PHA))+(CB*CKB*CKB*SIN((CKB*X)+PHB))
      2+(CC*CKC*CKC*SIN((CKC*X)+PHC)))
       RS=((1.0+(HP*HP))**1.5)/(-HPP)
       RETURN
       END
       FUNCTION TH(X)
       COMMON CA,CB,CKA,CKB,PHA,PHB,CC,CKC,PHC
       TH=ATAN2((CA*CKA*COS((CKA*X)+PHA))+(CB*CKB*COS((CKB*X)+PHB))
      2+(CC*CKC*COS((CKC*X)+PHC)),1.0)
C      THIS FUNCTION GIVES THE ANGLE BET. THE TANGENT TO H(X) AND THE
C       HORIZONTAL
       RETURN
       END


       FUNCTION H(X)
       COMMON CA,CB,CKA,CKB,PHA,PHB,CC,CKC,PHC
       H=(CA*SIN((CKA*X)+PHA))+(CB*SIN((CKB*X)+PHB))+CC*SIN((CKC*X)+PHC)
       RETURN
       END
```

```
      DIMENSION Y(10),ESSS(360)
C          THIS IS THE TM CASE .
C     THIS PROGRAM USES PHYSICAL OPTICS TO CALCULATE THE BACKSCATTERING
C     FROM A SEA SURFACE BY DIVIDING SURFACE INTO LIT AND UNLIT REGIONS
C     IN THE LIT REGIONS THE SURFACE CURRENT IN 2NXH
C     GAUSSIAN INTEGRATION  USED
C     FOR THIS PROGRAM TO GIVE USEFUL RESULTS THE SURFACE MUST HAVE
C     RADII OF CURVATURE NO LESS THAN 1*WE
C     NSP IS THE NUMBER OF SHADOW POINTS
C     SURFACE IS DESCRIBED BY AONE*SIN(CONE*X+PONE) +ATWO*SIN(CTWO*X
C     +PTWO)+ATRE*SIN(CTRE*X+PTRE)
C     SURFACE UNDER CONSIDERATION LIES BETWEEN ALEP AND REP
C     SN IS THE STEP SIZE TAKEN TO DETERMINE SHADOWING
C     IT MUST BE SMALLER THAN ANY SURFACE FEATURES AND MUST ALSO
C     ALLOW THE LOCATIONOF THE END POINTS OF INTEGRATION WITHIN
C     A SMALL FRACTION OF A WAVELENGTH
C     NANI IS THE NUMBER OF ANGLES (SCATTERING) TO BE EXAMINED
C     MAKE DIMENSIONS OF ESSS , SCANG,EFPA SMALL AS POSSIBLE TO AVOID
C     LAGE # OF CARDS RETURNED
C     NANI SHOULD BE THE DIMENSION OF ESSS,SCANG,EFPA
      NAMELIST/RON/AB,ANG,DTHS
      DIMENSION SCANG(360),EFPA(360)
      COMPLEX S,BINT
C     SCATTER SHADOWING HAS NOT BEEN ACCOUNTED FOR
      COMMON /DOG/AONE,CONE,PONE,ATWO,CTWO,PTWO,ATRE,CTRE,PTRE
      COMMON /HOG/ G,THI,THS,WE
      COMMON/PIG/ SECTOR,DX,REP,SECD10
      COMMON/GSNN/GW1,GW2,GW3,GW4,GW5,GU1,GU2,GU3,GU4,GU5
      WE=25.0
C     WE IS THE ELECTRICAL WAVELENGTH
      G=2.0*3.1415927/WE
      SRTWE=SQRT(WE)
      DX=WE/15.0
      AONE=50.0
      CONE=2.0*3.1415927/800.0
      PONE=3.14159/2.0
      ATWO=0.0
      CTWO=0.0
      PTWO=0.0
      ATRE=0.0
      CTRE=0.0
      PTRE=0.0
      NANI=360
      SECTOR=WE/2.0
      SECD10=SECTOR/10.0
C     CONSTANTS FOR GAUSSIAN INTEGRATION
      GW1=0.2369268
      GW2=0.47862867
      GW3=0.568889
      GW4=GW2
      GW5=GW1
      GU1=-0.9061798
      GU2=-0.53846931
      GU3=0.0
      GU4=-GU2
      GU5=-GU1
C     THE ANGLE OF INCIDENCE SHOULD NOT BE GREATER THAN 90 DEG
      THI=60.0*3.1415927/180.0
C     IF THE INCIDENCE ANGLE IS WITHIN TEN DEGREES OF 90 NO SHADOWING
C     TAKEN INTO ACCOUNT
      IF(ABS(THI-1.5707).LT.0.175) GO TO 563
      TANTHI=TAN(THI)
      DTHI=180.0*THI/3.1415927
      WRITE(6,1071) DTHI
 1071 FORMAT(' ',' ANG OF INC FROM POS X AXIS =',E15.8)
```

```
      REP=200.0
      ALEP=-REP
      SN=WE/10.0
      NSP=1
      DIMENSION  SX(1000)
      IF(DH(REP).GT.TANTHI) GO TO 106
      SX(NSP)=REP
      GO TO 105
  106 SLOPE=TANTHI
      B=H(REP)-(SLOPE*REP)
      X=REP
  109 X=X-SN
      IF((SLOPE*X)+B.GT.H(X)) GO TO 109
      IF(X.LE.ALEP) GO TO 1000
      SX(NSP)=X-(SN/2.0)
  105 CONTINUE
C     THIS ABOVE TAKES CARE OF THE FIRST RIGHTENDPOINT
   15 X=SX(NSP)
   22 X=X-SN
      XN=X-SN
      IF((DH(X).LT.TANTHI).AND.(DH(XN).GT.TANTHI)) GO TO 53
      IF(X.GT.ALEP) GO TO 22
      GO TO 92
   53 NSP=NSP+1
      SX(NSP)=XN
      SLOPE=TANTHI
      B=H(SX(NSP))-(SLOPE*SX(NSP))
      X=SX(NSP)-SN
   29 X=X-SN
      IF((SLOPE*X)+B.LT.H(X)) GO TO 39
      IF(X.GT.ALEP) GO TO 29
      GO TO 92
   39 NSP=NSP+1
      SX(NSP)=X-(SN/2.0)
      GO TO 15
   92 NSP=NSP+1
      SX(NSP)=ALEP
      GO TO 564
  563 SX(1)=REP
      SX(2)=ALEP
      NSP=2
  564 CONTINUE
C     LAST VALUE IN SX(J) IS ALEP
      WRITE (6,101) (K,SX(K),K=1,NSP)
  101 FORMAT(' ','SX(',I4,')=',E15.8)
      DO 317 JNX=1,NANI
      THS=FLOAT(JNX)*(0.8726646 E-02)
      DTHS=180.0*THS/3.1415927
      SCANG(JNX)=DTHS
      S=CMPLX(0.0,0.0)
      KKN=1
   10 CONTINUE
      ALOW=SX(KKN+1)
      AUPP=SX(KKN)
      S=S+BINT(ALOW,AUPP)
      KKN=KKN+2
      IF ((KKN.LT.NSP).AND.((KKN+1).LT.NSP)) GO TO 10
C      TO CONVERT TO TRUE SCATTERED E FIELD FOR EINC OF UNITY MAG.
      S=CMPLX(-0.70711,-0.70711)*S/SRTWE
      AB=CABS(S)
      ESSS(JNX)=AB
      ANG=180.0*ATAN2(AIMAG(S),REAL(S))/3.1415927
      EFPA(JNX)=ANG
  317 CONTINUE
      DO 531 JK=1,NANI
```

```
      E=ESSS(JK)
      DB=20.0*ALOG10(E)
      A=EFPA(JK)
      AS=SCANG(JK)
  531 WRITE (6,532) AS,E,A,DB
  532  FORMAT(' ',' SCAT ANG FROM HORIZ=' ,E15.8,' MAG OF E FIELD=',
     2  E15.8,'  PHASE ANG=',E15.8,'  DB=',E15.8)
      DO 535 IKE=1,NANI
      IND=IKE-1
      THSD=FLOAT(IKE)/2.00
      Y(1)=ESSS(IKE)
  535 CALL PLOT (THSD,Y,1,IND,50.0,0.0)
      GO TO 1002
 1000 WRITE(6,1592)
 1592 FORMAT('SURFACE IS NOT ILLUMINATED')
 1002 CONTINUE
      STOP
      END

      FUNCTION H(X)
      COMMON /DOG/AONE,CONE,PONE,ATWO,CTWO,PTWO,ATRE,CTRE,PTRE
      H=AONE*SIN(CONE*X+PONE)+ATWO*SIN(CTWO*X+PTWO)+ATRE*SIN(CTRE*X+PTRE
     2)
      RETURN
      END

      FUNCTION DH(X)
      COMMON /DOG/AONE,CONE,PONE,ATWO,CTWO,PTWO,ATRE,CTRE,PTRE
      DH=AONE*CONE*COS(CONE*X+PONE)+ATWO*CTWO*COS(CTWO*X+PTWO)
     2 +ATRE*CTRE*COS(CTRE*X+PTRE)
      RETURN
      END


      FUNCTION BINT(XX,YY)
C     XX IS LOWER LIMIT OF INTEGRATION,YY IS UPPER LIMIT
C     PHYSICAL OPTICS RADIATION INTEGRAL WITH PLANE WAVE INCIDENT
C     TM CASE
      COMPLEX S,BINT
      COMPLEX GASS5
      COMMON /HOG/  G,THI,THS,WE
      COMMON/PIG/ SECTOR,DX,REP,SECD10
C     BREAK INTEGRAL FROM XX TO YY INTO SMALLER SEGMENTS OF LENGTH
C     SECTOR AND INTEGRATE OVER EACH SEGMENT USING GAUSSIAN INTEGRATION
      S=CMPLX(0.0,0.0)
      LDS=INT((YY-XX)/SECTOR)
      IF(LDS.EQ.0) GO TO 10
      DO 100 INJ=1,LDS
      UL=XX+(FLOAT(INJ)*SECTOR)
      ALL=XX+(FLOAT(INJ-1)*SECTOR)
  100 S=S+GASS5(ALL,UL)
C     NOW TO GET LAST FRACTION OF SEGMENT LEFT OVER FROM SURFACE SEGMENTATION
      S=S+GASS5(XX+(FLOAT(LDS)*SECTOR),YY)
      GO TO 50
   10 S=GASS5(XX,YY)
   50 CONTINUE
      BINT=S
      RETURN
      END
```

```
      FUNCTION GASS5 (XL,XU)
      COMPLEX GASS5,FTBI
C     FIFTH ORDER GAUSSIN INTEGRATION
C     XL IS LOWER LIMIT,XU IS UPPER LIMIT
C     XU-XL IS LESS THAN OR EQUAL TO SECTOR
      COMMON/GSNN/GW1,GW2,GW3,GW4,GW5,GU1,GU2,GU3,GU4,GU5
      DVDFEP=(XU-XL)/2.0
      DVSMEP=(XU+XL)/2.0
      XU5=GU5*DVDFEP+DVSMEP
      XU4=GU4*DVDFEP+DVSMEP
      XU3=GU3*DVDFEP+DVSMEP
      XU2=GU2*DVDFEP+DVSMEP
      XU1=GU1*DVDFEP+DVSMEP
      GASS5=DVDFEP*(GW1*FTBI(XU1)+GW2*FTBI(XU2)+GW3*FTBI(XU3)
     2  +GW4*FTBI(XU4)+GW5*FTBI(XU5))
      RETURN
      END

      FUNCTION FTBI(X)
      COMPLEX FTBI
C     THIS IS THE FUNCTION TO BE INTEGRATED
C     THIS IS FOR THE TM CASE
      COMMON/HOG/G,THI,THS,WE
      COMMON/PIG/ SECTOR,DX,REP,SECD10
      GCC=G*(COS(THI)+COS(THS))
      GSS=G*(SIN(THI)+SIN(THS))
      RCK=REP-(2.0*WE)
      FTBI=SIN(THI-ATAN(DH(X)))*SQRT(1.0+(DH(X)**2))*
     2  CEXP(CMPLX(0.0,((X*GCC)+(H(X)*GSS))))
C     THE FOLLOWING ACCOUNTS FOR  TAPERING
      ABSX=ABS(X)
      IF(ABSX-RCK) 1500,1500,2000
 2000 IF(X.LE.(WE-REP)) FTBI=CMPLX(0.0,0.0)
      IF(X.GE.(REP-WE)) FTBI=CMPLX(0.0,0.0)
      IF((X.GT.(WE-REP)).AND.(X.LE.((2.0*WE)-REP)))
     2 FTBI=FTBI*(0.5+(0.5*SIN((G/2.0)*(X-((1.5*WE)-REP)))))
      IF((X.LT.(REP-WE)).AND.(X.GT.(REP-(2.0*WE))))
     2 FTBI=FTBI*(0.5-(0.5*SIN((G/2.0)*(X-(REP-(1.5*WE))))))
 1500  CONTINUE
      RETURN
      END
```

```
C     THIS IS THE TE CASE
C     THIS PROGRAM USES PHYSICAL OPTICS TO CALCULATE THE BACKSCATTERING
C     FROM A SEA SURFACE BY DIVIDING SURFACE INTO LIT AND UNLIT REGIONS
C     IN THE LIT REGIONS THE SURFACE CURRENT IN 2NXH
C     GAUSSIAN INTEGRATION  USED
C     FOR THIS PROGRAM TO GIVE USEFUL RESULTS THE SURFACE MUST HAVE
C     RADII OF CURVATURE NO LESS THAN 1*WE
C     NSP IS THE NUMBER OF SHADOW POINTS
C     SURFACE IS DESCRIBED BY AONE*SIN(CONE*X+PONE) +ATWO*SIN(CTWO*X
C     +PTWO)+ATRE*SIN(CTRE*X+PTRE)
C     SURFACE UNDER CONSIDERATION LIES BETWEEN ALEP AND REP
C     SN IS THE STEP SIZE TAKEN TO DETERMINE SHADOWING
C     IT MUST BE SMALLER THAN ANY SURFACE FEATURES AND MUST ALSO
C     ALLOW THE LOCATIONOF THE END POINTS OF INTEGRATION WITHIN
C     A SMALL FRACTION OF A WAVELENGTH
C     NANI IS THE NUMBER OF ANGLES (SCATTERING) TO BE EXAMINED
C     MAKE DIMENSIONS OF ESSS , SCANG,EFPA SMALL AS POSSIBLE TO AVOID
C     LAGE # OF CARDS RETURNED
C     NANI SHOULD BE THE DIMENSION OF ESSS,SCANG,EFPA
      DIMENSION Y(10),ESSS(360)
      NAMELIST/RON/AB,ANG,DTHS
      DIMENSION SCANG(360),EFPA(360)
      COMPLEX S,BINT
C     SCATTER SHADOWING HAS NOT BEEN ACCOUNTED FOR
      COMMON /DOG/AONE,CONE,PONE,ATWO,CTWO,PTWO,ATRE,CTRE,PTRE
      COMMON /HOG/ G,THI,THS,WE
      COMMON/PIG/ SECTOR,DX,REP,SECD10
      COMMON/GSNN/GW1,GW2,GW3,GW4,GW5,GU1,GU2,GU3,GU4,GU5
      WE=25.0
C     WE IS THE ELECTRICAL WAVELENGTH
      G=2.0*3.1415927/WE
      SRTWE=SQRT(WE)
      DX=WE/15.0
      AONE=40.0
      CONE=2.0*3.1415927/200.0
      PONE=0.0
      ATWO=0.0
      CTWO=0.0
      PTWO=0.0
      ATRE=0.0
      CTRF=0.0
      PTRE=0.0
      NANI=360
      SECTOR=WE/2.0
      SECD10=SECTOR/10.0
C     CONSTANTS FOR GAUSSIAN INTEGRATION
      GW1=0.2369268
      GW2=0.47862867
      GW3=0.568889
      GW4=GW2
      GW5=GW1
      GU1=-0.9061798
      GU2=-0.53846931
      GU3=0.0
      GU4=-GU2
      GU5=-GU1
C     THE ANGLE OF INCIDENCE SHOULD NOT BE GREATER THAN 90 DEG
      THI=60.0*3.1415927/180.0
C     IF THE INCIDENCE ANGLE IS WITHIN TEN DEGREES OF 90 NO SHADDOWING
C     TAKEN INTO ACCOUNT
      IF(ABS(THI-1.5707).LT.0.175) GO TO 563
      TANTHI=TAN(THI)
      DTHI=180.0*THI/3.1415927
      WRITE(6,1071) DTHI
 1071 FORMAT(' ',' ANG OF INC FROM POS X AXIS =',E15.8)
```

```
      REP=200.0
      ALEP=-REP
      SN=WE/10.0
      NSP=1
      DIMENSION  SX(1000)
      IF(DH(REP).GT.TANTHI) GO TO 106
      SX(NSP)=REP
      GO TO 105
  106 SLOPE=TANTHI
      B=H(REP)-(SLOPE*REP)
      X=REP
  109 X=X-SN
      IF((SLOPE*X)+B.GT.H(X)) GO TO 109
      IF(X.LE.ALEP) GO TO 1000
      SX(NSP)=X-(SN/2.0)
  105 CONTINUE
C     THIS ABOVE TAKES CARE OF THE FIRST RIGHTENDPOINT
   15 X=SX(NSP)
   22 X=X-SN
      XN=X-SN
      IF((DH(X).LT.TANTHI).AND.(DH(XN).GT.TANTHI)) GO TO 53
      IF(X.GT.ALEP) GO TO 22
      GO TO 92
   53 NSP=NSP+1
      SX(NSP)=XN
      SLOPE=TANTHI
      B=H(SX(NSP))-(SLOPE*SX(NSP))
      X=SX(NSP)-SN
   29 X=X-SN
      IF((SLOPE*X)+B.LT.H(X)) GO TO 39
      IF(X.GT.ALEP) GO TO 29
      GO TO 92
    39 NSP=NSP+1
      SX(NSP)=X-(SN/2.0)
      GO TO 15
   92 NSP=NSP+1
      SX(NSP)=ALEP
      GO TO 564
  563 SX(1)=REP
      SX(2)=ALEP
      NSP=2
  564 CONTINUE
C     SURFACE IS NOW  SEPERATED INTO LIT AND UNLIT ZONES
C     LAST VALUE IN SX(J) IS ALEP
      WRITE (6,101) (K,SX(K),K=1,NSP)
  101 FORMAT(' ','SX(',I4,')=',E15.8)
C     THE FOLLOWING FINDS THE SCATTERED FIELDS DUE TO THE LIT ZONES
      DO 317 JNX=1,NANI
      THS=FLOAT(JNX)*(0.8726646 E-02)
      DTHS=180.0*THS/3.1415927
      SCANG(JNX)=DTHS
      S=CMPLX(0.0,0.0)
      KKN=1
    10 CONTINUE
      ALOW=SX(KKN+1)
      AUPP=SX(KKN)
      S=S+BINT(ALOW,AUPP)
      KKN=KKN+2
      IF ((KKN.LT.NSP).AND.((KKN+1).LT.NSP)) GO TO 10
C      TO CONVERT TO TRUE SCATTERED H FIELD FOR HINC OF UNITY MAG
      S=S*CMPLX(0.70711,0.70711)/SRTWE
      AB=CABS(S)
      DB=20.0*ALOG10(AB)
      ESSS(JNX)=AB
      ANG=180.0*ATAN2(AIMAG(S),REAL(S))/3.1415927
      EFPA(JNX)=ANG
      WRITE(6,143) DTHS,AB,ANG,DB
```

```
 143  FORMAT('   SCATTERING ANG',E15.8,'    MAG=',E15.8,'  PHASE ANGLE=',
     2E15.8,'  DB=',E15.8)
  317 CONTINUE
      DO 531 JK=1,NANI
      E=ESSS(JK)
      A=EFPA(JK)
      AS=SCANG(JK)
  531 WRITE (6,532) AS,E,A
  532  FORMAT(' ',' SCAT ANG FROM HORIZ=' ,E15.8,' MAG OF H FIELD=',
     2  E15.8,'  PHASE ANG=',E15.8)
      DO 535 IKE=1,NANI
      IND=IKE-1
      THSD=FLOAT(IKE)/2.00
      Y(1)=ESSS(IKE)
  535 CALL PLOT (THSD,Y,1,IND,50.0,0.0)
      GO TO 1002
 1000 WRITE(6,1592)
 1592 FORMAT('SURFACE IS NOT ILLUMINATED')
 1002 CONTINUE
      STOP
      END

      FUNCTION H(X)
      COMMON /DOG/AONE,CONE,PONE,ATWO,CTWO,PTWO,ATRE,CTRE,PTRE
      H=AONE*SIN(CONE*X+PONE)+ATWO*SIN(CTWO*X+PTWO)+ATRE*SIN(CTRE*X+PTRE
     2)
      RETURN
      END


      FUNCTION DH(X)
      COMMON /DOG/AONE,CONE,PONE,ATWO,CTWO,PTWO,ATRE,CTRE,PTRE
      DH=AONE*CONE*COS(CONE*X+PONE)+ATWO*CTWO*COS(CTWO*X+PTWO)
     2 +ATRE*CTRE*COS(CTRE*X+PTRE)
      RETURN
      END


      FUNCTION BINT(XX,YY)
C     XX IS LOWER LIMIT OF INTEGRATION,YY IS UPPER LIMIT
C     PHYSICAL OPTICS RADIATION INTEGRAL WITH PLANE WAVE INCIDENT
C     TM CASE
      COMPLEX S,BINT
      COMPLEX GASS5
      COMMON /HOG/  G,THI,THS,WE
      COMMON/PIG/ SECTOR,DX,REP,SECDIO
C     BREAK INTEGRAL FROM XX TO YY INTO SMALLER SEGMENTS OF LENGTH
C     SECTOR AND INTEGRATE OVER EACH SEGMENT USING GAUSSIAN INTEGRATION
      S=CMPLX(0.0,0.0)
      LDS=INT((YY-XX)/SECTOR)
      IF(LDS.EQ.0) GO TO 10
      DO 100 INJ=1,LDS
      UL=XX+(FLOAT(INJ)*SECTOR)
      ALL=XX+(FLOAT(INJ-1)*SECTOR)
  100 S=S+GASS5(ALL,UL)
      S=S+GASS5(XX+(FLOAT(LDS)*SECTOR),YY)
      GO TO 50
   10 S=GASS5(XX,YY)
   50 CONTINUE
      BINT=S
      RETURN
      END
```

```
      FUNCTION GASS5 (XL,XU)
      COMPLEX GASS5,FTBI
C     FIFTH ORDER GAUSSIN INTEGRATION
C     XL IS LOWER LIMIT,XU IS UPPER LIMIT
C     XU-XL IS LESS THAN OR EQUAL TO SECTOR
      COMMON/GSNN/GW1,GW2,GW3,GW4,GW5,GU1,GU2,GU3,GU4,GU5
      DVDFEP=(XU-XL)/2.0
      DVSMEP=(XU+XL)/2.0
      XU5=GU5*DVDFEP+DVSMEP
      XU4=GU4*DVDFEP+DVSMEP
      XU3=GU3*DVDFEP+DVSMEP
      XU2=GU2*DVDFEP+DVSMEP
      XU1=GU1*DVDFEP+DVSMEP
      GASS5=DVDFEP*(GW1*FTBI(XU1)+GW2*FTBI(XU2)+GW3*FTBI(XU3)
     2  +GW4*FTBI(XU4)+GW5*FTBI(XU5))
      RETURN
      END

      FUNCTION FTBI(X)
      COMPLEX FTBI
C     THIS IS THE FUNCTION TO BE INTEGRATED
C     THIS IS FOR THE TM CASE
      COMMON/HOG/G,THI,THS,WE
      COMMON/PIG/ SECTOR,DX,REP,SECD10
      GCC=G*(COS(THI)+COS(THS))
      GSS=G*(SIN(THI)+SIN(THS))
      RCK=REP-(2.0*WE)
      FTBI=SIN(THS-ATAN(DH(X)))*SQRT(1.0+(DH(X)**2))*
     2  CEXP(CMPLX(0.0,((X*GCC)+(H(X)*GSS))))
C     THE FOLLOWING ACCOUNTS FOR TAPPERING
      ABSX=ABS(X)
      IF(ABSX-RCK) 1500,1500,2000
 2000 IF(X.LE.(WE-REP)) FTBI=CMPLX(0.0,0.0)
      IF(X.GE.(REP-WE)) FTBI=CMPLX(0.0,0.0)
      IF((X.GT.(WE-REP)).AND.(X.LE.((2.0*WE)-REP)))
     2 FTBI=FTBI*(0.5+(0.5*SIN((G/2.0)*(X-((1.5*WE)-REP)))))
      IF((X.LT.(REP-WE)).AND.(X.GT.(REP-(2.0*WE))))
     2 FTBI=FTBI*(0.5-(0.5*SIN((G/2.0)*(X-(REP-(1.5*WE))))))
 1500  CONTINUE
      RETURN
      END
```

```
C      THIS IS A METHOD OF MOMENTS SOLUTION
C      TM POLARIZATION   SYMMETRIC MATRIX
C      NSUB SEGMENTS HAVE N MIDPOINTS
C      NSUB IS THE SUBSCRIPT WHICH COUNTS THE END POINTS
C      N    IS THE SUBSCRIPT WHICH COUNTS THE MIDPOINTS
C       WATCH MAX SLOPE SO THAT THE X INCREMENTS ARE SMALL ENOUGH
C      THE REGION UNDER CONSIDERATION LIES BETWEEN -EP AND EP
       DIMENSION Y(10),CMC(360)
       COMPLEX SNN,SST
       COMPLEX FSS
       DOUBLE PRECISION DAL,DDX,DDC2,DDC,DALC,DR
       COMPLEX FINC(30 ),STS
       COMMON /PIG/ AONE,CONE,PONE,ATWO,CTWO,PTWO,N
       COMPLEX AHAN20
       COMPLEX F(300),S(45150),SS,T
       COMPLEX FIN
       DIMENSION X(300)
       DIMENSION XMID(300)
       COMPLEX STO
C      WE  IS THE ELECTRICAL WAVELENGTH
       WE=25.0
       G=6.2831853        /WE
       STS=SQRT(WE)*CMPLX(1.0,1.0)*(+0.707107)/3.1415927
       DC=WE/10.0
       DX=DC/1000.0
       DC2=DC/2.0
       EP=200.0
       API=3.1415927
C      THE FOLLOWING CONSTANTS DEFINE THE SURFACE
       AONE=25.0
       CONE=2.0*3.1415927/200.0
       PONE=0.0
       ATWO=0.0
       CTWO=0.0
       PTWO=0.0
       CALL SCLOK1
C      THE FOLLOWING BREAKS THE SURFACE INTO SEGMENTS DC CENTIMETERS LONG
C      BY LINE INTEGRATION USING STEPS OF LENGTH DX FOR THE INTEGRATION
       NSUB=1
       X(NSUB)=-EP
       DDC=DBLE(DC)
       DDX=DBLE(DX)
       DDC2=DBLE(DC2)
 1002  DAL=0.00D 00
       DR=DBLE(X(NSUB))
 1001  DR=DR+DDX
       R=SNGL(DR)
       DALO=DAL
       DAL=DAL+(DDX*DSQRT(1.0D 00 +((DBLE(DH(R)))**2)))
       IF(((DDC2-DAL).LE.0.0D 00).AND.((DDC2-DALO).GE.0.0D 00))
      2  XMID(NSUB)=R
       IF(DAL.LT.DDC)GO TO 1001
       NSUB=NSUB+1
       X(NSUB)=R
       AL=SNGL(DAL)
       WRITE (6,352) AL,NSUB
  352  FORMAT(' ','AL=',E15.8,'   NSUB=',I4)
       IF (R.LT.EP) GO TO 1002
       TIME=RCLCK1(1.0)
       WRITE(6,3276 ) TIME
 3276  FORMAT(' ','TIME=',F10.6,'SECONDS')
       N=NSUB-1
       DO 1004 J=1,NSUB
       IF (J.EQ.NSUB) XMID(NSUB)=0.0
       XXX=X(J)
       XMD=XMID(J)
```

```
 1004 WRITE (6,1003) XXX,XMD,J
 1003 FORMAT (6H X(J)=,E15.8,9H XMID(J)=,E15.8,3H J=,I3)
C      THIS ENDS THE SURFACE SUBDIVISION
       NM0=N-1
       NM3=N-3
C      DIMENSION OF S IS N(N+1)/2
C      DIMENSION OF FINC,F IS N
       DPIF=0.7853982
       EE=2.71828
       GA=G*DC/(2.0*EE)
C     SNN IS THE DIAGONAL ELEMENT OF THE INPUT MATRIX
       SNN=AHAN20(GA)
       WRITE (6,400) SNN
  400  FORMAT (5H SNN=,2E15.8)
       DO 100 NJ=1,N
       NJP0=NJ+1
       S(ISUB(NJ,NJ))=SNN
C      THIS FINDS ELEMENTS ON THE DIAGONAL
       IF (NJP0.GT.N) GO TO 100
       DO 100 NA=NJP0,N
C      THIS FINDS OFF DIAGONAL ELEMENTS
       XM=XMID(NJ)
       XN=XMID(NA)
       RHO=SQRT(((XN-XM)**2)+((H(XN)-H(XM))**2))
       RHG=RHO*G
       S(ISUB(NJ,NA))=AHAN20(RHG)
  100  CONTINUE
C     THIS COMPLETES THE FILLIN OF THE MATRIX

C      THIS BEGINS THE CONVERSION TO UPPER TRIANGULAR MATRIX
       S(1)=CSQRT(S(1))
       DO 1 K=2,N
    1  S(K)=S(K)/S(1)
       DO 2 I=2,N
       IM0=I-1
       IP0=I+1
       T=CMPLX(0.0,0.0)
       DO 3 L=1,IM0
       LI=(L*N)-((((L-1)*L)/2)+N-I)
    3  T=T+(S(LI)**2)
       II=(I*N)-((((I-1)*I)/2)+N-I)
       S(II)=CSQRT(S(II)-T)
       IF(IP0.GT.N) GOTO 2
       DO 5 J=IP0,N
       T=CMPLX(0.0,0.0)
       DO 6 M=1,IM0
       MI=(M*N)-((((M-1)*M)/2)+N-I)
       MJ=(M*N)- (((M*(M-1))/2)+N-J)
    6  T=T+(S(MJ)*S(MI))
       IJ=(I*N)-((((I-1)*I)/2)+N-J)
    5  S(IJ)=(S(IJ)-T)/S(II)
    2  CONTINUE
C      THIS ENDS THE CONVERSION TO UPPER TRIANGULAR MATRIX
       WRITE (6,1222) N,WE
 1222  FORMAT(3H N=,I3,4H WE=,E15.8)
       TH=60.0*3.1415927/180.0
       THXD=180.0*TH/3.1415927
       WRITE (6,9333) THXD
 9333  FORMAT(9H INC ANG=,E15.8)
C      TH IS THE ANGLE OF INCIDENCE FROM THE HORIZONTAL
       STH=SIN(TH)
       CTH=COS(TH)
C      THIS FINDS THE INCIDENT FIELD ION THE NJTH SEGMENT
       DO 455 NJ=1,N
       ENJ=FLOAT(NJ)
       XM=XMID(NJ)
       F(NJ)=CEXP(CMPLX(0.0,G*((XM*CTH)+(H(X1)*STH))))
```

```
C
C
C     TAPERED ILLUMINATION  ****************************    ***********
C
C
      IF(XM.LE.((WE*1.C)-EP)) F(NJ)=CMPLX(0.0,0.0)
      IF(XM.GE.(EP-(1.0*WE))) F(NJ)=CMPLX(0.0,0.0)
      IF((XM.GT.((1.C*WE)-EP)).AND.(XM.LE.((2.0*WE)-EP)))
     2 F(NJ)=F(NJ)*(0.5+(0.5*SIN((G/2.0)*(XM    -((1.5*WE)-EP)))))
      IF((XM    .GE.(EP-(2.0*WE))).AND.(XM    .LT.(EP-(1.0*WE))))
     2  F(NJ)=F(NJ)*(0.5-(0.5*SIN((G/2.0)*(XM    -(EP-(1.5*WE))))))
  455 CONTINUE
      WRITE(6,2948) (NJ,F(NJ),NJ=1,N)
 2948 FORMAT(' ',' INC FIELD F(',I4,')=',2E15.8)
C     THIS BEGINS THE BACK SUBSTUTION
      F(1)=F(1)/S(1)
      DO 10 I=2,N
      IMO=I-1
      T=CMPLX(0.0,0.0)
      DO 11 L=1,IMO
      LI=(L*N)-((((L-1)*L)/2)+N-I)
   11 T=T+(S(LI)*F(L))
      II=(I*N)-((((I-1)*I)/2)+N-I)
   10 F(I)=(F(I)-T)/S(II)
      NN=(N*(N+1))/2
      F(N)=F(N)/S(NN)
      NMO=N-1
      DO 25 I=1,NMO
      K=N-I
      KPO=K+1
      T=CMPLX(0.0,0.0)
      DO 26 L=KPO,N
      KL=(K*N)-((((K-1)*K)/2)+N-L)
   26 T=T+(S(KL)*F(L))
      KK=(K*N)-((((K-1)*K)/2)+N-K)
      F(K)=(F(K)-T)/S(KK)
   25 CONTINUE
C     THIS ENDS THE BACK SUBSTITUTIONS
      DO 491 K=1,N
      STT=CABS(F(K))
      STO=F(K)
      ANNN=ATAN2(AIMAG(F(K)),REAL(F(K)))*180.0/3.1415927
  491 WRITE(6,492) K,STO,STT,ANNN
  492 FORMAT(' ','F(',I4,')=',2E15.8,'  OR  ','AMP=',E15.8,'AT ANGLE=',
     2 E15.8)
      DO 317 JNX=1,360
      TH=0.872664625E-02 *FLOAT(JNX)
      T=CMPLX(0.0,0.0)
      DO 310 I=1,N
      XN=XMID(I)
  310 T=T+ ((F(I)*CEXP(CMPLX(0.0,G*((XN*COS(TH))+(H(XN)*SIN(TH))))))))
C     THIS CORRECTS T TO TRUE SCATTERED FIELD
      T=STS*T
      CM=CABS(T)
      CMC(JNX)=CM
      CANG=57.296*ATAN2(AIMAG(T),REAL(T))
      THD=TH*57.296
      DB=20.0*ALOG10(CM)
  317 WRITE (6,312) CM,CANG,THD,DB
  312 FORMAT (18H RELATIVE E FIELD=,E15.8,7H ANGLE=,E15.8,
     2 23H ANGLE FROM HORIZONTAL=,E15.8,7H    DB=,E15.8)
```

```
      DO 576 IKE=1,360
      THSD=FLOAT(IKE)/2.0
      IND=IKE-1
      Y(1)=CMC(IKE)
  576 CALL PLOT(THSD,Y,1,IND,50.0,0.0)
      STOP
      END

      FUNCTION  H(X)
C     THIS DEFINES THE SURFACE
      COMMON /PIG/ AONE,CONE,PONE,ATWO,CTWO,PTWO,N
      H=AONE*SIN(CONE*X+PONE)+ATWO*SIN(CTWO*X+PTWO)
      RETURN
      END

      FUNCTION DH(X)
C         DH(X) IS THE DERIV. OF H(X)
      COMMON /PIG/ AONE,CONE,PONE,ATWO,CTWO,PTWO,N
      DH=AONE*CONE*COS(CONE*X+PONE)+ATWO*CTWO*COS(CTWO*X+PTWO)
      RETURN
      END

      FUNCTION  ISUB(J,K)
      COMMON /PIG/ AONE,CONE,PONE,ATWO,CTWO,PTWO,N
C     THIS CONVERTS ELEMENTS OF UPPER TRIANGULAR MATRIX TO A LINEAR
      ISUB=(N*J)-((((J-1)*J)/2)+N-K)
C     ARRAY  COUNTING LEFT TO RIGHT STARTING WITH FIRST ROW
      RETURN
      END
```

```
C     THIS IS A METHOD OF MOMENTS SOLUTION FOR BISTATIC SCATT  TM  CASE
C     GAUSSIAN INTEGRATION IS USED TO CALCULATE THE MATRIX ELEMENTS
C     UNIT INCIDENT ELECTRIC FIELD IS ASSUMED,OF COURSE THIS IS MODIFIED
C     NEAR THE ENDPOINTS OF THE SURFACE BY ILLUMINATION TAPPERING
C     NSUB SEGMENTS HAVE N MIDPOINTS
C     NSUB IS THE SUBSCRIPT WHICH COUNTS THE END POINTS
C     N    IS THE SUBSCRIPT WHICH COUNTS THE MIDPOINTS
C      WATCH MAX SLOPE SO THAT THE X INCREMENTS ARE SMALL ENOUGH
C     THE SURFACE UNDER CONSIDERATION LIES BETWEEN -EP AND +EP
C     THE ARRAY XM(J) CONTAINS THE X COORDINATES OF THE MIDPOINTS OF THE
C     SEGMENTS,XM(I) IS THE MIDPOINT OF THE I'TH SEGMENT
C     THE ARRAY X(J) CONTAINS THE X COORDINATES OF THE ENDPOINTS OF THE
C     SURFACE SEGMENTS,X(I),X(I+1) ARE THE LOWER AND UPPER X COORDINATES
C     OF THE ENDPOINTS OF THE I'TH SEGMENT
C     PHASE REFFERENCE IS AT THE ORIGIN OF THE COORDINATE SYSTEM
      COMPLEX SNN,SST
      COMPLEX S
      DIMENSION Y(10),CMC(360)
      NAMELIST/D/ WE,EP,THXXD,AONE,CONE,PONE,ATWO,CTWO,PTWO,N
      NAMELIST /E/F,XMID
      COMPLEX FSS
      COMPLEX STS
      COMMON /PIG/ AONE,CONE,PONE,ATWO,CTWO,PTWO,N
      COMPLEX C(236,236)
      COMPLEX  F(236),SS,T,CTEST
C     THE DIMENSIONS OF C AND F MUST BE COMMENSURATE
C     THAT IS  C(L,L) ---- F(L)
      COMPLEX FIN
      COMPLEX HAN2
      DIMENSION X(500)
      DIMENSION XM(500)
C     THE FOLLOWING CONSTANTS DESCRIBE THE SURFACE
      ACNE=-50.0
      CONE=6.28318/800.0
      PONE=3.1415927/2.0
      ATWO=0.0
      CTWO=0.0
      PTWO=0.0
C     WE  IS THE ELECTRICAL WAVELENGTH
      WE=25.0
      G=6.2831853        /WE
      DC=WE/10.0
      DX=DC/1000.0
      DC2=DC/2.0
      EP=200.0
C     THE FOLLOWING BREAKS THE SURFACE INTO SEGMENTS DC CENTIMETERS LONG
C     BY LINE INTEGRATION USING STEPS OF LENGTH DX FOR THE INTEGRATION
      NSUB=1
      X(NSUB)=-EP
 1002 AL=0.000
      R=X(NSUB)
 1001 R=R+DX
      ALO=AL
      AL=AL+(DX*SQRT(1.0+(DH(R)**2)))
      IF(((DC2-AL).LE.0.0).AND.((DC2-ALO).GT.0.0))   XM(NSUB)=R
      IF(AL.LT.DC)GO TO 1001
      WRITE (6,352) AL,NSUB
  352 FORMAT(' ','AL=',E15.8,'   NSUB=',I4)
      NSUB=NSUB+1
      X(NSUB)=R
      IF (R.LT.EP) GO TO 1002
      N=NSUB-1
      DO 1004 J=1,NSUB
      IF (J.EQ.NSUB)   XM(NSUB)=0.0
      XXX=X(J)
      XMD=  XM(J)
```

```
 1004 WRITE (6,1003) XXX,XMD,J
 1003 FORMAT (6H X(J)=,E15.8,9H    XM(J)=,E15.8,3H J=,I3)
C      THIS ENDS THE SURFACE SUBDIVISION
       NMO=N-1
       NM3=N-3
C      DIMENSION OF FINC,F IS N
       DPIF=0.7853982
       EE=2.71828
       GA=G*DC/(2.0*EE)
C     SNN IS THE DIAGONAL ELEMENT OF THE INPUT MATRIX
       SNN=HAN2(GA)*DC
       WRITE (6,400) SNN
  400  FORMAT (5H SNN=,2E15.8)
       DO 100 NJ=1,N
       C(NJ,NJ)=SNN
  100  CONTINUE
C           CONSTANTS FOR GAUSSIAN INTEGRATION 5 TH  ORDER
       GU1=-0.9061798
       GU2=-0.53846931
       GU3=0.0
       GU4=-GU2
       GU5=-GU1
       GW1=0.2369268
       GW5=0.2369268
       GW4=0.47862867
       GW2=0.47862867
       GW3=0.5688888
       DO 3361 MR=1,N
       XMM=XM(MR)
       HXMM=H(XMM)
       DO 3361 MC=1,N
       IF (MC.EQ.MR) GO TO 3361
       EPL=X(MC)
       EPU=X(MC+1)
       DVDFEP=(EPU-EPL)/2.0
       DVSMEP=(EPU+EPL)/2.0
       XU5=GU5*DVDFEP+DVSMEP
       XU1=GU1*DVDFEP+DVSMEP
       XU2=GU2*DVDFEP+DVSMEP
       XU3=GU3*DVDFEP+DVSMEP
       XU4=GU4*DVDFEP+DVSMEP
       C(MR,MC)=DVDFEP*(
      2+GW1*HAN2(G*SQRT(((XU1-XMM)**2)+((H(XU1)-HXMM)**2)))*SQRT(1.0+(DH(
      2 XU1)**2))
      2+GW2*HAN2(G*SQRT(((XU2-XMM)**2)+((H(XU2)-HXMM)**2)))*SQRT(1.0+(DH(
      2 XU2)**2))
      2+GW3*HAN2(G*SQRT(((XU3-XMM)**2)+((H(XU3)-HXMM)**2)))*SQRT(1.0+(DH(
      2 XU3)**2))
      2+GW4*HAN2(G*SQRT(((XU4-XMM)**2)+((H(XU4)-HXMM)**2)))*SQRT(1.0+(DH(
      2 XU4)**2))
      2+GW5*HAN2(G*SQRT(((XU5-XMM)**2)+((H(XU5)-HXMM)**2)))*SQRT(1.0+(DH(
      2 XU5)**2)))
 3361 CONTINUE
C     THIS COMPLETES THE FILLIN OF THE MATRIX
C      NONSYMMETRIC CROUT
C      FIRST COLUMN OK
C      TOO GET FIRST ROW
       DO 10 J=2,N
  10   C(1,J)=C(1,J)/C(1,1)
C            NOW WORK ON ROW AND COLUMN SET K
       DO 11 K=2,N
       KMO=K-1
       KPO=K+1
```

```
C       TO GET DIAGONAL ELEMENT
        S=CMPLX(0.0,0.0)
        DO 12 IK=1,KMO
 12     S=S+C(K,IK)*C(IK,K)
        C(K,K)=C(K,K)-S
C               TO GET ELEMENTS IN COLUMN  K BELOW ROW K
        IF (KPO.GT.N) GO TO 17
        DO 13 IROW=KPO,N
        S=CMPLX(0.0,0.0)
        DO 14 JJ=1,KMO
 14     S=S+C(IROW,JJ)*C(JJ,K)
 13     C(IROW,K)=C(IROW,K)-S
C           TO GET ELEMENTS IN ROW K TO THE RIGHT OF COLUMN K
        DO 15 ICOL=KPO,N
        S=CMPLX(0.0,0.0)
        DO 16 JR=1,KMO
  16    S=S+C(K,JR)*C(JR,ICOL)
  15    C(K,ICOL)=(C(K,ICOL)-S)/C(K,K)
  17    CONTINUE
  11    CONTINUE
        WRITE (6,1222) N,WE
  1222  FORMAT(3H N=,I3,4H WE=,E15.8)
        THI=3.1415927*60.0/180.0
        THXXD=THI*180.0/3.1415927
        WRITE (6,9333) THXXD
  9333  FORMAT(9H INC ANG=,E15.8)
C       THI IS THE ANGLE OF INCIDENCE MEASURED FROM THE HORIZONTAL
C     I.E.  THE POSITIVE X AXIS
        STH=SIN(THI)
        CTH=COS(THI)
C       THIS FINDS THE INCIDENT FIELD ION THE NJTH SEGMENT
        DO 455 NJ=1,N
        XG=XM(NJ)
        F(NJ)=CEXP(CMPLX(0.0,G*((XG*CTH)+(F(XG)*STH))))
C
C
C         TAPERD ILLUMINATION
C
C
        IF(XG.LE.((WE*1.0)-EP)) F(NJ)=CMPLX(0.0,0.0)
        IF(XG.GE.(EP-(1.0*WE))) F(NJ)=CMPLX(0.0,0.0)
        IF((XG.GT.((1.0*WE)-EP)).AND.(XG.LE.((2.0*WE)-EP)))
      2 F(NJ)=F(NJ)*(0.5+(0.5*SIN((G/2.0)*(XG     -((1.5*WE)-EP)))))
        IF((XG     .GE.(EP-(2.0*WE))).AND.(XG     .LT.(EP-(1.0*WE))))
      2  F(NJ)=F(NJ)*(0.5-(0.5*SIN((G/2.0)*(XG     -(EP-(1.5*WE))))))
        ABSF=CABS(F(NJ))
        WRITE(6,83) NJ,ABSF
  83    FORMAT('  INC FIELD AT XM(',I4,')=',E15.8)
  455   CONTINUE
C       THIS BEGINS THE BACK SUBSTUTION
C       CONVERSION OF SOURCE SIDE
        F(1)=F(1)/C(1,1)
        DO 90 IJ=2,N
        S=CMPLX(0.0,0.0)
        IJMO=IJ-1
        DO 91 IK=1,IJMO
  91    S=S+C(IJ,IK)*F(IK)
  90    F(IJ)=(F(IJ)-S)/C(IJ,IJ)
C           NOW FOR FINAL BACK SUBSTITUTION
```

```
      NMO=N-1
      DO 160 L=1,NMO
      K=N-L
      KPO=K+1
      S=CMPLX(0.0,0.0)
      DO 175 JO=KPO,N
  175 S=S+C(K,JO)*F(JO)
  160 F(K)=F(K)-S
      DO 425 KCURR=1,N
      ABF=CABS(F(KCURR))
      ANGF=180.0*ATAN2(AIMAG(F(KCURR)),REAL(F(KCURR))) /3.1415927
  425 WRITE(6,553) KCURR,ABF,ANGF
  553 FORMAT( ' F(',I4,')=',E15.8,'   AT. ANGLE',E15.8)
C     THIS ENDS THE BACK SUBSTITUTIONS
      DO 439 KURR=1,N
      IND=KURR-1
      Y(1)=CABS(F(KURR))*4.0*WE/(6.28318*377.0)
      XORD=FLOAT(KURR)
  439 CALL PLOT(XORD,Y,1,IND,0.0200,0.0)
      DO 440 KURR=1,N
      IND=KURR-1
      Y(1)=180.0*ATAN2(AIMAG(F(KURR)),REAL(F(KURR)))/3.1415927
      XORD=FLOAT(KURR)
  440 CALL PLOT(XORD,Y,1,IND,180.0,-180.0)
      DO 317 JNX=1,360
      TH=0.87266463 E-02*FLOAT(JNX)
      T=CMPLX(0.0,0.0)
      DO 310 I=1,N
      XN=XM(I)
  310 T=T+ ((F(I)*CEXP(CMPLX(0.0,G*((XN*COS(TH))+(H(XN)*SIN(TH))))))
      T=T*DC*SQRT(WE)*CMPLX(-0.707107,-0.707107)/3.1415927
      CM=CABS(T)
      DB=20.0*ALOG10(CM)
      CMC(JNX)=CM
      CANG=57.296*ATAN2(AIMAG(T),REAL(T))
      THD=TH*57.296
  317 WRITE (6,312) CM,CANG,THD,DB
  312 FORMAT (18H RELATIVE E FIELD=,E15.8,7H ANGLE=,E15.8,
     2 23H ANGLE FROM HORIZONTAL=,E15.8,6H   DB= ,E15.8)
      DO 441 IES=1,360
      IND=IES-1
      Y(1)=CMC(IES)
      THS=FLOAT(IES)/2.0
  441 CALL PLOT(THS,Y,1,IND,50.0,0.0)
      STOP
      END
      FUNCTION  H(X)
C     THIS DEFINES THE SURFACE
      COMMON /PIG/ AONE,CONE,PONE,ATWO,CTWO,PTWO,N
      H=AONE*SIN(CONE*X+PONE)+ATWO*SIN(CTWO*X+PTWO)
      RETURN
      END
      FUNCTION HAN2(X)
C     I DO THIS TO AVOID RETYPING THE WHOLE GAUSS INT. PART
      COMPLEX HAN2
      COMPLEX AHAN20
      HAN2=AHAN20(X)
      RETURN
      END


      FUNCTION DH(X)
C         DH(X) IS THE DERIV. OF H(X)
      COMMON /PIG/ AONE,CONE,PONE,ATWO,CTWO,PTWO,N
      DH=AONE*CONE*COS(CONE*X+PONE)+ATWO*CTWO*COS(CTWO*X+PTWO)
      RETURN
      END
```

```
C     THIS IS A METHOD OF MOMENTS SOLUTION FOR BISTATIC SCATT  TM  CASE
C      USING TWO POINT INTERPOLATION
C     GAUSSIAN INTEGRATION IS USED TO CALCULATE THE MATRIX ELEMENTS
C     NSUB SEGMENTS HAVE N MIDPOINTS
C     NSUB IS THE SUBSCRIPT WHICH COUNTS THE END POINTS
C     N    IS THE SUBSCRIPT WHICH COUNTS THE MIDPOINTS
C      WATCH MAX SLOPE SO THAT THE X INCREMENTS ARE SMALL ENOUGH
C     THE SURFACE UNDER CONSIDERATION LIES BETWEEN -EP AND +EP
      COMPLEX SNN,SST
      COMPLEX S,CO
      COMPLEX FSS
      COMPLEX FINC(20),STS
      COMMON /PIG/ AONE,CONE,PONE,ATWO,CTWO,PTWO,N
      COMMON /HOG/ XM(400),X(400),GA,G,DC
      COMMON/GASSN/ GU1,GU2,GU3,GU4,GU5,GW1,GW2,GW3,GW4,GW5
      COMPLEX C(150,150)
      COMPLEX F(400),FP(400),SS,T,CTEST
      COMPLEX FIN
      COMPLEX HAN2
      DIMENSION        ABES(360),Y(10)
C     WE  IS THE ELECTRICAL WAVELENGTH
      WE=25.0
C     THE FOLLOWING CONSTANTS DESCRIBE THE SURFACE
      AONE=15.0
      CONE=2.0*3.1415927/200.0
      PONE=0.0
      ATWO=0.0
      CTWO=0.0
      PTWO=0.0
      DC=WE/10.0
      DX=DC/1000.0
      DC2=DC/2.0
      DPIF=0.7853982
      G=6.2831853        /WE
      EE=2.71828
      GA=G*DC/(2.0*EE)
C     EP IS THE END POINT
      EP=200.0
C          CONSTANTS FOR GAUSSIAN INTEGRATION 5 TH  ORDER
      GU1=-0.9061798
      GU2=-0.53846931
      GU3=0.0
      GU4=-GU2
      GU5=-GU1
      GW1=0.2369268
      GW5=0.2369268
      GW4=0.47862867
      GW2=0.47862867
      GW3=0.5688888
C          CONSTANTS FOR GAUSSIAN INTEGRATION 5 TH  ORDER
C     THE FOLLOWING BREAKS THE SURFACE INTO SEGMENTS DC CENTIMETERS LONG
C     BY LINE INTEGRATION USING STEPS OF LENGTH DX FOR THE INTEGRATION
      NSUB=1
      X(NSUB)=-EP
 1002 AL=0.000
      R=X(NSUB)
 1001 R=R+DX
      ALO=AL
      AL=AL+(DX*SQRT(1.0+(DH(R)**2)))
      IF(((DC2-AL).LE.0.0).AND.((DC2-ALO).GT.0.0))   XM(NSUB)=R
      IF(AL.LT.DC)GO TO 1001
      NSUB=NSUB+1
      X(NSUB)=R
      IF (R.LT.EP) GO TO 1002
```

```
      N=NSUB-1
      DO 1004 J=1,NSUB
      IF (J.EQ.NSUB)   XM(NSUB)=0.0
      XXX=X(J)
      XMD=  XM(J)
 1004 WRITE (6,1003) XXX,XMD,J
 1003 FORMAT (6H X(J)=,E15.8,9H   XM(J)=,E15.8,3H J=,I3)
C     THIS ENDS THE SURFACE SUBDIVISION
C     THIS INSURES THAT N IS ODD
      KK=0
 5733 KK=KK+1
      IF ((2*(K-1).EQ.N) GO TO 5731
      IF (2*KK.EQ.N) GO TO 5732
      GO TO 5733
 5732 N=N-1
 5731 CONTINUE
      WRITE (6,3728) N,KK
 3728 FORMAT(' ','CORRECTED VALUE OF N=',I4,'KK=',I4,'2*KK-1=N')
      NMO=N-1
      NM3=N-3
C     DIMENSION OF FINC,F IS N
C     MATRIX FILL IN
C     DO BY COLUMNS
C     FOR FIRST COLUMN
      DO 3661 I=1,KK
 3661 C(I,1)=CO(2*I-1,1)+(CO(2*I-1,2)/2.0)
C     FOR LAST COLUMN
      DO 3678 I=1,KK
 3678 C(I,KK)=(CO(2*I-1,2*KK-2)/2.0)+CO(2*I-1,2*KK-1)
C     FOR MIDDLE COLUMNS
      DO 56 I=1,KK
      II=2*I-1
      KKM1=KK-1
      DO 56 J=2,KKM1
      JJ=2*J-1
      C(I,J)=(CO(II,JJ-1)/2.0)+CO(II,JJ)+(CO(II,JJ+1)/2.0)
 56   CONTINUE
C    THIS COMPLETES THE FILLIN OF THE MATRIX
C     NONSYMMETRIC CROUT
C     FIRST COLLOM OK
C     TO GET THE FIRST ROW
      DO 10 J=2,KK
 10   C(1,J)=C(1,J)/C(1,1)
C          NOW WORK ON ROW AND COLUMN SET K
      DO 11 K=2,KK
      KMO=K-1
      KPO=K+1
C      TO GET DIAGONAL ELEMENT
      S=CMPLX(0.0,0.0)
      DO 12 IK=1,KMO
 12   S=S+C(K,IK)*C(IK,K)
      C(K,K)=C(K,K)-S
C            TO GET ELEMENTS IN COLUMN  K BELOW ROW K
      IF(KPO.GT.KK) GO TO 17
      DO 13 IROW=KPO,KK
      S=CMPLX(0.0,0.0)
      DO 14 JJ=1,KMO
 14   S=S+C(IROW,JJ)*C(JJ,K)
 13   C(IROW,K)=C(IROW,K)-S
C          TO GET ELEMENTS IN ROW K TO THE RIGHT OF COLUMN K
      DO 15 ICOL=KPO,KK
      S=CMPLX(0.0,0.0)
      DO 16 JR=1,KMO
 16   S=S+C(K,JR)*C(JR,ICOL)
 15   C(K,ICOL)=(C(K,ICOL)-S)/C(K,K)
 17   CONTINUE
 11   CONTINUE
```

```
      WRITE (6,1222) KK,WE
 1222 FORMAT(' ',' KK=',I4,'  WE=',E15.8)
      TH=3.1415927*60.0/180.0
      THDEG=57.29578*TH
      WRITE (6,9333) THDEG
 9333 FORMAT(9H INC ANG=,E15.8)
C     TH IS THE ANGLE OF INCIDENCE FROM THE HORIZONTAL
      STH=SIN(TH)
      CTH=COS(TH)
C     THIS FINDS THE INCIDENT FIELD ION THE NJTH SEGMENT
      DO 455 NJ=1,KK
      XG=XM(2*NJ-1)
      FP(NJ)=CEXP(CMPLX(0.0,G*((XG*CTH)+(H(XG)*STH))))
      IF(XG.LE.((WE*1.0)-EP)) FP(NJ)=CMPLX(0.0,0.0)
      IF(XG.GT.(EP-1.0*WE))  FP(NJ)=CMPLX(0.0,0.0)
      IF((XG.GT.((1.0*WE)-EP)).AND.(XG.LE.((2.0*WE)-EP)))
     2 FP(NJ)=FP(NJ)*(0.5+(0.5*SIN((G/2.0)*(XG -((1.5*WE)-EP)))))
      IF((XG.GE.(EP-(2.0*WE))).AND.(XG.LT.(EP-(1.0*WE))))
     2  FP(NJ)=FP(NJ)*(0.5-(0.5*SIN((G/2.0)*(XG-(EP-(1.5*WE))))))
 455  CONTINUE
      WRITE(6,9410) (NJ,FP(NJ),NJ=1,KK)
 9410 FORMAT(' ','INCIDENT FIELD FINC(',I4,')=',2E15.8)
C     THIS BEGINS THE BACK SUBSTUTION
C     CONVERSION OF SOURCE SIDE
      FP(1)=FP(1)/C(1,1)
      DO 90 IJ=2,KK
      S=CMPLX(0.0,0.0)
      IJMO=IJ-1
      DO 91 IK=1,IJMO
 91   S=S+C(IJ,IK)*FP(IK)
 90   FP(IJ)=(FP(IJ)-S)/C(IJ,IJ)
C          NOW FOR FINAL BACK SUBSTITUTION
      NMO=KK-1
      DO 160 L=1,NMO
      K=KK-L
      KPO=K+1
      S=CMPLX(0.0,0.0)
      DO 175 JO=KPO,KK
 175  S=S+C(K,JO)*FP(JO)
 160  FP(K)=FP(K)-S
      KKM1=KK-1
C     TO RECONSTRUCT THE CURRENTS
      DO 47 IRA=1,KKM1
 47   F(2*IRA)=(FP(IRA)+FP(IRA+1))/2.0
      DO 48 IRA=1,KK
 48   F(2*IRA-1)=FP(IRA)
      WRITE (6,4970)((J,FP(J)),J=1,KK)
 4970 FORMAT(' ','FP(',I5,')=',2E15.8)
      WRITE (6,553) (F(K),K=1,N)
 553  FORMAT (6H F(K)=,2E15.8)
C     THIS ENDS THE BACK SUBSTITUTIONS
      DO 439 KURR=1,N
      IND=KURR-1
      Y(1)=CABS(F(KURR))*4.0*WE/(6.28318*377.0)
      XORD=FLOAT(KURR)
 439  CALL PLOT(XORD,Y,1,IND,0.0200,0.0)
      DO 440 KURR=1,N
      IND=KURR-1
      Y(1)=180.0*ATAN2(AIMAG(F(KURR)),REAL(F(KURR)))/3.1415927
```

```
      XORD=FLOAT(KURR)
  440 CALL PLOT(XORD,Y,1,IND,180.0,-180.0)
      DO 317 JNX=1,360
      TH=0.01745329*FLOAT(JNX)/2.0
      T=CMPLX(0.0,0.0)
      DO 310 I=1,N
      XN=XM(I)
  310 T=T+ ((F(I)*CEXP(CMPLX(0.0,G*((XN*COS(TH))+(H(XN)*SIN(TH)))))))
C     ********** THIS CORRECTS THE OUTPUT TO TRUE ELE. FIELD
      T=T*DC*SQRT(WE)*CMPLX(-0.707107,-0.707107)/3.1415927
      CM=CABS(T)
      DB=20.0*ALOG10(CM)
      CANG=57.296*ATAN2(AIMAG(T),REAL(T))
      THD=TH*57.296
      ABES(JNX)=CM
  317 WRITE (6,312) CM,CANG,THD,DB
  312 FORMAT (18H RELATIVE E FIELD=,E15.8,7H ANGLE=,E15.8,
     2 23H ANGLE FROM HORIZONTAL=,E15.8,6H    DB=,E15.8)
      DO 9500 JC=1,360
      Y(1)=ABES(JC)
      E=FLOAT(JC)/2.0
      IND=JC-1
 9500 CALL PLOT(E,Y,1,IND,50.0,0.0)
      STOP
      END


      FUNCTION  CO(MR,MC)
      COMPLEX CO
      COMPLEX  AHAN20
      COMMON/GASSN/ GU1,GU2,GU3,GU4,GU5,GW1,GW2,GW3,GW4,GW5
      COMMON /HOG/ XM(400),X(400),GA,G,DC
      IF(MR.NE.MC) GO TO 100
      CO=DC*AHAN20(GA)
      GO TO 200
  100 CONTINUE
      XMM=XM(MR)
      HXMM=H(XMM)
      EPL=X(MC)
      EPU=X(MC+1)
      DVDFEP=(EPU-EPL)/2.0
      DVSMEP=(EPU+EPL)/2.0
      XU5=GU5*DVDFEP+DVSMEP
      XU1=GU1*DVDFEP+DVSMEP
      XU2=GU2*DVDFEP+DVSMEP
      XU3=GU3*DVDFEP+DVSMEP
      XU4=GU4*DVDFEP+DVSMEP
      CO=DVDFEP*(
     2+GW1*AHAN20(G*SQRT(((XU1-XMM)**2)+((H(XU1)-HXMM)**2)))*SQRT(1.0
     2+(DH(XU1)**2))
     2+GW2*AHAN20(G*SQRT(((XU2-XMM)**2)+((H(XU2)-HXMM)**2)))*SQRT(1.0
     2+(DH(XU2)**2))
     2+GW3*AHAN20(G*SQRT(((XU3-XMM)**2)+((H(XU3)-HXMM)**2)))*SQRT(1.0
     2+(DH(XU3)**2))
     2+GW4*AHAN20(G*SQRT(((XU4-XMM)**2)+((H(XU4)-HXMM)**2)))*SQRT(1.0
     2+(DH(XU4)**2))
     2+GW5*AHAN20(G*SQRT(((XU5-XMM)**2)+((H(XU5)-HXMM)**2)))*SQRT(1.0
     2+(DH(XU5)**2)))
  200 CONTINUE
      RETURN
      END
```

```
      FUNCTION DH(X)
C          DH(X) IS THE DERIV. OF H(X)
      COMMON /PIG/ AONE,CONE,PONE,ATWO,CTWO,PTWO,N
      DH=AONE*CONE*COS(CONE*X+PONE)+ATWO*CTWO*COS(CTWO*X+PTWO)
      RETURN
      END


      FUNCTION  H(X)
C     THIS DEFINES THE SURFACE
      COMMON /PIG/ AONE,CONE,PONE,ATWO,CTWO,PTWO,N
      H=AONE*SIN(CONE*X+PONE)+ATWO*SIN(CTWO*X+PTWO)
      RETURN
      END
```

```
C       TE CASE ,GAUSSIAN INTEGRATION USED TO FILL IN MATRIX,INTEGRAL EQN.
C       NSUB SEGMENTS HAVE N MIDPOINTS
C       NSUB IS THE SUBSCRIPT WHICH COUNTS THE END POINTS
C       N    IS THE SUBSCRIPT WHICH COUNTS THE MIDPOINTS
C        WATCH MAX SLOPE SO THAT THE X INCREMENTS ARE SMALL ENOUGH
C       THE ARRAY XM(J) CONTAINS THE X COORDINATES OF THE MIDPOINTS OF THE
C       SURFACE SEGMENTS,X(I),X(I+1) ARE THE LOWER AND UPPER X COORDINATES
C       OF THE ENDPOINTS OF THE I'TH SEGMENT
C       THE SURFACE UNDER CONSIDERATION LIES BETWEEN -EP AND +EP
        COMPLEX SNN,SST
        COMPLEX S,CO
        COMPLEX FSS
        COMMON/GASSN/ GU1,GU2,GU3,GU4,GU5,GW1,GW2,GW3,GW4,GW5
        COMPLEX FINC(20),STS
        COMMON /PIG/ AONE,CONE,PONE,ATWO,CTWO,PTWO,N
        COMPLEX C(235,235)
        COMMON/HOG/  XM(400),G,X(400)
        COMMON /DOG/ DJC
        COMPLEX DJC
        COMPLEX F(235),SS,T,CTEST
        COMPLEX FIN
        COMPLEX HAN2
        DIMENSION        ABES(360),Y(10)
C       THE FOLLOWING CONSTANTS DESCRIBE THE SURFACE
        AONE=40.0
        CONE=6.28318/200.0
        PONE=0.0
        ATWO=0.0
        CTWO=0.0
        PTWO=0.0
C       WE  IS THE ELECTRICAL WAVELENGTH
        WE=25.0
        G=6.2831853        /WE
        DC=WE/10.0
        DX=DC/1000.0
        DC2=DC/2.0
        EP=200.0
        STS=-DC*CMPLX(0.707107,0.707107)/(2.0*SQRT(WE))
        DJC=CMPLX(0.0,1.0)*G/4.0
C            CONSTANTS FOR GAUSSIAN INTEGRATION 5 TH  ORDER
        GU1=-0.9061798
        GU2=-0.5384693 1
        GU3=0.0
        GU4=-GU2
        GU5=-GU1
        GW1=0.2369268
        GW5=0.2369268
        GW4=0.47862867
        GW2=0.47862867
        GW3=0.5688888
C            CONSTANTS FOR GAUSSIAN INTEGRATION 5 TH  ORDER
C       THE FOLLOWING BREAKS THE SURFACE INTO SEGMENTS DC CENTIMETERS LONG
C       BY LINE INTEGRATION USING STEPS OF LENGTH DX FOR THE INTEGRATION
        NSUB=1
        X(NSUB)=-EP
 1002   AL=0.000
        R=X(NSUB)
 1001   R=R+DX
        ALO=AL
        AL=AL+(DX*SQRT(1.0+(DH(R)**2)))
        IF(((DC2-AL).LE.0.0).AND.((DC2-ALO).GT.0.0))    XM(NSUB)=R
        IF(AL.LT.DC)GO TO 1001
```

```
      WRITE(6,352) AL,NSUB
  352 FORMAT('  AL=',E15.8,'  NSUB=',I4)
      NSUB=NSUB+1
      X(NSUB)=R
      IF (R.LT.EP) GO TO 1002
      N=NSUB-1
      WRITE(6,251) N,NSUB
  251 FORMAT( '   N=',I4,'   NSUB=',I4)
      DO 1004 J=1,NSUB
      IF (J.EQ.NSUB)   XM(NSUB)=0.0
      XXX=X(J)
      XMD=  XM(J)
 1004 WRITE (6,1003) XXX,XMD,J
 1003 FORMAT (6H X(J)=,E15.8,9H   XM(J)=,E15.8,3H J=,I3)
C     THIS ENDS THE SURFACE SUBDIVISION
      NMC=N-1
      NM3=N-3
C     DIMENSION OF FINC,F IS N
      DPIF=0.7853982
C     MATRIX FILL IN
      DO 3661 IR=1,N
      DO 3661 IC=1,N
 3661 C(IR,IC)=CO(IR,IC)
C    THIS COMPLETES THE FILLIN OF THE MATRIX
C     NONSYMMETRIC CROUT
C     FIRST COLUMN OK
C     TO GET THE FIRST ROW
      DO 10 J=2,N
  10  C(1,J)=C(1,J)/C(1,1)
C          NOW WORK ON ROW AND COLUMN SET K
      DO 11 K=2,N
      KMC=K-1
      KPO=K+1
C      TO GET DIAGONAL ELEMENT
      S=CMPLX(0.0,0.0)
      DO 12 IK=1,KMO
  12  S=S+C(K,IK)*C(IK,K)
      C(K,K)=C(K,K)-S
C            TO GET ELEMENTS IN COLUMN K BELOW ROW K
      IF (KPO.GT.N) GO TO 17
      DO 13 IROW=KPO,N
      S=CMPLX(0.0,0.0)
      DO 14 JJ=1,KMC
  14  S=S+C(IROW,JJ)*C(JJ,K)
  13  C(IROW,K)=C(IROW,K)-S
C          TO GET ELEMENTS IN ROW K TO THE RIGHT OF COLUMN K
      DO 15 ICOL=KPO,N
      S=CMPLX(0.0,0.0)
      DO 16 JR=1,KMO
  16  S=S+C(K,JR)*C(JR,ICOL)
  15  C(K,ICOL)=(C(K,ICOL)-S)/C(K,K)
  17  CONTINUE
  11  CONTINUE
C     THIS ENDS THE MATRIX FACTORIZATION
      WRITE (6,1222) N,WE
 1222 FORMAT(3H N=,I3,4H WE=,E15.8)
      THI=60.0*3.14159/180.0
      WRITE (6,9333) THI
 9333 FORMAT(9H INC ANG=,E15.8)
C     THI IS THE ANGLE OF INC. MEAS. FROM THE +VE X AXIS
      STH=SIN(THI)
      CTH=COS(THI)
C     THIS FINDS THE INCIDENT FIELD ION THE NJTH SEGMENT
      DO 455 NJ=1,N
      XG=XM(NJ)
```

```
C      THE SIGN ON THE INCIDENT FIELD HAS BEEN ADJUSTED TO AGREE WITH
C      THE INTEGRAL EQUATION
       F(NJ)=CEXP(CMPLX(0.0,G*((XG*CTH)+(H(XG)*STH))))*CMPLX(-1.0,0.0)
C
C
C      TAPPERED ILLUMINATION
       IF(XG.LE.((WE*1.0)-EP)) F(NJ)=CMPLX(0.0,0.0)
       IF(XG.GE.(EP-(1.0*WE))) F(NJ)=CMPLX(0.0,0.0)
       IF((XG.GT.((1.0*WE)-EP)).AND.(XG.LE.((2.0*WE)-EP)))
      2 F(NJ)=F(NJ)*(0.5+(0.5*SIN((G/2.0)*(XG     -((1.5*WE)-EP)))))
       IF((XG     .GE.(EP-(2.0*WE))).AND.(XG     .LT.(EP-(1.0*WE))))
      2  F(NJ)=F(NJ)*(0.5-(0.5*SIN((G/2.0)*(XG     -(EP-(1.5*WE))))))
  455  CONTINUE
       WRITE(6,2948) (NJ,F(NJ),NJ=1,N)
 2948  FORMAT(' ',' INC FIELD F(',I4,')=',2E15.8)
C      THIS BEGINS THE BACK SUBSTUTION
C      CONVERSION OF SOURCE SIDE
       F(1)=F(1)/C(1,1)
       DO 90 IJ=2,N
       S=CMPLX(0.0,0.0)
       IJMO=IJ-1
       DO 91 IK=1,IJMO
  91   S=S+C(IJ,IK)*F(IK)
  90   F(IJ)=(F(IJ)-S)/C(IJ,IJ)
C          NOW FOR FINAL BACK SUBSTITUTION
       NMO=N-1
       DO 160 L=1,NMO
       K=N-L
       KPO=K+1
       S=CMPLX(0.0,0.0)
       DO 175 JO=KPO,N
  175  S=S+C(K,JO)*F(JO)
  160  F(K)=F(K)-S
C      THIS ENDS THE BACK SUBSTITUTIONS
       DO 554 IKUR=1,N
       AAF=CABS(F(IKUR))
       ANF=57.296*ATAN2(AIMAG(F(IKUR)),REAL(F(IKUR)))
  554  WRITE(6,553)IKUR,AAF,ANF
  553  FORMAT (' ','F(',I4,')=', E15.8,'    AT ANGLE=',E15.8)
       DO 9553 IRRO=1,N
       IND=IRRO-1
       Y(1)=CABS(F(IRRO))
       XRRO=FLOAT(IRRO)
 9553  CALL PLOT(XRRO,Y,1,IND,5.00,0.0)
       DO 9554 IRRO=1,N
       IND=IRRO-1
       Y(1)=57.2958*ATAN2(AIMAG(F(IRRO)),REAL(F(IRRO)))
       XRRO=FLOAT(IRRO)
 9554  CALL PLOT(XRRO,Y,1,IND,180.0,-180.0)
       DO 317 JNX=1,360
       THS=0.01745329*FLOAT(JNX)/2.0
       T=CMPLX(0.0,0.0)
       DO 310 I=1,N
       XN=XM(I)
       THN=1.5707963+ATAN(DH(XN))
  310  T=T+ ((F(I)*CEXP(CMPLX(0.0,G*((XN*COS(THS))+(H(XN)*SIN(THS))))))
      2 *COS(THN-THS))
C      ********** THIS CORRECTS THE OUTPUT TO TRUE MAG. FIELD
       T=T*STS
       CM=CABS(T)
       DB=20.0*ALOG10(CM)
       CANG=57.296*ATAN2(AIMAG(T),REAL(T))
       THSD=THS*57.296
       ABES(JNX)=CM
  317  WRITE (6,312) CM,CANG,THSD,DB
```

```
  312  FORMAT (18H RELATIVE H FIELD=,E15.8,7H ANGLE=,E15.8,
     2 23H ANGLE FROM HORIZONTAL=,E15.8,6H    DB=,E15.8)
       DO 9500 JC=1,360
       Y(1)=ABES(JC)
       U=FLOAT(JC)/2.0
       IND=JC-1
 9500  CALL PLOT(U,Y,1,IND,50.0,0.0)
       STOP
       END


       FUNCTION  H(X)
C      THIS DEFINES THE SURFACE
       COMMON /PIG/ AONE,CONE,PONE,ATWO,CTWO,PTWO,N
       H=AONE*SIN((CONE*X)+PONE)+ATWO*SIN((CTWO*X)+PTWO)
       RETURN
       END


       FUNCTION DH(X)
C           DH(X) IS THE DERIV. OF H(X)
       COMMON /PIG/ AONE,CONE,PONE,ATWO,CTWO,PTWO,N
       DH=AONE*CONE*COS((CONE*X)+PONE)+ATWO*CTWO*COS((CTWO*X)+PTWO)
       RETURN
       END

       FUNCTION  CO(MR,MC)
C      THIS GIVES THE OLD MATRIX COEFFICIENTS
       COMPLEX CO
       COMPLEX DJC
       COMMON/GASSN/ GU1,GU2,GU3,GU4,GU5,GW1,GW2,GW3,GW4,GW5
       COMMON/HOG/  XM(400),G,X(400)
       COMMON /DOG/ DJC
       COMPLEX AHAN21
       IF(MR.NE.MC) GO TO 100
       CO=CMPLX(0.500,0.0)
       GO TO 200
  100  CONTINUE
       XMM=XM(MR)
       HXMM=H(XMM)
       EPL=X(MC)
       EPU=X(MC+1)
       DVDFEP=(EPU-EPL)/2.0
       DVSMEP=(EPU+EPL)/2.0
       XU5=GU5*DVDFEP+DVSMEP
       XU1=GU1*DVDFEP+DVSMEP
       XU2=GU2*DVDFEP+DVSMEP
       XU3=GU3*DVDFEP+DVSMEP
       XU4=GU4*DVDFEP+DVSMEP
       HXU1=H(XU1)
       HXU2=H(XU2)
       HXU3=H(XU3)
       HXU4=H(XU4)
       HXU5=H(XU5)
       DHXU1=DH(XU1)
       DHXU2=DH(XU2)
       DHXU3=DH(XU3)
       DHXU4=DH(XU4)
       DHXU5=DH(XU5)
       CO=DVDFEP*(
      2+(GW1*AHAN21(G*SQRT(((XU1-XMM)**2)+((HXU1-HXMM)**2)))
      2   *((-DHXU1*(XMM-XU1))+(HXMM-HXU1))
      2/SQRT(((XMM-XU1)**2)+((HXMM-HXU1)**2)))
      2+(GW2*AHAN21(G*SQRT(((XU2-XMM)**2)+((HXU2-HXMM)**2)))
      2   *((-DHXU2*(XMM-XU2))+(HXMM-HXU2))
```

```
     2/SQRT(((XMM-XU2)**2)+((HXMM-HXU2)**2)))
     2+(GW3*AHAN21(G*SQRT(((XU3-XMM)**2)+((HXU3-HXMM)**2)))
     2   *((-DHXU3*(XMM-XU3))+(HXMM-HXU3))
     2/SQRT(((XMM-XU3)**2)+((HXMM-HXU3)**2)))
     2+(GW4*AHAN21(G*SQRT(((XU4-XMM)**2)+((HXU4-HXMM)**2)))
     2   *((-DHXU4*(XMM-XU4))+(HXMM-HXU4))
     2/SQRT(((XMM-XU4)**2)+((HXMM-HXU4)**2)))
     2+(GW5*AHAN21(G*SQRT(((XU5-XMM)**2)+((HXU5-HXMM)**2)))
     2   *((-DHXU5*(XMM-XU5))+(HXMM-HXU5))
     2/SQRT(((XMM-XU5)**2)+((HXMM-HXU5)**2))))
      CO=CO*DJC
200   CONTINUE
      RETURN
      END
```

```
C       THIS IS TE CASE USING TWO POINT INTERPOLATION
C      THIS PROGRAM USES GAUSSIAN INTEGRATION TO GET MATRIX ELEMENTS
C      NSUB SEGMENTS HAVE N MIDPOINTS
C      NSUB IS THE SUBSCRIPT WHICH COUNTS THE END POINTS
C      N    IS THE SUBSCRIPT WHICH COUNTS THE MIDPOINTS
C       WATCH MAX SLOPE SO THAT THE X INCREMENTS ARE SMALL ENOUGH
C      EP IS THE END POINT
       COMPLEX SNN,SST
       COMPLEX S,CO
       COMPLEX FSS
       COMMON/GASSN/ GU1,GU2,GU3,GU4,GU5,GW1,GW2,GW3,GW4,GW5
       COMPLEX FINC(20),STS
       COMMON /PIG/ AONE,CONE,PONE,ATWO,CTWO,PTWO,N
       COMPLEX C(150,150)
       COMMON/HOG/  XM(400),G,X(400)
       COMMON /DOG/ DJC
       COMPLEX DJC
       COMPLEX F(400),FP(400),SS,T,CTEST
       COMPLEX FIN
       COMPLEX HAN2
       DIMENSION         ABES(360),Y(10)
C      WE  IS THE ELECTRICAL WAVELENGTH
       WE=25.0
       G=6.2831853        /WE
       AONE=5.0
       CONE=6.28318/200.0
       PONE=0.0
       ATWO=0.0
       CTWO=0.0
       PTWO=0.0
       DC=WE/15.0
       DX=DC/1000.0
       DC2=DC/2.0
       EP=200.0
       STS=DC*CMPLX(-0.70711,-0.70711)/(2.0*SQRT(WE))
       DJC=CMPLX(0.0,1.0)*G/4.0
C           CONSTANTS FOR GAUSSIAN INTEGRATION 5 TH  ORDER
       GU1=-0.9061798
       GU2=-0.53846931
       GU3=0.0
       GU4=-GU2
       GU5=-GU1
       GW1=0.2369268
       GW5=0.2369268
       GW4=0.47862867
       GW2=0.47862867
       GW3=0.5688888
C           CONSTANTS FOR GAUSSIAN INTEGRATION 5 TH  ORDER

C      THE FOLLOWING BREAKS THE SURFACE INTO SEGMENTS DC CENTIMETERS LONG
C      BY LINE INTEGRATION USING STEPS OF LENGTH DX FOR THE INTEGRATION
       NSUB=1
       X(NSUB)=-EP
 1002  AL=0.000
       R=X(NSUB)
 1001  R=R+DX
       ALO=AL
       AL=AL+(DX*SQRT(1.0+(DH(R)**2)))
       IF(((DC2-AL).LE.0.0).AND.((DC2-ALO).GT.0.0))   XM(NSUB)=R
       IF(AL.LT.DC)GO TO 1001
       WRITE(6,352) AL,NSUB
  352  FORMAT('  AL=',E15.8,'  NSUB=',I4)
```

```
      NSUB=NSUB+1
      X(NSUB)=R
      IF (R.LT.EP) GO TO 1002
      N=NSUB-1
      WRITE(6,251) N,NSUB
  251 FORMAT( '   N=',I4,'   NSUB=',I4)
      DO 1004 J=1,NSUB
      IF (J.EQ.NSUB)   XM(NSUB)=0.0
      XXX=X(J)
      XMD=  XM(J)
 1004 WRITE (6,1003) XXX,XMD,J
 1003 FORMAT (6H X(J)=,E15.8,9H    XM(J)=,E15.8,3H J=,I3)
C     THIS ENDS THE SURFACE SUBDIVISION
C     THIS INSURES THAT N IS ODD
      KK=0
 5733 KK=KK+1
      IF ((2*KK-1).EQ.N) GO TO 5731
      IF (2*KK.EQ.N) GO TO 5732
      GO TO 5733
 5732 N=N-1
 5731 CONTINUE
      WRITE (6,3728) N,KK
 3728 FORMAT(' ','CORRECTED VALUE OF N=',I4,'KK=',I4,'2*KK-1=N')
      NMO=N-1
      NM3=N-3
C     DIMENSION OF FINC,F IS N
      DPIF=0.7853982
C     MATRIX FILL IN
C     DO BY COLUMNS
C     FOR FIRST COLUMN
      DO 3661 I=1,KK
 3661 C(I,1)=CO(2*I-1,1)+(CO(2*I-1,2)/2.0)
C     FOR LAST COLUMN
      DO 3678 I=1,KK
 3678 C(I,KK)=(CO(2*I-1,2*KK-2)/2.0)+CO(2*I-1,2*KK-1)
C     FOR MIDDLE COLUMNS
      DO 56 I=1,KK
      II=2*I-1
      KKM1=KK-1
      DO 56 J=2,KKM1
      JJ=2*J-1
      C(I,J)=(CO(II,JJ-1)/2.0)+CO(II,JJ)+(CO(II,JJ+1)/2.0)
   56 CONTINUE
C    THIS COMPLETES THE FILLIN OF THE MATRIX
C     NONSYMMETRIC CROUT
C     FIRST COLLOM OK
C     TWO GET FIRST ROW
      DO 10 J=2,KK
   10 C(1,J)=C(1,J)/C(1,1)
C          NOW WORK ON ROW AND COLUMN SET K
      DO 11 K=2,KK
      KMO=K-1
      KPO=K+1
C      TO GET DIAGONAL ELEMENT
      S=CMPLX(0.0,0.0)
      DO 12 IK=1,KMO
   12 S=S+C(K,IK)*C(IK,K)
      C(K,K)=C(K,K)-S
C            TO GET ELEMENTS IN COLUMN  K BELOW ROW K
      IF(KPO.GT.KK) GO TO 17
      DO 13 IROW=KPO,KK
      S=CMPLX(0.0,0.0)
      DO 14 JJ=1,KMO
   14 S=S+C(IROW,JJ)*C(JJ,K)
   13 C(IROW,K)=C(IROW,K)-S
C          TO GET ELEMENTS IN ROW K TO THE RIGHT OF COLUMN K
```

```
      DO 15 ICOL=KPO,KK
      S=CMPLX(0.0,0.0)
      DO 16 JR=1,KMO
   16 S=S+C(K,JR)*C(JR,ICOL)
   15 C(K,ICOL)=(C(K,ICOL)-S)/C(K,K)
   17 CONTINUE
   11 CONTINUE
      WRITE (6,1222) KK,WE
 1222 FORMAT(' ',' KK=',I4,' WE=',E15.8)
      TH=3.1415927*60.0/180.0
      THDEG=57.29578*TH
      WRITE (6,9333) THDEG
 9333 FORMAT(9H INC ANG=,E15.8)
C     TH IS THE ANGLE OF INCIDENCE FROM THE HORIZONTAL
      STH=SIN(TH)
      CTH=COS(TH)
C     THIS FINDS THE INCIDENT FIELD ION THE NJTH SEGMENT
C
C      TAPERED ILLUMINATION  *********      ********     ********
C
      DO 455 NJ=1,KK
      XG=XM(2*NJ-1)
      FP(NJ)=CEXP(CMPLX(0.0,G*((XG*CTH)+(H(XG)*STH))))*CMPLX(-1.0,0.0)
C     INCIDENT FIELD HAS BEEN ADJUSTED TO AGREE WITH INTEGRAL EQTN.
      IF(XG.LE.((WE*1.0)-EP)) FP(NJ)=CMPLX(0.0,0.0)
      IF(XG.GT.(EP-1.0*WE))  FP(NJ)=CMPLX(0.0,0.0)
      IF((XG.GT.((1.0*WE)-EP)).AND.(XG.LE.((2.0*WE)-EP)))
     2 FP(NJ)=FP(NJ)*(0.5+(0.5*SIN((G/2.0)*(XG -((1.5*WE)-EP)))))
      IF((XG.GE.(EP-(2.0*WE))).AND.(XG.LT.(EP-(1.0*WE))))
     2  FP(NJ)=FP(NJ)*(0.5-(0.5*SIN((G/2.0)*(XG-(EP-(1.5*WE))))))
  455 CONTINUE
      WRITE(6,9410) (NJ,FP(NJ),NJ=1,KK)
 9410 FORMAT(' ',' INCIDENT FIELD FINC(',I4,')=',2E15.8)
C     THIS BEGINS THE BACK SUBSTUTION
C     CONVERSION OF SOURCE SIDE
      FP(1)=FP(1)/C(1,1)
      DO 90 IJ=2,KK
      S=CMPLX(0.0,0.0)
      IJMO=IJ-1
      DO 91 IK=1,IJMO
   91 S=S+C(IJ,IK)*FP(IK)
   90 FP(IJ)=(FP(IJ)-S)/C(IJ,IJ)
C         NOW FOR FINAL BACK SUBSTITUTION
      NMO=KK-1
      DO 160 L=1,NMO
      K=KK-L
      KPO=K+1
      S=CMPLX(0.0,0.0)
      DO 175 JO=KPO,KK
  175 S=S+C(K,JO)*FP(JO)
  160 FP(K)=FP(K)-S
      KKM1=KK-1
C     TO RECONSTRUCT THE CURRENTS
      DO 47 IRA=1,KKM1
   47 F(2*IRA)=(FP(IRA)+FP(IRA+1))/2.0
      DO 48 IRA=1,KK
   48 F(2*IRA-1)=FP(IRA)
      WRITE (6,4970)((J,FP(J)),J=1,KK)
 4970 FORMAT(' ',' FP(',I5,')=',2E15.8)
      WRITE (6,553) (F(K),K=1,N)
  553 FORMAT (6H F(K)=,2E15.8)
      DO 9553 IRRO=1,N
      IND=IRRO-1
      Y(1)=CABS(F(IRRO))
      XRPO=FLOAT(IRRO)
```

```
 9553 CALL PLOT(XRRO,Y,1,IND,5.00,0.0)
      DO 9554 IRRO=1,N
      IND=IRRO-1
      Y(1)=57.2958*ATAN2(AIMAG(F(IRRO)),REAL(F(IRRO)))
      XRRO=FLOAT(IRRO)
 9554 CALL PLOT(XRRO,Y,1,IND,180.0,-180.0)
C     THIS ENDS THE BACK SUBSTITUTIONS
      DO 317 JNX=1,360
      THS=0.01745329*FLOAT(JNX)/2.0
      T=CMPLX(0.0,0.0)
      DO 310 I=1,N
      XN=XM(I)
      THN=1.5707963+ATAN(DH(XN))
 310  T=T+ ((F(I)*CEXP(CMPLX(0.0,G*((XN*COS(THS))+(H(XN)*SIN(THS))))))
     2 *COS(THN-THS))
C     ********** THIS CORRECTS THE OUTPUT TO TRUE ELE. FIELD
      T=T*STS
      CM=CABS(T)
      DB=20.0*ALOG10(CM)
      CANG=57.296*ATAN2(AIMAG(T),REAL(T))
      THSD=THS*57.296
      ABES(JNX)=CM
 317  WRITE (6,312) CM,CANG,THSD,DB
 312  FORMAT (18H RELATIVE E FIELD=,E15.8,7H ANGLE=,E15.8,
     2 23H ANGLE FROM HORIZONTAL=,E15.8,6H   DB=,E15.8)
      DO 9500 JC=1,360
      Y(1)=ABES(JC)
      U=FLOAT(JC)/2.0
      IND=JC-1
 9500 CALL PLOT(U,Y,1,IND,50.0,0.0)
      STOP
      END


          FUNCTION  H(X)
     C    THIS DEFINES THE SURFACE
          COMMON /PIG/ AONE,CONE,PONE,ATWO,CTWO,PTWO,N
          H=AONE*SIN((CONE*X)+PONE)+ATWO*SIN((CTWO*X)+PTWO)
          RETURN
          END


        FUNCTION DH(X)
  C         DH(X) IS THE DERIV. OF H(X)
        COMMON /PIG/ AONE,CONE,PONE,ATWO,CTWO,PTWO,N
        DH=AONE*CONE*COS((CONE*X)+PONE)+ATWO*CTWO*COS((CTWO*X)+PTWO)
        RETURN
        END

        FUNCTION  CO(MR,MC)
  C     THIS GIVES THE OLD MATRIX COEFFICIENTS
        COMPLEX CO
        COMPLEX OJC
        COMMON/GASSN/ GU1,GU2,GU3,GU4,GU5,GW1,GW2,GW3,GW4,GW5
        COMMON/HOG/   XM(400),G,X(400)
        COMMON /DOG/ OJC
        COMPLEX AHAN21
        IF(MR.NE.MC) GO TO 100
        CO=CMPLX(0.500,0.0)
        GO TO 200
   100  CONTINUE
        XMM=XM(MR)
        HXMM=H(XMM)
```

```
      EPL=X(MC)
      EPU=X(MC+1)
      DVDFEP=(EPU-EPL)/2.0
      DVSMEP=(EPU+EPL)/2.0
      XU5=GU5*DVDFEP+DVSMEP
      XU1=GU1*DVDFEP+DVSMEP
      XU2=GU2*DVDFEP+DVSMEP
      XU3=GU3*DVDFEP+DVSMEP
      XU4=GU4*DVDFEP+DVSMEP
      ATDH1=ATAN(DH(XU1))
      ATDH2=ATAN(DH(XU2))
      ATDH3=ATAN(DH(XU3))
      ATDH4=ATAN(DH(XU4))
      ATDH5=ATAN(DH(XU5))
      HXU1=H(XU1)
      HXU2=H(XU2)
      HXU3=H(XU3)
      HXU4=H(XU4)
      HXU5=H(XU5)
      CO=DVDFEP*(
     2+GW1*AHAN21(G*SQRT(((XU1-XMM)**2)+((H(XU1)-HXMM)**2)))*SQRT(1.0+(
     2DH(XU1)**2))*((-SIN(ATDH1)*(XMM-XU1))+(COS(ATDH1)*(HXMM-HXU1)))
     2/SQRT(((XMM-XU1)**2)+((HXMM-HXU1)**2))
     2+GW2*AHAN21(G*SQRT(((XU2-XMM)**2)+((H(XU2)-HXMM)**2)))*SQRT(1.0+(
     2DH(XU2)**2))*((-SIN(ATDH2)*(XMM-XU2))+(COS(ATDH2)*(HXMM-HXU2)))
     2/SQRT(((XMM-XU2)**2)+((HXMM-HXU2)**2))
     2+GW3*AHAN21(G*SQRT(((XU3-XMM)**2)+((H(XU3)-HXMM)**2)))*SQRT(1.0+(
     2DH(XU3)**2))*((-SIN(ATDH3)*(XMM-XU3))+(COS(ATDH3)*(HXMM-HXU3)))
     2/SQRT(((XMM-XU3)**2)+((HXMM-HXU3)**2))
     2+GW4*AHAN21(G*SQRT(((XU4-XMM)**2)+((H(XU4)-HXMM)**2)))*SQRT(1.0+(
     2DH(XU4)**2))*((-SIN(ATDH4)*(XMM-XU4))+(COS(ATDH4)*(HXMM-HXU4)))
     2/SQRT(((XMM-XU4)**2)+((HXMM-HXU4)**2))
     2+GW5*AHAN21(G*SQRT(((XU5-XMM)**2)+((H(XU5)-HXMM)**2)))*SQRT(1.0+(
     2DH(XU5)**2))*((-SIN(ATDH5)*(XMM-XU5))+(COS(ATDH5)*(HXMM-HXU5)))
     2/SQRT(((XMM-XU5)**2)+((HXMM-HXU5)**2)))
      CO=DJC*CO
200   CONTINUE
      RETURN
      END
```

```
      FUNCTION AHAN21(X)
C     THIS IS THE HANKEL FUNCTION OF TYPE 2 AND OF ORDER 1
      DOUBLE PRECISION XD,DX,A1,A2,A3,A4,A5,A6,HJ1,B1,B2,B3,B4,B5,AHJ1,
     2TDX,A1,A2,A3,A4,A5,A6,T1,T2,T3,T4,T5,T6,T7,DSQX,B6
      COMPLEX AHAN21
      DX=DBLE(X)
      IF (X.GT.3.0) GO TO 200
      XD=DX*DX/9.0D+00
      A1=-0.31761D-03+0.11C9D-04*XD
      A2=0.00443319D+00+A1*XD
      A3=-0.03954289D+00+A2*XD
      A4=0.21093573D+00+A3*XD
      A5=-0.56249985D+00+A4*XD
      A6=0.5D+00+A5*XD
      HJ1=A6*DX
      B1=-0.0400976D+00+0.0027873D+00*XD
      B2=0.3123951D+00+B1*XD
      B3=-1.3164827D+00+B2*XD
      B4=2.1682709D+00+B3*XD
      B5=0.2212091D+00+B4*XD
      B6=-0.6366198D+00+B5*XD
      AHJ1=(B6/DX)+HJ1*DLOG(DX/2.0)*0.63661977
      AHAN21=CMPLX(SNGL(HJ1),-SNGL(AHJ1))
      GO TO 300
  200 TDX=3.0/DX
      A1=0.00113653D+00-0.00020033*TDX
      A2=-0.00249511D+00+A1*TDX
      A3=.0001710 5D+00+A2*TDX
      A4=0.01659667D+00+A3*TDX
      A5=0.156D-05+A4*TDX
      A6=0.79788456D+00+A5*TDX
      T1=0.00079824D+00-0.00029166D+00*TDX
      T2=0.00074348D+00+T1*TDX
      T3=-0.00637879D+00+T2*TDX
      T4=0.00005650D+00+T3*TDX
      T5=0.12499612D+00+T4*TDX
      T6=-2.35619449D+00+T5*TDX
      T7=DX+T6
      DSQX=A6/DSQRT(DX)
      AHAN21=CMPLX(SNGL(DSQX*DCOS(T7)),-SNGL(DSQX*DSIN(T7)))
  300 CONTINUE
      RETURN
      END
```

```
      FUNCTION AHAN20(X)
C     THIS IS THE HANKEL FUNCTION OF ORDER  0 AND OF TYPE 2
      DOUBLE PRECISION  XSQ,B10,B8,B6,B4,B2,C10,C8,C6,C4,C2,D5,D4,D3,
     2D2,D1,E5,E4,E2,E1,E0,XD,DX,F0,E3,HJ,DSX
      COMPLEX AHAN20
      DX=DBLE(X)
      IF (X.GT.3.0) GO TO 100
      XSQ=DX*DX/9.0D+01
      B10=-0.39444D-02+XSQ*0.21D-03
      B8=0.0444479D+00+XSQ*B10
      B6=-0.3163866D+00+XSQ*B8
      B4=1.2656208D+00+XSQ*B6
      B2=-2.2499997D+00+XSQ*B4
      HJ=1.0D+00+XSQ*B2
      C10=0.427916D-02-XSQ*0.24846D-03
      C8=-0.4261214D-01+XSQ*C10
      C6=0.2530117D+00+XSQ*C8
      C4=-0.74350384D+00+XSQ*C6
      C2=0.60559366D+00+XSQ*C4
      HY=SNGL(0.36746691D+00+0.6366198D+00*HJ*DLOG(DX/2.0)+XSQ*C2)
      AHAN20=CMPLX(SNGL(HJ),-HY)
      GO TO 200
  100 XD=3.0/DX
      E5=-0.72805D-03+XD*0.14476D-03
      D4=0.137237D-02+D5*XD
      D3=-0.9512D-04+D4*XD
      D2=-0.55274CD-02+D3*XD
      D1=-0.77D-06+D2*XD
      F0=0.79788456D+00+XD*D1
      E5=-0.29333D-03+XD*0.13558D-03
      E4=-0.54125D-03+E5*XD
      E3=0.262573D-02+E4*XD
      E2=-0.3954D-04+E3*XD
      E1=-0.4166397D-01+E2*XD
      E0= (-0.78539816D+00+XD*E1)+DX
      DSX=DSQRT(DX)
      AHAN20=CMPLX(SNGL(F0*DCOS(E0)/DSX),-SNGL(F0*DSIN(E0)/DSX))
  200 CONTINUE
      RETURN
      END
```

```
      SUBROUTINEPLOT( X,Y,N,IND,YMAX,YMIN)
      DIMENSIONM(119),YLABEL(6),Y(10),MARK(10)
      DATA MARK(1),MARK(2),MARK(3),MARK(5),MARK(6),MARK(7),MARK(8),
     2MARK(9),MARK(10),MARK(4)/1H*,1H.,1HI,1HO,1HN,1HH,1H1,1HZ,1H-,1HX/
      DATA IBLANK,NOPT,IPLUS/1H ,1H$,1H+/
      IF (IND)1,1,11
    1 WRITE(6,3)
    3 FORMAT(1H1//25X,48HORDER IN WHICH PLOT SYMBOLS ARE USED  *.IXONH1Z
     *-//30X,39HTHE SYMBOL ($) INDICATES OFF-SCALE DATA//)
      DO7J=9,119
    7 M(J)=MARK(10)
      NCOUNT=10
      SCALE=100.0/(YMAX-YMIN)
      LLL=(-YMIN*SCALE)+11.5
      DO8J=1,6
      R=J-1
    8 YLABEL(J)=R*20.0/SCALE+YMIN
      WRITE(6,9) (YLABEL(I),I=1,6)
    9 FORMAT(6X,1PE9.2,5(1PE20.2) /  )
      GOTO132
   11 NCOUNT=NCOUNT+1
      DO99J=1,119
   99 M(J)=IBLANK
      IF(LLL.GE.11.AND.LLL.LE.110)M(LLL)=MARK(10)
      IF(NCOUNT-10)133,132,133
  132  DO89J=11,111,20
   89   M(J)=IPLUS
  133 DO20J=1,N
      L=(Y(J)-YMIN)*SCALE+0.5
      IF(L)14,17,17
   14 IF(L+10)15,16,16
   15 M(1)=NOPT
      GOTO20
   16   LL=L+11
        M(LL)=MARK(J)
      GOTO20
   17 IF(L-108)18,19,19
   18  LL=L+11
       M(LL)=MARK(J)
      GOTO20
   19 M(119)=NOPT
   20 CONTINUE
      IF(NCOUNT-10)21,25,21
   21 WRITE(6,24) (M(J ), J=1,119)
   24 FORMAT(1X,119A1)
      GOTO27
   25 WRITE(6,26) (X,(M(J),J=9,119))
   26 FORMAT(1X,F7.3  ,111A1)
      NCOUNT=0
   27  CONTINUE
      RETURN
      END
```

APPENDIX B

SOLUTION OF SYSTEMS OF SIMULTANEOUS LINEAR EQUATIONS

Several direct methods exist which find the solution vector, [X], when the system of equations

(99) $[C]\,[X] = [B]$

is given. The two methods used here were the square root (or Cholesky) method for symmetric systems, and the Crout method for non-symmetric systems (Ref. [33]). Both methods take advantage of the fact that a non-singular matrix [C] is equivalent to [L][U], where [L] is a lower triangular matrix and [U] is an upper triangular matrix. So

(100)
$$\begin{bmatrix} \ell_{11} & 0 & 0 & \cdots & 0 \\ \ell_{21} & \ell_{22} & 0 & \cdots & 0 \\ \ell_{31} & \ell_{32} & \ell_{33} & 0 & 0 \\ \cdot & & & & \\ \ell_{N1} & \cdot & \cdot & \cdots & \ell_{NN} \end{bmatrix} \begin{bmatrix} u_{11} & u_{12} & \cdots & u_{1N} \\ 0 & u_{22} & \cdots & u_{2N} \\ & & & \\ 0 & \cdot & 0 & u_{NN} \end{bmatrix} = \begin{bmatrix} c_{11} & c_{12} & \cdots & c_{1N} \\ c_{21} & c_{22} & \cdots & \cdot \\ \cdot & & & \cdot \\ & & & \\ c_{N1} & \cdot & \cdots & c_{NN} \end{bmatrix}$$

or

$$(101) \qquad \sum_{k=1}^{\min(i,j)} \ell_{ik}\, u_{kj} = c_{ij}$$

since

$$(102) \qquad \ell_{ik} \equiv 0 \quad \text{if } k > i \quad \text{and}$$

$$(103) \qquad u_{kj} \equiv 0 \quad \text{if } k > j.$$

In order to specify [L] and [U], N^2+N unknowns must be determined. Since there are only N^2 equations, (values of C_{ij}), N unknowns may be specified. In the square root method the diagonal elements are assumed equal, i.e.,

$$u_{ii} = \ell_{ii} \text{ for } i = 1, \cdots, N$$

which gives the N extra conditions; in the Crout method one set of diagonals is specified, namely

$$(104) \qquad u_{kk} = 1 \quad \text{for } k = 1, \cdots, N.$$

Suppose that [C] has been broken up into [L][U], then

$$(105) \qquad [L][U][X] = [B]$$

whence by defining

$$(106) \qquad [R] = [U][X]$$

there results

(107) $[L][R] = [B]$

which has the solution

(108) $$r_i = (b_i - \sum_{k=1}^{i-1} \ell_{ik}\, x_k)/\ell_{ii} \qquad \text{for } i=1,\cdots,N$$

and the sum is omitted, if i equals 1. Once the [R] vector is known the system

(109) $[U][X] = [R]$

is solved by

(110) $$x_i = (r_i - \sum_{k=i+1}^{N} u_{ik}\, x_k)/u_{ii} \qquad \text{for } i=1,\cdots,N$$

where the sum is omitted if i equals N. Wilkinson (Ref. [34]) has shown that most of the error in a solution of Eq. (99) by triangularization methods comes from the decomposition of [C] into [L][U] and not in the double back substitution (Eqs. (108) and (110)).

The details of the decomposition of [C] into [L][U] will now be considered. For Crout factorization the diagonal elements of [U] are set equal to unity leaving N^2 equations and N^2 unknowns in the set of Eqs. (101), (102) and (103), which can be solved as follows:

(111) $$\ell_{ik} = c_{ik} - \sum_{m=1}^{k-1} \ell_{im}\, u_{mk} \qquad \text{for } i=k,\cdots,N$$

$$u_{kj} = \frac{1}{\ell_{kk}} \left(c_{kj} - \sum_{m=1}^{k-1} \ell_{km}\, u_{mj}\right) \qquad \text{for } j=k+1,\cdots,N \tag{112}$$

$$\ell_{ik} = 0 \quad \text{if } i < k \tag{113}$$

$$u_{kj} = 0 \quad \text{if } j < k. \tag{114}$$

These equations are used in the order: first column of [L], first row of [U]; second column of [L], second row of [U]; third column of [L], ect. In a computer solution the elements of [U] and [L] may be written over the original matrix [C] as they are generated. Once this is done the matrix becomes

$$\left[\,C\,\right] \xrightarrow[\text{AND STORED}]{\text{FACTORED}} \begin{bmatrix} \ell_{11} & u_{12} & \cdots & u_{1N} \\ & \ell_{22} & & \vdots \\ & & \ddots & \\ \ell_{N1} & \cdots & & \ell_{NN} \end{bmatrix}$$

and the fact that the diagonal elements of [U] are unity is used only in the previously described back substitution portion of the solution.

If [C] is symmetric then [C] can be factored into

$$[C] = [U]^T [U] \tag{115}$$

where $[U]^T$ is the transpose of [U]. Equation (101) becomes

$$(116) \qquad \sum_{k=1}^{\min \text{ of } (i,j)} u_{ki}\, u_{kj} = c_{ij}.$$

The $u_{i,j}$'s are found from

$$(117) \qquad u_{11} = \sqrt{c_{11}}$$

$$(118) \qquad u_{ij} = c_{ij}/u_{11} \quad \text{for} \quad j=2,\cdots,N$$

$$(119) \qquad u_{ii} = \left(c_{ii} - \sum_{k=1}^{i-1} u_{ki}^2\right)^{1/2} \quad \text{for} \quad i=2,\cdots,N$$

$$(120) \qquad u_{ij} = \left(c_{ij} - \sum_{k=1}^{i-1} u_{ki}\, u_{kj}\right)/u_{ii} \quad \text{for} \begin{cases} j=i+1,\cdots,N \\ i=2,\cdots,N \end{cases}$$

and

$$(121) \qquad u_{ij} = 0 \quad \text{if } i > j.$$

The value of this method lies in the reduction of storage space required for a given N. With the usual Crout method N^2 storage locations are required, but the square root method requires $N(N+1)/2$ storage locations since only the upper triangular portion of [C] need be stored and [U] can be found using only the upper triangular part of [C].

A small trick is required if this saving is to be realized in practice, since in FORTRAN IV the use of the dimension statement "COMPLEX C(N,N)" would set aside N^2 complex storage locations for

the elements of [C] even if only the upper triangular part of [C] were to be filled in and manipulated. To economize on storage a way was found to load the elements of the upper triangular part of [C] into a linear array N(N+1)/2 positions long. It was convenient to preserve the double subscript notation for the matrix manipulations and use a simple formula to access the proper location in the singly subscripted linear array. A symmetric matrix [C] is shown in Fig. 43 with the elements of the linear array S inserted into the corresponding locations of [C]. The order of the matrix is chosen to be 6 for this example.

s_1	s_2	s_3	s_4	s_5	s_6
	s_7	s_8	s_9	s_{10}	s_{11}
		s_{12}	s_{13}	s_{14}	s_{15}
			s_{16}	s_{17}	s_{18}
				s_{19}	s_{20}
					s_{21}

Fig. 43.--Storing a symmetric matrix in a linear array.

Element c_{11} is stored in position s_1, a_{12} in c_2, etc. The element c_{ij} $(i \leq j)$ can be accessed in the following way. The rows above the i-th row contain N(i-1) - ((i-1)(i-2)/2) elements and in the i-th row there are j - i+1 elements up to and including the one to be accessed, hence

$$(122) \qquad c_{ij} = s\left(N(i-1) - \frac{(i-1)(i-2)}{2} + j - i + 1\right)$$

$$= \left(sN \cdot i - \left[\left(\frac{i(i-1)}{2}\right) + N - j\right]\right) .$$

In the programs the subscript manipulations are performed directly in the subscript or accessed by calling a function named ISUB(i,j) [Integer Subscript corresponding to i,j]. If, for example, c_{15} were needed in a computation the element s(ISUB(1,5)) is used. Once the factorization is completed, the back substitutions are performed.

Notice that in either the Crout method or the square root method there are two distinct steps. The first is factoring the matrix and the second is the back substitution. The first step is independent of the driving column [B] and hence need be done only once for any given matrix [C] so any number of driving columns may be considered without re-factoring [C].

REFERENCES

1. Wright, J.W., "Backscattering from capillary waves with applications to sea clutter," IEEE Trans. on Antennas and Propagation, vol. AP-14, pp. 749-754, (November 1966).
2. Valenzuela, G.R., "Scattering of EM waves from a tilted slightly rough surface," Radio Science, Vol. 3, pp. 1057-1064, (July 1968).
3. Guinard, N.W., et al., "An Experimental Study of a Sea Clutter Model," Proc. IEEE, Vol. 58, pp. 543-550, (April 1970).
4. Stogryn, A., "The Apparent Temperature of the Sea at Microwave Frequencies," IEEE Trans. on Antennas and Propagation, Vol. AP-15, pp. 278-285, (March 1967).
5. Barrick, D.E. and Peake, W.H., "A review of scattering from surfaces with different roughness scales," Radio Science, Vol. 3, pp. 865-868, (August 1968).
6. Semenov, B., "An approximate calculation of scattering of electromagnetic waves from a rough surface," Radiotekh. Elektron., Vol. 11, pp. 1351-1361, (August 1966).
7. Fuks, I., "Contribution to the theory of radio wave scattering on the perturbed sea surface," Izv. Vyssh. Ucheb. Zaved. Radiofiz., Vol. 9, pp. 876-887, (May 1966).

8. Phillips, O.M., The Dynamics of the Upper Ocean, Cambridge University Press, (1966).

9. Barrick, D.E., "Unacceptable height correlation coefficients and the quasi-specular component in rough surface scattering," Radio Science, Vol. 5, pp. 647-654, (April 1970).

10. Silver, S., Microwave Antenna Theory and Design, pp. 138-143, Dover, New York, (1965).

11. Kay, I. and Keller, J.B., "Asymptotic evaluation of the field at a caustic," J. Appl. Physics, Vol. 25, pp. 876-883, (July 1954).

12. Kouyoumjian, R.G., "Asymptotic high frequency methods," Proc. IEEE, Vol. 53, pp. 864, 876 (August 1965).

13. Beckmann, P., and Spizzichino, A., The Scattering of Electromagnetic Waves from Rough Surfaces, Pergammon, New York, pp. 9-16, (1963).

14. Harrington, R.F., Time Harmonic Electromagnetic Fields, McGraw-Hill, p. 127, (1961).

15. Kouyoumjian, R.G., "Asymptotic High-Frequency Methods," Proceedings of the IEEE, Vol. 53, pp. 864-876.

16. Kodis, R.D., "A Note on the Theory of Scattering from an Irregular Surface," IEEE Trans. on Antennas and Propagation, Vol. AP-14, pp. 77-82, (January 1966).

17. Silver, S., Microwave Antenna Theory and Design, Dover, New York, p. 121, (1965).

18. Van Bladel, J., Electromagnetic Field, McGraw-Hill, New York, pp. 360-361, (1964).

19. Beckman, Petr, Depolarization of Electromagnetic Waves, Golem, pp. 82-86, (1968).

20. Richmond, J.H., "Scattering by an Arbitrary Array of Parallel Wires," IEEE Trans. on Microwave Theory and Technique, Vol. MTT-13, No. 4, July 1965, pp. 408-412.

21. Richmond, J.H., "The Calculation of Radome Diffraction Patterns," Report 1180-13, 15 September 1963, The Ohio State University ElectroScience Laboratory; prepared under Contract AF 33(616)-7614, Air Force Avionics Laboratory, Air Force Systems Command, United States Air Force, Wright-Patterson Air Force Base, Ohio.

22. Harrington, R.F., Field Computation by Moment Methods, MacMillan, New York, 1968.

23. Mei, K.K., "Scattering of Radio Waves by Rectangular Cylinders," University of Wisconsin Dissertation, (1962).

24. Harrington, R.F., Field Computation by Moment Methods, MacMillan, New York, (1968), p. 42.

25. Abramowitz, M. and Stegun, I.A., Ed., Handbook of Mathematical Functions, National Bureau of Standards, Appl. Math. Series 55, (1964), p. 916.

26. Richmond, J.H., private communications.

27. Rudduck, R.C., "Application of Wedge Diffraction Theory to Antenna Theory," Ohio State University ElectroScience Laboratory Report, N.A.S.A. Grant Number NsG-448, (1965), pp. 1-6.

28. Poggio, A.J. and Miller, E.K., "Integral Equation Solutions of Three Dimensional Scattering Problems," Computer Techniques for Electromagnetics and Antennas, Part 2, University of Illinois Short Course, (1970).

29. Zaki, K.A. and Neureuther, A.R., "Scattering from a Perfectly Conducting Surface with a Sinusoidal Hiehgt Profile: TE Polarization," IEEE Trans. on Antennas and Propagation, Vol. AP-19, (March 1971), pp. 208-214.

30. Lysanov, Iu.P., "One Approximation for the Problem of the *Scattering of Acoustic Waves by an Uneven Surface*," Soviet Physics - Acoustics, Vol. 2, pp. 190-197.

31. Leporskii, A.N., "Experimental Investigation of Diffraction of Acoustic Waves by Periodic Structures," Soviet Physics - Acoustics, Vol. 1, pp. 50-59.

32. Phillips, O.M., op. cit.

33. Westlake, J., A Handbook of Numerical Matrix Inversion and Solution of Linear Equations, Wiley, (1968), pp. 10-14.

34. Wilkinson, J.H., Rounding Errors in Algebraic Processes, Prentice-Hall, New Jersey, (1963).